Hexavalent Chromium Removal from Aqueous Solutions Using Novel Adsorbents

A Thesis

Submitted in Partial Fulfillment of the Requirements

for the Degree of

DOCTOR OF PHILOSOPHY

by

Shravan Kumar

Department of Chemical Engineering

Indian Institute of Technology Guwahati

GUWAHATI – 781039, ASSAM, INDIA

AUGUST, 2020

Dedicated

To

Almighty, My Parents, Parents in law

Mentors

And

Family Members

Department of Chemical Engineering
Indian Institute of Technology Guwahati

DECLARATION STATEMENT

I, hereby declare that the content embodied in this thesis entitled **"Hexavalent Chromium Removal from Aqueous Solutions Using Novel Adsorbents"** is the result of investigations carried out by me at the Department of Chemical Engineering, Indian Institute of Technology Guwahati, Guwahati, India, under the supervision of **Dr. Prasanna Venkatesh Rajaraman** and **Dr. Selvaraju Narayanasamy.**

In keeping with the general practice of reporting scientific observations, the thesis has been prepared without resorting to plagriasm and due acknowledgement and citation has been made wherever the work described is based on the findings of other investigations

Place: IIT Guwahati, India **Shravan Kumar**

August 2020 (Roll No. 146107030)

Department of Chemical Engineering
Indian Institute of Technology Guwahati

CERTIFICATE

It is certified that the work contained in this thesis entitled **"Hexavalent Chromium Removal from Aqueous Solutions Using Novel Adsorbents"** submitted by **Mr. Shravan Kumar** for the award of the degree of Doctor of Philosophy has been carried out in the department of Chemical Engineering, Indian Institute of Technology Guwahati, Assam, India under our supervision and this work has not been submitted elsewhere for award of any other degree or diploma.

This thesis in my opinion, has reached the standard fulfilling the requirement for award of degree of Doctor of Philosophy in accordance with regulations of the institute.

Date:

Dr. Prasanna Venkatesh Rajaraman
(Main-Supervisor)
Associate Professor
Department of Chemical Engineering
IIT Guwahati, Assam, India-781039

Dr. Selvaraju Narayanasamy
(Co- Supervisor)
Assistant Professor
Department of BSBE
IIT Guwahati ,Assam, India-781039

ACKNOWLEDGEMENT

I would like to take this opportunity to express my deep gratitude and sincere thanks to each and everyone, for helping me some way or the other, towards the completion of my research work and making this thesis possible. I convey my utmost respect to every person.

In the first place, I wish to express my deepest sense of gratitude, appreciation and trustworthiness to my PhD supervisors **Dr. Prasanna Venkatesh Rajaraman** and **Dr. Selvaraju Narayanasamy** for their patient guidance, monitoring and suggestions throughout the due course of my research work. This thesis would not have been possible without their support.

I would like to thank them for encouraging, inspiring and enriching me with the necessary research skills, which is desirable for a researcher. Their professional approach, constructive criticism and insightful comments helped me immensely in the completion of this thesis. I am indebted to them for providing their valuable time, fruitful discussions and motivating me for exploring new ideas and opportunities during the course of my investigation. Under their supervision, I grew professionally, which I believe, will have a far-reaching impact on my career. It was really a great honor and privilege to work under their esteemed guidance.

Beside of my supervisors, I would also like to express my sincere appreciation to my Doctoral Committee members, **Prof. G. Pugazhenthi** (Department of Chemical Engineering), **Prof. Tamal Banerjee** (Department of Chemical Engineering) and **Dr. Souptick Chanda** (Department of Biosciences and Bioengineering) for providing their invaluable time, advices and suggestions throughout my research period.

I am thankful to my present and former head of Department of Chemical Engineering for their kind support. I also grate full to the faculty members of Department of Chemical Engineering of Indian Institute of Technology Guwahati, for their benevolent support, encouragement and assistance.

I acknowledge with thanks to the Central Instrument Facility, Department of Chemical Engineering and BSBE of Indian Institute of Technology Guwahati, for providing me necessary instrument facility which has been very important in this research work.

I acknowledge Ministry of Human Resource Development *(MHRD)* and our institute for providing fellowship throughout the Ph.D program. I would also like to thank all the technical and non-technical staff members of Department of Chemical Engineering for their kind support.

I would like to thanks all my lab members like *Dr. Prince Kumar Baranwal, Dr. Apeksha gupta, Ms. Anusuya Talukdar, Ms. Jenasree Hazarika, Ms. Sayani adhikari, Mr. Nikhil dhongade, Ms. Chetana Patil, Mr. Sudip Das, Mr. shaimpu babu, Mr. Manish Rajput, Dr. Abhishek Ajmani, Ms. Tasrin Shahnaz, Mr. Chandi Patra, Mr. Vivek Sharma, Mr. Medisetti Raj mohan Naidu, Mr. Ajit Kumar, Mr. Vishnu Priyan V, Mr. Fazil SMM, and Mr. Rishabh Gupta,* for their suggestions in performing experiments, co-operative assistance and friendly support during my stay in Indian Institute of Technology Guwahati.

Further, I would like to thanks all my seniors, juniors and friends *like Dr. Venkatanarasimha Rao Chelli, Dr. Raj Kumar Das, Dr.Shyam Kumar Yadav, Dr. Rahul Saha, Dr. Pallab Das, Dr. Ali Shemesedin Reshad, Dr. Melaku Tesfaye, Dr. Santosh Kumar Yedla, Mr. Mahboob*

Alam, Ms. Devi Priya, Mr. Rambabu, Mr. Anirban, Mr. Bharath Velaga, Ms. Pooja Saxena, Mr. Sourdip choudary, Mr. Prudhviraj, , Mr. Dharmalingam K, Dr.Mood Mohan, Mr. Ranjeeth Kr Mishra, Mr. Amit Batghare, Dr. Pankaj Jha, Dr. Abishek Sharma, Dr. Mrutyunjay Maharana, Mr. Jitendra Singh Rawat, Mr. Debasis Maharana, Dr. Sanjeev Kumar, Ms. Remya kommadath, Mr. Harshal D. kawale for the lovely support and making my stay in IITG memorable.

I acknowledge the people who mean a lot to me, my parents for showing faith in me and giving me liberty to choose what I desired. I salute you all for the selfless love, care, pain and sacrifice you did to shape my life. Although you hardly understood what I researched on, you were willing to support any decision I made. I would never be able to pay back the love and affection showered upon me by my parents. I feel that my mother who passed away recently is looking at this work from the Heaven.

Also I express my thanks to my elder brother *Mr. Akhilesh kumar*, younger sisters, *Ms. Mamta kumari*, *Ms. Basundhra Kumari* and *Ms. Shweta Kumari* for their support and valuable prayers.

I owe thanks to a very special person, my wife, ***Dr. Deepa Lal*** for her continued and unfailing love, support and understanding during my pursuit of Ph.D degree that made the completion of thesis possible. You were always around at times I thought that it is impossible to continue, you helped me to keep things in perspective. I greatly value her contribution and deeply appreciate her belief in me. I appreciate my baby, my little son *Prarabdh* for withstanding my ignorance and the patience he showed during my thesis writing. Words would never say how grateful I am to both of you. I consider myself the luckiest in the world

to have such a lovely and caring family, standing beside me with their love and unconditional support.

My heartfelt regard goes to my father in law, mother in law, brother in law and sister in law for their love and limitless for their moral support.

I wish to thank many other people also whose names might have been overlooked but this does not mean that I have forgotten their help.

I thank the Almighty for giving me the strength and patience to work through all these years so that today I can stand proudly with my head held high.

Thank You

Shravan Kumar

August, 2020

Abstract

Urbanization and industrialization activities release large amount of hazardous pollutants in water stream and turn it non-potable form. Among the several pollutants, heavy metals found in water are needed special attention for many reasons; they are non biodegradable and their high toxicity causes adverse affect to living organisms even at very low concentrations. Among the heavy metals found in the water, Cr(VI) is one of the top toxic heavy metals by virtue of more carcinogenic and recalcitrant nature. Chromium has a wide range of applications in several industries such as paints, electroplating, cooling towers, dyes, metal finishing and largely used in tannery industry. Therefore, effluent discharge from these industries in water stream causes a serious threat to aquatic and humane life. Long exposure to Cr(VI) results in adverse effects such as lung cancer, skin irritation, kidney and liver damage. Therefore, for a long time, decontamination of Cr(VI) from wastewater has been become a challenging task. Numerous scientific methods have been used in this regards such as adsorption, reverse osmosis, precipitation, ion exchange, electrochemical treatments and membrane filtration processes. However, these conventional methods have some disadvantages due to generation of toxic sludge, high reagent and energy consumption, and incomplete metal removal. Among these methods, adsorption technology based on natural agriculture waste is a suitable choice due to inexpensive use of adsorbent and easy to operate.

In this framework, the present study was aimed to evaluate the potential of locally available biosorbents (water caltrop (*Trapa Natans*) shell and Datura *(Datura Stramonium) fruit*) and activated carbon developed from it towards the hexavalent chromium removal from waste water through batch and continuous system.

Several characterization techniques such as FESEM, EDX, TGA, FTIR and BET were employed to study physical and chemical properties of the adsorbents before and after biosorption.

Batch system was applied to study the effect of various influence parameters such as biosorbents dosage, particle size, initial metal ion concentration, contact time, temperature and pH of solution. Several adsorption isotherm and kinetic models were used to test the equilibrium data obtained from biosorbents on the basis of regression coefficient and chi square values determination.

The removal of Cr(VI) on water caltrop shell was well explained by Langmuir isotherm (R^2 = 0.989) and pseudo-second-order (R^2 = 0.998) compared to that of other models with separation factor (R_L) observed between 0.11 and 0.37. The monolayer adsorption capacity of waste caltrop shell was found to be 98.04 mg g^{-1}.

Using linear and non-linear regression analysis with high R^2 and low χ^2 value, Langmuir and pseudo-second order models were employed to explain the equilibrium data of Cr(VI) adsorption on PDSF (phosphoric activated Datura *(Datura Stramonium)* fruit), SDSF (sulphuric activated Datura *(Datura Stramonium)* fruit) and RDSF (raw Datura *(Datura Stramonium)* fruit) biosorbents. The monolayer adsorption capacity of developed adsorbents RDSF, SDSF and PDSF was found to be 85.916, 119.632, and 138.074 mg g^{-1} respectively towards the adsorption of Cr(VI) at pH 2 of solution.

Thermodynamic results of batch investigation revealed that the adsorption of Cr(VI) on adsorbents was spontaneous, endothermic and randomness in nature. The studied adsorbents were regenerated using 0.1 m HCl as an eluent.

Adsorptive performance of phosphoric treated water caltrop shell (*Trapa Natans*) was investigated in fixed bed column for the removal of Cr(VI) from waste water. Characteristics of breakthrough curve were obtained by investigating the effect of several operating parameters viz. inlet flow rate (2 - 6 mL min^{-1}), initial metal ion concentration (50 - 150 mg L^{-1}) and bed height (1 - 3 cm). The breakthrough curves of column experiment were well described by the Thomas model, Yoon-Nelson and BDST model based on regression equation and the maximum adsorption capacity was found to be 87.31 mg g^{-1}.

Research carried out in this thesis provide an insight that the developed adsorbent can be serve as alternative efficient, eco-friendly and low cost adsorbent for removal of Cr(VI) from waste water in order to meet the regulatory limits of Cr(VI) release in effluent.

Keywords: Water caltrop (*Trapa Natans*); Datura (*Dataura Staramonium);* Activated carbon; Low cost adsorbent; Cr(VI); Biosorption; Isotherm; Kinetics; Column studies; Breakthrough curve; Model.

TABLE OF CONTENTS

LIST OF FIGURES

LIST OF TABLES

INTRODUCTION

Chapter – 1
Introduction

1.1 Water Contamination

Water is considered as one of the important natural resources to survive life on earth for human beings and for all forms of living organisms. Therefore maintaining quality of water resources (ground water, rivers and lakes) is very important challenge in today's scenario as rapid industrialization, urbanization and expansion of population have led to deterioration of both quantity and quality of water. Poor quality of water, which does not meet the standard of world health organization (WHO), causes 3.1% death and also 80 % water borne diseases [Khan et al., 2013; Pawari and Gawande, 2015]. Undesirable changes in physical, chemical and biological properties of water implied that water are polluted which would cause deleterious effect on human health and aquatic life. Discharge of organic, inorganic and biological pollutants from industries, domestic and marine dumping are accountable for water pollution. Among many pollutants, inorganic heavy metals are the growing concern for environment as these are most toxic, non-biodegradable and persistence in environment [Keshavarzi et al., 2018; Sud et al., 2008; Barakat, 2011]. Therefore heavy metal contaminated water is a serious problem for aquatic life and human health [Demirbas, 2008].

1.2 Heavy Metal Pollutants

The term heavy metals refer to metallic element that possesses specific gravity more than 5.0 g cm^{-3}. In general, atomic weight of heavy metal lies in the range between 63.5 and 200.6 g mol^{-1} [Srivastava and Majumder, 2008]. Generally heavy metals found in the waste water are the elements of 4^{th} period of periodic table such as Chromium (Cr), Zinc (Zn), Arsenic (As), Cobalt (Co), Nickel (Ni), Copper, Lead (Pb) and Mercury (Hg). Although the metals are

required for organisms in trace amount for biological functions, the consumption of excess amount of heavy metals would cause adverse effects. The maximum allowable limit of heavy metals in water is given by the maximum contaminant level (MCL) standards and the same are given in Table 1.1 [Barakat, 2011; Sud et al., 2008].

Table 1.1: The MCL standards for the most hazardous heavy metals

Heavy metal	Toxicity	MCL (mg L^{-1})
Arsenic (As)	Skin irritation and visceral cancers	0.050
Cadmium (Cd)	Kidney malfunction, human carcinogen and renal sickness	0.01
Chromium Cr)	Nausea, head-ache, vomiting, diarrhea, cancer causing agent and lung cancer	0.05
Copper (Cu)	Liver disorder, wilson disease and insomnia	0.25
Nickel (Ni)	Human carcinogen, dermatitis, prolonged asthma, nausea and coughing	0.20
Zinc (Zn)	lethargy, neurological symbol and causes thirst	0.80
Lead (Pb)	Circulatory system and nervous system and infections of kidney	0.006
Mercury (Hg)	Affect to the neural system	0.00003

Among various heavy metals, chromium is highly toxic and persistent in nature. It is on the top of toxic metals list, suggested by United States Environmental Protection Agency (USAEPA). Besides, Chromium is also highly soluble and the degree of toxicity depends on particular oxidation state [Das and Singh, 2011].

1.3 Sources of Cr(VI) in Aqueous Solution

Chromium is the 7th most abundant elements on earth. Chromium possesses silver color and have high melting point (1907 °C). Furthermore, atomic weight, atomic number and density

of Chromium are 51.996 g mol^{-1}, 24 and 7.19 g cm^{-3} respectively [Shahid et al., 2017]. Rocks, volcanic dust, gases, plants and animals are the sources of natural form of chromium. In nature, chromium is found in the form of ores, mainly in chromites ($FeOCr_2O_3$) and does not exist in elemental form or found in the other metal complexes such as rocoites ($PbCrO_4$), bentorite $Ca_6(Cr,Al)_2(SO4)_3$ and tarapacaite (K_2CrO_4), vauquelinite ($CuPb_2CrO_4PO_4OH$) [Babula et al., 2008]. Owing to unique properties of chromium such as hardness, color and high corrosion resistances, it has got large applications in several industries [Zayed and Terry, 2003]. The existence of Cr(VI) in waste water is mainly due to different anthropogenic activities like industries development and mining. Specifically, metallurgy, chemical and refectory foundries discharge Cr(VI) pollutants into water bodies [Dhal et al., 2013]. Cr(VI) is mainly used as oxidizing agent and also for manufacturing chromium based compounds in chemical industries. The consumption of total chrome ore by various industries is listed in Fig. 1.1. Effluents of these industries are accountable for contamination of Cr(VI) in water stream [Dhal et al., 2013]. Tanning industry is the largest contributor of chromium in waste water.

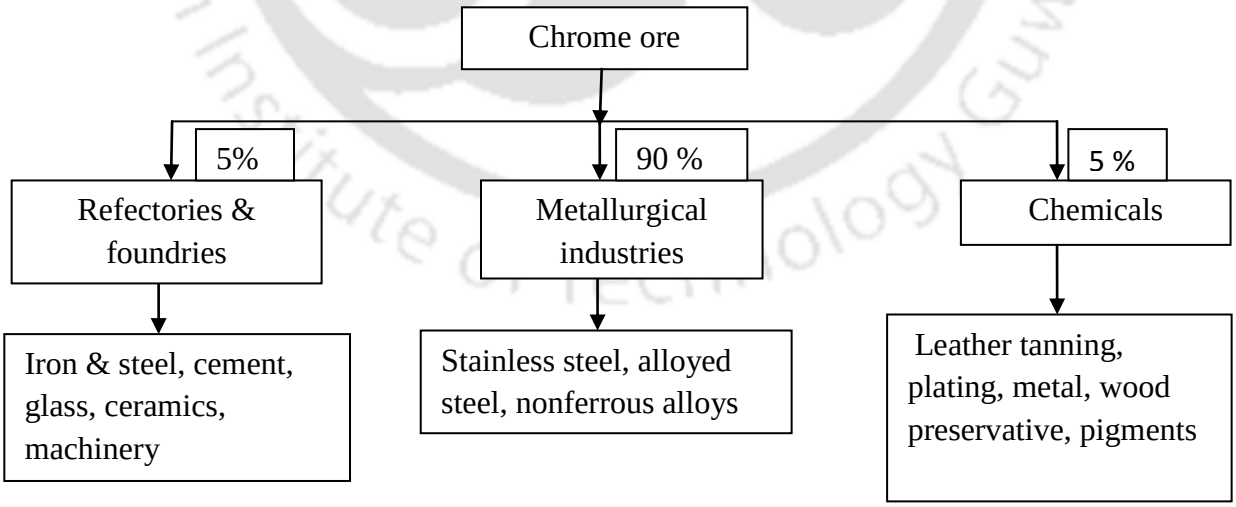

Fig. 1.1: Chromium ore percentage consumption in different industries

In addition, hexavalent form of chromium is being consumed by various industries as given in Table 1.2.

Table 1.2: Types of hexavalent chromium consumed in industry **[**Das and Mishra, 2008**]**

Industries	**Types of Cr(VI) chemical used**
Lather	Ammonium dichromate ($(NH_4)_2Cr_2O_7$)
Plastic, pigments in paints and inks	Barium chromate, lead chromate ($PbCrO_4$), sodium chromate, zinc chromate($ZnCrO_4$), calcium chromate, potassium dichromate
Wood preservation	Chromium trioxide
Anti-corrosion coating (chrome plating, spray coating)	Barium chromate ($BaCrO_4$), chromic trioxide, strontium chromate ($SrCrO_4$), chromate of zinc ($ZnCrO_4$), sodium and calcium
Stainless steel	Potassium chromate, hexavalent chromium (welded, torch cut), - potassium dichromate, sodium chromate, ammonium dichromate ($(NH4)_2Cr_2O_7$)

1.4 Chemistry of Hexavalent Chromium Ion in Liquid Phase

Chromium exists in more than one oxidation states i.e. from 2 to 6 forms. However, Cr(III) and Cr(IV) are the most two stable and common oxidation form of compounds in aqueous solution [Miretzky and Cirelli, 2010]. Hydrogen chromate ($HCrO^-_4$), chromate (CrO^{-2}_4), and dichromate ($Cr_2O_7^{-2}$) compounds are formed because hexavalent chromium shows strong oxidizing behaviour particularly in acidic region and therefore it associated with oxygen [Huang et al., 2015]. The distribution of Cr(VI) ions in solution are highly depend on pH of solution and concentration of total chromium.

As shown in Fig. 1.2, H_2CrO_4 prevails at pH < 1, $HCrO_4^{2-}$ are more in numerous than $Cr_2O_7^{-2}$ at pH between 1- 6.5 while Chromate ion (CrO_4^-) is predominant at pH > 6.5. Besides, dichromate ion $Cr_2O_7^{-2}$ formation take place when the concentration of Cr increases beyond 1g L^{-1} at low pH (1- 6.5) as shown in Fig. 1.2 [Ksakas et al., 2015]. The existence of various forms of Cr ion is characterized using constant at equilibrium as shown in equation 1.1,1.2 and 1.3 [Saha et al., 2011; Balan et al., 2013].

$$H_2CrO_4 \leftrightarrow HCrO_4^- + H^+ \qquad k_1 = 1.21 \qquad (1.1)$$

$$HCrO_4^- \leftrightarrow CrO_4^{2-} + H^+ \qquad k_3 = 3\times10^{-7} \qquad (1.2)$$

$$Cr_2O_7^{2-} + H_2O \leftrightarrow 2HCrO_4^- \qquad k_2 = 35.5 \qquad (1.3)$$

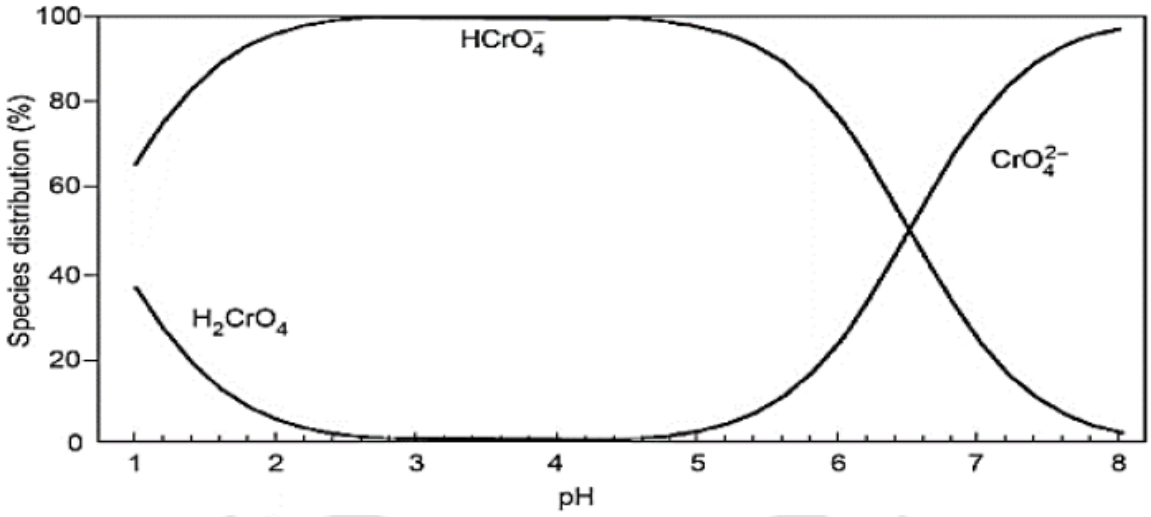

Fig.1.2: The distribution diagram of Cr(VI) at different pH values [Ksakas et al., 2015]

1.5 Toxicity of Chromium and Health Effects

The effluent stream discharge from the industries is primarily containing chromium ions in two stable oxidation states as Cr(III) and Cr(VI). The relationship between these two oxidation forms is given in equation no 1.4. In order to promote the rate of reduction reactions of Cr(VI) species, it is required to provide numerous protons supply. Acidic medium in the presence of electron donor group may allow the reduction of high toxic Cr(VI) (E° = 1.33 V) to less toxic Cr(III) [Balan et al., 2013].

$$Cr_2O_7^{2-} + 14H^+ + 6e \Leftrightarrow 2Cr^{3+} + 7H_2O + 1.33\ V \qquad (1.4)$$

These two forms are very easily inter convertible in aqueous solution. Out of these two oxidation sates, toxicity of Cr(VI) in comparison to Cr(III) is 500 times more because it accountable for cancer causes disease [Kan et al., 2017]. Toxicity and hazardous effect of Cr(VI) are attributed to more mobility and high solubility of Cr(VI) in aqueous solution. Moreover, Cr(VI) ions could easily penetrate through biological cell membrane which will damage DNA structure [Pal et al., 2013]. In addition, intake of Cr(VI) depends on various route such as inhalation, ingestion and dermal contact. Notably, exposure of Cr(VI) can cause several health issues such as skin irritation, severe diarrhoea, epigastric pain, dermatitis, nausea, vomiting and haemorrhage. The exposure of Cr(VI) through ingestion and inhalation can cause stomach ulcers, irritation of the gastrointestinal tract, respiratory distress, kidney and liver damage [Shrivastava et al., 2002; Banerjee et al., 2018; Abbas et al., 2014]. On the other hand, Cr(III) is more essential micronutrient to enhance the metabolism of protein, lipid and carbohydrate. Also, small dose of Cr(III) is required as dietary supplement and it have shown significant health benefit in mammals [Munoz et al., 2015; Shrivastava et al., 2002; Mishra et al., 2015].

However Cr(III) also have adverse effect on human health and on aquatic life at higher concentrations such as irritation to the eyes and skin [Nunez et al., 2014; Rakhunde et al., 2012]. Hence contamination of water by chromium metal pollutant is a great concern for environment and human being. According to WHO, the maximum permissible limit of Cr(VI) in potable water must be less than 0.05 mg L^{-1}.Total chromium pollutant is regulated in discharge effluent and it must be less than 2 mg L^{-1} and Cr(VI) controlled limit in surface water should be 0.1 mg L^{-1}. Therefore it is necessary to remove the Cr(VI) pollutant from effluent prior to discharge in the environment for the protection of aquatic life and public health [Albadarin et al., 2012; Kumar and Jena, 2017]. In order to meet the acceptable limit of Cr(VI) pollutant in waste water, researchers have employed several methods to control the chromium limit in discharge water as given in Table 1.3.

1.6 Water Treatment Methods

1.6.1 Conventional Methods for Removal of Cr(VI)

Various conventional methods have been adopted by researchers to remove the Cr(VI) from waste water for many years. Advantages and disadvantages of widely used methods are represented in Table 1.3.

Table 1.3: Several conventional technologies are reported to remove the Cr(VI) from effluent to an environmental tolerance limit

Sr. No.	Treatment Method	Advantage	Disadvantage	References
1.	Membrane based filtration	Extraction and striping in single step offer higher selectivity and space saving	Membrane fouling and limited flow rates, Low thermal stability , high capital cost and , maintenance, high power consumption	Kaur et al., 2012; Kulkarni et al., 2007; Fu and Wang, 2011
3.	Chemical precipitation	Most simple, selective and cost effective	Production of large quantity of toxic sludge and addition of more chemicals	Ku and Jung, 2001; Xie et al., 2017
4.	Ion exchange	High capacity, Ion exchange process removes the heavy metal selectively from solution to a solid matrix. It seems to produce the sludge in order to meet the strict discharge limit.	It involves high cost of maintenance and operation process. The synthetic organic ion exchangers are not so widely used for waste water purification, more expensive than activated carbon	Zewail and Yousef, 2015 ; Kononova et al., 2019
5.	Electrochemical	Require minimum additive, less labour, low maintenance cost, fast result obtained	Corrosion, More consumption of electricity	Taweel et al., 2015; Pena et al., 2012
6.	Adsorption	low operation cost, reusability of the adsorbent, improved selectivity of certain metal ions, great availability of adsorbent, simple operational process	High cost, low mechanical efficiency and poor removal efficiency, which limit their application, A high cost of activated carbon limited its use , Lack of active sites and binding capacity, the search of new adsorbents is important to improve the efficiency of removal of metal ions	Feng et al., 2018; Fu and Wang, 2011; Shrestha et al., 2016

1.6.2 Alternative Treatment Methods

However, the conventional methods suffer from some limitation such as less effective in reduction of Cr(VI), high consumption of chemical, more operation and maintenance expenditure and production of toxic sludge that require again treatment [Ghosh and Mitra, 2018; Bishnoi et al., 2004]. Therefore, most of these conventional methods turned unsuccessful for the removal of the Cr(VI) from waste water. Therefore, a cost effective, eco-friendly, and sustainable alternative method are required for the reduction of Cr(VI) from waste water. In this context, researchers have employed the adsorption process which offer the significant benefit like low cost operation, less sludge generation, high removal efficiency, easy operation and regeneration of metal from adsorbent for the reduction of Cr(VI) from waste water [Kan et al., 2017; Hyder et al., 2015]. Basically, adsorption is the surface phenomenon in which a molecule or atom are accumulated on the surface of solid due to chemical or physical interaction [Barakat, 2011]. In adsorption process, activated carbon exhibited significant efficiency for removal of Cr(VI) from aqueous solution owing to its beneficial characteristics such as high surface area and beneficial surface chemical properties. However, the material cost of activated carbon is significantly high [Kobya et al., 2005]. Thus, nowadays, activated carbon based sources are depleted which further leads to increase in activated carbon price [Fu and Wang, 2011]. Thus, adsorption process becomes an expensive one due to high cost associated with commercial activated carbon. In general, adsorbents can be considered as low cost if it possesses properties such as abundantly available in nature, requiring little processing steps or deriving from agriculture or industries waste material [Hegazi, 2013]. Therefore nowadays researchers have been focused on agriculture based by product as adsorbent for removing Cr(VI) from aqueous solution. Adsorption of Cr(VI) from effluent by using agriculture based adsorbent is known as biosorption process [Barakat, 2011]. Accordingly, several researchers have reported the

development of adsorbent derived from low cost and abundantly available material such as *Bagasse* [Mohan and Singh, 2002], *Coconut coir* [Gonzalez et al., 2008], *Groundnut hull* [Owalude and Tella, 2016], *Saw dust* [Shukla et al., 2005], *Rice husk* [Mohan and Sreelakshmi, 2008], *Swietenia mahagoni* shell [Rangabhashiyam et al., 2016], *Syzygium Jambolanum* nut [Muthukumaran and Beulah, 2011], *Mango kernel* [Rai, et al., 2016], *Bael* fruit [Anandkumar and Mandal, 2009], *Pineapple* leaves [Ponou et al., 2011], *Peanut* shell activated carbon [Othman et al., 2012] and *Terminali aarjuna* nuts [Mohanty et al., 2005]. Generally, agriculture based biosorbents can be classified into three categories such as cellulose, lignin and hemicelluloses [Nor et al., 2013]. In addition, adsorption on lignocelluloses based adsorbent is promoted by some oxygenated groups such as hydroxyl, carboxylic, carbonyl, alkoxy and amino [Ali et al., 2016]. Moreover, pre-treated lignocelluloses based adsorbent could provide enhanced surface area and chelating efficiency than raw adsorbents [Ngah and Hanafiah, 2008]. Moreover, biosorbent can be modified by various techniques such as pyrolysis, physical (heat treatment, size reduction) and chemical modifications (using organic solvents acids or bases) to increase the biosorption capacity [Kumar and Jena, 2017]. Hence still, investigation are required to develop sustainable efficient biosorbent from agriculture based biosorbent such as inexpensive, unexplored material for removal of Cr(VI) from waste water [Hegazi, 2013].

1.6.3 Biosorption

Biosorption process is defined as the removal of metal, metalloid or metal complex by biological material derived from waste material through physicochemical or metabolically pathway. Moreover, biosorption is recognized as passive and independent metabolic energy process for the sequestration of heavy metals from waste water. Biosorption process is performed by single or combination of various mechanisms. The several mechanisms like ion

exchange, surface complexation and precipitation, adsorption on surface and pores are involved in binding of metal on biosorbent surface [Gadd, 2009; Fomina and Gadd, 2014; Srivastava et al., 2015]. The mechanism underlying the biosorption process affected by operating and environmental conditions. Characteristics of biosorbent are more significant in addition to other parameters such as pH, temperature, concentration of solute and nature of effluent in biosorption of heavy metals [Vendruscolo et al., 2017]. Thus, finding an suitable biosorbent and optimizing the experimental conditions for the removal of Cr(VI) from waste water is still of great concern. In addition, to understand the equilibrium adsorption behavior as well as rate of biosorption process in batch mode, several mathematical models are used such as isotherm and kinetics models. Further, breakthrough curve analysis is predicted by using various mathematical models in continuous mode biosorption process. [Fawzy et al., 2016; Papirio et al., 2017].

1.6.3.1 Biosorption Isotherm

Biosorption isotherm is used to find out the qualitative analysis of biosorption equilibrium. Biosorption isotherm explains the interaction between metal concentration in liquid phase and metal adsorbed on adsorbent at given constant temperature. Several isotherm models such as Langmuir, Freundlich and D-R are used to understand the interaction behavior of adsorbent and solute in solution at equilibrium. Regression coefficients are used to indicate the better fitting criteria for this isotherm model [Pradhan et al., 2019; Ferreira et al., 2019; Foo and Hameed, 2010].

1.6.3.1.1 Langmuir Isotherm

Langmuir isotherm explains the qualitative distribution of a solute on adsorbent surface and in liquid phase. This is based on basic assumptions as given by following [Langmuir, 1918]:

- Adsorbent surface covered with monolayer adsorbed solute
- The entire active site on adsorbents surface is energetically equivalent
- Adsorbed solute do not interact with each other on adsorbent surface
- Adsorption of molecule occur on specific localized active site on adsorbent surface

The empirical non-linear and linear form equations of Langmuir isotherm are represented as follow:

$$q_e = Q_{max} \frac{bC_e}{1 + b\,C_e} \tag{1.5}$$

$$\frac{C_e}{q_e} = \frac{1}{Q_{max}\,b} + \frac{C_e}{Q_{max}} \tag{1.6}$$

Where C_e (mg L^{-1}) represents amount of solute in liquid phase at equilibrium, q_e (mg g^{-1}) indicates the adsorption capacity at equilibrium on adsorbent per unit mass. The parameters Q_{max} (mg g^{-1}) and b (L mg^{-1}) of Langmuir isotherm are related to maximum monolayer adsorption capacity and binding energy or affinity respectively. The value of Q_{max} and b of Langmuir isotherm equation are observed from the plot of C_e/q_e against C_e using intercept and slope of the line. The essential characteristics of Langmuir isotherm can be represented as dimensionless constant and it referred as equilibrium parameter or separation factor (R_L). Adsorption process can be predicted on the basis of R_L value i.e. it considered as

unfavourable if $R_L > 1$, irreversible if $R_L = 0$, linear if $R_L = 1$ and favourable if $0 < R_L < 1$ [Khan et al., 2016; Ghosal and Gupta, 2017].

The parameter R_L is represented as

$$R_L = {}^{1}/_{1 + bC_i} \quad (1.7)$$

Where b (L mg^{-1}) represents the energy constant and C_0 (mg L^{-1}) indicates the initial constant of metal in solution.

1.6.3.1.2 Freundlich Isotherm

The Freundlich isotherm model describes the relationship between adsorbed solute on heterogeneous surface and in liquid phase. In addition, it assumes that multilayer adsorption occurs by interaction between adsorbed molecules on adsorbent. Moreover, it involves the logarithmic decrease in energy of sorption as fraction of occupied site increases. The non-linear and linear form expression are represented as follow: [Freundlich and Helle, 1939]

$$q_e = K_f C_e^{1/n} \quad (1.8)$$

$$\log q_e = \log K_f + {}^{1}/_{n_f} \log C_e \quad (1.9)$$

Where C_e (mg L^{-1}) and q_e (mg g^{-1}) represent the amount of metal in liquid phase and the amount of solute adsorbed on adsorbent at saturation respectively. The Freundlich isotherm parameters like adsorption intensity and adsorption capacity are expressed by n and K_f ($mg^{1-1/n}$ $L^{1/n/g}$) respectively. Freundlich empirical equation can be employed to calculate K_f and n using slope and intercept of linear equation. When the calculated value of slope $1/n$ for Freundlich empirical equation ranges between 0 to 1, then it suggests that adsorption process

is favorable. In addition, the slope (*n*) value less than one (1) indicate that the adsorption process is chemisorptions. On the other hand, the calculated value of slope more than one predicts that adsorption occurs through physical process [Abdelnaeim et al., 2016; Ali et al., 2016].

1.6.3.1.3 D-R Isotherm Model

D-R isotherm model generally implied to describe the adsorption process on heterogeneous and homogeneous surfaces. This model usually expresses the adsorption mechanism on micro porous adsorbent surface. Moreover it predicts the information about nature of adsorption process on adsorbent i.e. whether it is physical adsorption or chemical ion exchange [Hutson and Ralph, 1997].

The non-linear and linear form of D-R isotherm model is expressed as follow:

$$q_e = Q_{max} \exp(-K_{DR} \in^2) \quad (1.10)$$

$$\ln q_e = \ln Q_{m,DR} - K_{DR} \in^2 \quad (1.11)$$

Where q_e denotes the adsorption of solute per weight unit of adsorbent and $Q_{m,DR}$ represents the maximum monolayer adsorption capacity (mg g^{-1}), K_{DR} is related to the activity coefficient from which the mean adsorption energy *E* (kJ mol^{-1}) can be calculated and $\in$ represent the Polanyi potential. *E* and $\in$ are estimated by following equations

$$E = \frac{1}{\sqrt{2K_{DR}}} \quad (1.12)$$

$$\in = RT \ln\left(1 + \frac{1}{C_e}\right) \quad (1.13)$$

Where R (kJ mol^{-1} K^{-1}) represents the gas constant, T (K) denotes temperature and C_e is amount of solute in liquid phase. Values of K_{DR} and $Q_{m,DR}$ can be observed from the plot of of $ln\, q_e$ against $\in^2$ using slope and intercept of linear form of D-R equation.

E is the mean free adsorption energy; it can be defined as amount of solute transferred from liquid phase to solid phase. The magnitude of E can be used to predict about the adsorption process like physical or chemical ion exchange **[**Rafatullah et al., 2009].

When the value of E lies between 8 to 16, KJ mol^{-1} then adsorption process can be considered as chemical ion exchange while if value of E ranges from 1 to 8 KJ mol^{-1} then it depicted the adsorption process follow the physical adsorption [Zhu et al., 2009].

1.6.3.2 Biosorption Kinetics

The study of adsorption kinetics provide significant insight on uptake rate which explains about residence time, the rate of adsorption for design and operation control in sorption reaction [Sooksawat et al., 2016]. It is important to understand the mechanism involve in transportation of solute from the solution to adsorbent surface. Therefore, it is very necessary to choose mathematical model which comply with experimental data. The distribution of the solute species between the liquid and solid phases is carried out by transfer of mass and it is controlled by either internal diffusion or external diffusion. Moreover, the adsorption mechanism of solute on adsorbent surfaces involves various steps such as given below [Tatah et al., 2017].

a. Bulk diffusion process in which adsorbate particle moves from solution to the film surrounding of adsorbent
b. External diffusion process in which adsorbate moves from film surface to the external surface of adsorbent

c. Internal diffusion process, which can be defined as transport of solute from adsorbent surface to the pores

d. Pore diffusion process which involves the adsorption of solute on the interior surface of the adsorbent through binding of the solute to the active sites

Several kinetic models are proposed to examine the experimental data in order to understand the biosorption mechanism and rate controlling step that include mass transport and chemical reaction processes. The Coefficients of determination can be applied for conformity between the experimental data and kinetic rate equation [Rafatullah et al., 2009; Febrianto et al., 2016].

1.6.3.2.1 Pseudo-First-Order Model

The Lagergren's proposed the mathematical expression which is widely used to describe the adsorption process from liquid phase to surface of adsorbent. This model assumes that rate of adsorption is related to the number of unoccupied site. The pseudo-first-order equation in differential form is expressed as below [Lagergren, 1898]:

$$\frac{dq_t}{dt} = k_1(q_e - q_t) \qquad (1.14)$$

The equation can be linearized by using boundary conditions such as $q_t = 0$ at $t = 0$ and $q_t = q_e$ at time $t = t_e$, and this is given as

$$log(q_e - q_t) = log\, q_{e\,cal} - \frac{k_1}{2.030}t \qquad (1.15)$$

Where q_e and q_t denote the amount of Cr(VI) adsorbed (mg g^{-1}) at equilibrium and at any time t and the rate constant is represented by k_1 (min^{-1}). The plot of $log(q_e\text{-}q_t)$ against t gives

the straight line with negative slope and intercept enables the calculation of the sorption rate k_1 and equilibrium adsorption capacity q_e.

1.6.3.2.2 Pseudo-Second-Order Model

Pseudo-second-order also predicts the sorption kinetics rate and it assumes that the adsorption process occur through chemisorptions process. This mechanism occurs by exchange of electron between the functional group and solute. In addition, number of active sites on surface is related to adsorption capacity; therefore kinetic rate law can be expressed as [Ho and McKay, 1999].

$$\frac{dq_t}{dt} = k_1(q_e - q_t)^2 \qquad (1.16)$$

Linear form of pseudo-second-order rate expression can be obtained by integrating the equation 1.12 by using boundary conditions such as $q_t = 0$ at $t = 0$ and $q_t = q_e$ at $t = t_e$ and it is expressed as follow:

$$\frac{t}{q_t} = \frac{1}{k_2 q_t^2} + \frac{t}{q_e} \qquad (1.17)$$

Where q_t and q_e are amount of adsorbate adsorbed per unit mass of adsorbent at any time t and at equilibrium time respectively and k_2 is the rate constant of adsorption (g mg^{-1} min^{-1}). The plot of t/q_t versus t can be applied for observing the value of equilibrium adsorption amount (q_e) and the pseudo second-order rate parameters (k_2) with help of slope and intercept of the equation.

1.6.3.2.3 Intra-Particle Diffusion Model

Weber-Morris proposed this model to get an insight of diffusion mechanism for adsorption of solute from bulk liquid solution to solid phase. Moreover, this proposal is used to assess the

rate limiting step in biosorption. According to this proposal, the adsorption of solute varies proportional to square of root of contact time $\sqrt{t}$ instead of *t*. Mathematical model of Weber equation is expressed as below [Weber and Morris, 1963].

$$q_t = k_{id} t^{1/2} + c \quad (1.18)$$

Where q_t (mg g-^{1}) is representing the concentration of adsorbate adsorbed on surface adsorbent per unit mass, rate constant of interparticle diffusion process is indicated by k_{id} (mg g^{-1}min$^{1/2}$) and the intercept is denoted by c . When the plot of q_t against $\sqrt{t}$ passes through origin and gives straight line, then it describes that biosorption process is only controlled by intraparticle diffusion with slope k_{id} and intercept *c*. In addition, increase in *c* value attributed to the increase in boundary layer thickness which result to the surface adsorption in the rate controlling step [Kavitha and Namasivayam, 2007]. However if plot of weber equation is not passes through the origin and may showed multi-linearity, then it indicates that adsorption process is controlled by either one or combination of two mechanisms such as interparticle diffusion, external diffusion, adsorption on pore surface, pore diffusion and surface diffusion [Jianying et al., 2015].

1.6.3.3 Thermodynamics

Thermodynamic studies provide information about nature of biosorption process i.e. either biosorption process is feasible, spontaneous, exothermic or endothermic. The thermodynamic factors including ΔG^0 (standard Gibb's free energy change), ΔH^0 (enthalpy change) and ΔS^0 (entropy change) can be calculated to understand the biosorption process [Bhatnagar and Minocha, 2010].

The mathematical expression for thermodynamics parameters are expressed by following equations 1.19, 1.20 and 1.21.

$$\Delta G^0 = RT \ln K_C \quad (1.19)$$

$$K_C = \frac{C_a}{C_e} \quad (1.20)$$

$$\ln K_C = \frac{\Delta H^0}{RT} + \frac{\Delta S^0}{R} \quad (1.21)$$

Where K_C represent the thermodynamic equilibrium constant, and it can be obtained from the ratio of C_a (weight of solute adsorbed per liter, mgL^{-1}) and C_e (at equilibrium, amount of metal in liquid phase, $mg\ L^{-1}$). Universal gas constant are represented by R ($8.314\ Jmol^{-1}\ K^{-1}$) and temperature (K) by T. Standard Gibb's free energy change ΔG^0 can be evaluated from determining equilibrium constant K_C values at various adsorption temperatures. The thermodynamic parameters such as ΔH^0 and ΔS^0 can observed from the slope and intercept of the $ln\, K_C$ against $1/T$ plot. Accordingly, negative values of free energy imply that the biosorption process is spontaneous and feasible and conversely positive value indicates that process is non-spontaneous. Moreover, with increase in temperature, decrease in free energy value implies that feasibility of biosorption decreases. In general, the obtained values of free energy up to 20 kJ mol^{-1} implies that the biosorption process follow physical sorption while the values between 20 kJ mol^{-1} to 40 kJ mol^{-1}suggest that chemisorptions is the dominating process [Zafar et al., 2015]. The positive and negative values of enthalpy (ΔH^0) imply that biosorption process is endothermic and exothermic nature respectively. When value of entropy (ΔS^0) is positive, it suggests that randomness of adsorbate increases and conversely for negative value of entropy, the degree of freedom decreases at solid-solution interface during the biosorption process [Fan et al., 2008].

1.6.4 Column Study

The batch mode experiments are ineffective to treat large amount of industrial waste water. Hence, there is a requirement to perform the adsorption experiments in continuous mode. Several parameters such as bed height, flow rate and initial solute concentration are used to design the fixed column. The performance of column is explained by the breakthrough curve. An effective performance of column and thorough understanding of breakthrough curve can be better explained by using various mathematical models such as Thomas, Adams–Bohart, Yoon−Nelson and Bed Depth Service Time (BDST).

1.6.4.1 Thomas Model

Thomas model is widely employed to describe the performance of column and it follows the Langmuir assumption adsorption process without axial dispersion. It explains about adsorption process which obey the second order reversible kinetics and linearized form of Thomas model equation (1.22) is given as follow [Thomas, 1944]:

$$\ln\left(\frac{C_0}{C_t}-1\right)=\frac{K_{TH}\,q_0 W}{Q}-K_{TH}\,C_0 t \qquad (1.22)$$

Where K_{TH} (mL min^{-1} mg^{-1}) and q_0 (mg g-1) represent the Thomas model constant and the adsorption capacity respectively; W (g) is weight of adsorbent in column; Q indicates the volumetric flow rate (ml min^{-1}) in column; and C_0/C_t denotes the ratio of influent to effluent concentration of metal solution. The unknown values K_{TH} and q_0 of Thomas equation can be determined by the linear plot of $ln((C_0/C_t) - 1)$ against time (t) using linear regression from the slope and intercept of the plot.

1.6.4.2 Adams–Bohart Model

Bohart-Adams uses surface reaction theory to describe the fundamental equations. It explains the initial breakthrough curve using the relationship between C_t/C_0 and t in a fixed bed column. The approach based on some assumption such as equilibrium does not take place sudden and the rate of the adsorption is directly related to the fraction of adsorption capacity still remained on the adsorbent [Bohart and Admas, 1920]. The performance of fixed bed column for adsorption can be observed by following equation:

$$\ln\left(\frac{C_t}{C_0}\right) = K_{AB}\, C_0\, t - K_{AB}\, N_{AB}\left(\frac{Z}{u}\right) \qquad (1.23)$$

Where C_t and C_0 represent the effluent and influent concentration of Cr(VI); K_{AB} (L mg^{-1} min^{-1}) and N_{AB} (mg L^{-1}) indicate the kinetics constant and saturation constant respectively; Z is the bed height of column and u (cm min^{-1}) denote the superficial velocity that can be determined by dividing the volumetric flow rate to the cross sectional area of bed. The linear plot of $ln\left(\frac{C_t}{C_0}\right)$ against time (t) is used to determine the unknown parameters.

1.6.4.3 Yoon–Nelson Model

The Yoon–Nelson model followed the assumption that the rate of decrease in the probability of adsorption for each sorbate molecule is proportional to the probability of sorbate adsorption and the probability of sorbate breakthrough on the sorbent [Yoon and Nelson, 1984].

Yoon-Nelson Model expression in linearized form is given in following equation:

$$\ln\left(\frac{C_t}{C_0 - C_t}\right) = K_{YN}\, t - K_{YN}\, \tau \qquad (1.24)$$

Where K_{YN} and τ indicate the rate constant (L min^{-1}) and the time to reach 50% sorbate breakthrough (min) respectively and t is processing time. The two unknown parameters of Yoon–Nelson model K_{YN} and τ can be determined from the linear plot of $ln\ (C_t/C_0\text{-}C_t)$ against time (t) using slope and intercept of graph.

1.6.4.4 Bed Depth Service Time (BDST) Model

BDST model are used to extend the lab scale design for pilot scale application to predict the behaviour of fixed bed column and it is the modified model form of Bohart–Adams model. BDST model explained the physical adsorption without considering the external mass resistance and intraparticle mass transfer resistance [Baral et al., 2009]. BDST is a simple model and it described the relationship between the processing time (t) and bed height (Z). BDST model expression is represented as follow:

$$t = \left(\frac{N_0 Z}{C_0\, u}\right) - \left(\frac{1}{C_0 K_a}\right) \ln\left(\frac{C_0}{C_b} - 1\right) \qquad (1.25)$$

Where C_b and C_0 represent the breakthrough metal concentration and influent concentration respectively, u is the linear velocity (cm min^{-1}), K_a indicate the rate constant (L $(mg\ min)^{-1}$) and No is the adsorption capacity (mg L^{-1}).

Here, in the present work, the main focus is to find a suitable low cost biosorbent for the removal of Cr(VI) ions from the waste water. In this regard, an extensive literature survey is conducted to find lacunae and is presented in the next chapter-2.

LITERATURE SURVEY

Chapter -2
Literature Survey

2.1 Overview

According to Owa, (2014), water is considered as polluted when it is no long appropriate for drinking, bathing, cooking or specific purpose. Anthropogenic activities, rapid industrialization and urbanization are the results of water pollution. According to Mubarak et al., (2014), several types of pollutant are discharged from various industries such as tannery, fossil fuel refineries, metallurgical, production of plastics, battery manufacturing industries and so forth which lead to contamination of water. Among all the pollutants, heavy metals are reported as greatest environmental threat due to their toxicity and non-biodegradability in nature [Abdolali et al., 2015]. Chromium in hexavalent form is one of the most toxic heavy metals which discharge into the waste water through several anthropogenic activities [Mohan et al., 2005]. Thus, Chromium removal from waste water is of great concern.

2.2 Methods for the Removal of Chromium

A wide range of conventional treatment methods such as chemical precipitation [Matlock et al., 2002], ion exchange [Dabrowski et al., 2004], membrane processes [Hernaandez et al., 2005], and adsorption [Moon and Lee, 2005] has been introduced by researchers and scientists to control the environmental problem concerning chromium contaminated waste water. Chapter- 2 gives a detailed report on conventional methods and Table 1.3 represents the comparison of several conventional methods used for reduction of chromium. Recently, the biosorption has been addressed towards one of the alternative treatment techniques for the removal of chromium. According to Ahalya et al., (2008) biosorption can be considered as promising process for sequestration of heavy metal or metalloid species, compounds and

particulates from a solution by biological origin materials. Biosorption has been considered as alternative potential technique and widely used in industries due to the low cost and easily obtained biosorbents, minimization of the volume of chemical and biological sludge to be disposed of, and high efficiency in removal of heavy metal [Feng et al., 2011].

2.3 Biosorption Affecting Parameters

Biosorption performance can be affected by various physico-chemical factors such as pH, temperature, agitation speed, other pollutant, initial adsorbate concentration, biomass particle size, biosorbent nature and doses of it [Park et al., 2010]. The same has been discussed in detail below:

2.3.1 pH of Solution

Biosorption is highly depending on pH value of the solution. Solution chemistry of metal and functional activity of biosorbents is strongly affected by the solution pH. Generally, the lower pH value of solution favors the maximum adsorption which is attributed to the electrostatic interaction between the solute and adsorbent surface. In aqueous solution Cr(VI) co-exist in various form which depend on concentration of Cr(VI) and pH of solution which is very well described in introduction chapter-1. Furthermore, at same concentration of Cr(VI) the hydrogen chromate ion ($HCrO_4^-$) predominately adsorbed than other chromate ions which is attributed to lower adsorption free energy of ($HCrO_4^-$) than CrO_4^{-2} and $Cr_2O_7^{-2}$ ions [Chen et al., 2014; Liu et al., 2018].

2.3.2 Temperature

Generally, biosorption capacity is enhanced with increase in solution temperature due to increase in kinetic energy and surface activity of the adsorbent. However, surface structure of biosorbent gets damaged at higher temperature. Therefore, higher temperature is undesirable

for biosorption process [Park et al., 2010]. Thus, optimal temperature needs to be employed in biosorption process.

2.3.3 Agitation Speed

Biosorption removal efficiency can be enhanced with increasing agitation speed of aqueous solution in appropriate system; it is true up to some extent of agitation speed. Slow agitation speed causes to assemble the sorbent in solution instead of spreading it, which lead to less exposure of active site. Whereas at later stages, increase in agitation speed results in detachments of loosely bound solute. Beside, sorbate and sorbent do not get considerable contact time to interact with each other [Rangabhashiyam and Selvaraju, 2015]. Hence, optimization of agitation speed is critical in biosorption process.

2.3.4 Biosorbent Nature

Biosorption performance can be influenced by active sites on biosorbent, prehistory of growth and physical or chemical modification of biosorbent [Fomina and Gadd, 2014]. Therefore, metal sequestration should be enhanced by understanding the biosorbent nature and suitable treatments must be employed if necessary.

2.3.5 Biomass Particle Size

It is well known that the decrease in particle size of biomass offers more surface area, which result in increase in adsorption capacity. Beside, smaller particle size biosorbent possess a tendency to equilibrate in lesser time. The reason of this phenomenon may be attributed to increase in active site and contact surface, which in turn increase in mass transfer and lesser time in equilibrium.

Moreover, the extent of adsorption is directly related to surface area because adsorption process is a surface phenomenon [Aliabadi et al., 2012; Rangabhashiyam and Selvaraju, 2015]. Thus, biosorbent of suitable size should be chosen based on the techniques used.

2.3.6 Biosorbent Doses

Biosorbent dose is considered as one of the significant parameters for biosorption of heavy metal. The maximum biosorption capacity decreases as biomass concentration increases in solution. This result can be ascribed to the formation of aggregates of biomass at higher concentration. This phenomenon describes that the higher biomass concentration offering lower utilization of biomass active surface area. Conversely, percentage removal of Cr(VI) increases with increase in biosorbent dosages. This can be attributed to an increase in surface area for a given concentration of Cr(VI) adsorption with an increase in biosorbent dosages [Hanif et al., 2007; Park et al., 2010; Aliabadi et al., 2012].

2.3.7 Initial Metal Concentration

Initial metal ion concentration is an important characteristic of biosorption process as it is related to saturation of biosorbent surface. The initial metal concentration is a significant parameter which provides a driving force for the metal ions to diffuse from the aqueous phase to the solid phase by overcoming all mass transfer resistances. Moreover, higher concentration metal ion leads to more collision, which results in a higher biosorption capacity [Madrid et al., 2011; Kuppusamy et al., 2016].

2.3.8 Regeneration of Saturated Adsorbent

Regeneration investigation is performed to evaluate the potential of reusability of adsorbent which make the adsorption process to be economically feasible. Further, the potential of

regeneration and lower cost of adsorbent allow the process more useful for industrial application. Generally, the reusability of the adsorbent are carried out by using acid and the limitation is that adsorbent should not be damaged. Beside, loaded metal on adsorbent after adsorption are needed to recover. Therefore, regeneration of loaded adsorbent should be performed to understand the biosorbent potential [Gupta et al., 2015].

2.3.9 Other pollutant

If concentration of other pollutant increases then it leads to competition for binding on active site or it offers resistance on surface of biosorbent. Consequently, biosorptive removal efficiency of target pollutant is reduced [Fomina and Gadd, 2014].

2.4 Biosorption Mechanism

Biosorption is a promising method for the metal to be taken up by the bio-origin material from aqueous solution. In order to get the information about the metal binding within biosorbent, it is necessary to understand the biosorption process. Due to the effects of several parameters of biosorption process and environmental condition, the biosorption process cannot be explained by a single mechanism. Therefore several biosorption mechanisms have been proposed by researchers to understand the sequestration of metal from waste water by lignocelluloses biomass which include chemisorptions, ion-exchange, complexation, coordination, chelation, physical adsorption and micro precipitation [Volesky, 2001; Farooq et al., 2010]. Basically, there are many polar functional groups present on lignocellulose biosorbent such as alcohols, aldehydes, ketones, carboxylic acids and ethers which favor the better metal complexation, resulting in more biosorption [Hashem, 2007].

2.5 Analytical Characterization Techniques Used in Studies of Biosorption

In order to get on insight on mechanism of biosorption process, several characterization techniques have been used by researchers. Therefore metal-free control and metal-loaded biomass are used for analysis by numerous analytical techniques such as, field emission scanning electron microscopy coupled (FESEM) with energy dispersive X-ray spectroscopy (EDX), infrared spectroscopy or Fourier-transform infrared spectroscopy (IR or FTIR), thermo gravimetric analysis (TGA) Brunauer–Emmett–Teller (BET) and Barrett–Joyner–Halenda (BJH). In addition, metal ion concentration of solution is observed by UV–Vis spectrophotometer.

2.5.1 Field Emission Scanning Electron Microscope (FESEM)

FESEM is the abbreviation of Field Emission Scanning Electron Microscope. FESEM working principle is based on the fact that it works with electron instead of light. The specimen is examined by electron which is emitted by field emission source. FESEM images show the morphology of the biosorbent both before and after the bisorption process. The microstructure surface of adsorbent can be directly examined by FESEM [Bind et al., 2018; Park et al., 2010]. This could really help us to understand the surface of biosorbent after metal sequestration.

2.5.2 Energy Dispersive X-Ray Spectroscopy (EDX)

Energy dispersive X-ray spectroscopy is coupled with Field emission scanning electron microscopy. EDX is employed to get the element analysis of metal ions bound on the biosorbent surface after biosorption process which can be observed from the peak of corresponding individual metal ions on the biosorbent surface [Muñoz et al., 2015; Bind et al., 2018].

2.5.3 Fourier-Transform Infrared Spectroscopy (FTIR)

FTIR analysis are required to confirm and determine the functional groups of metal free control and metal loaded biomass which play significant role in sequestration of heavy metal to understand the role of various functional groups involved in bio sorption process. The change in vibration frequency of functional groups (C=O, carboxylate and hydroxylate anions etc.) upon interaction with metal ion are carried out by the FTIR spectroscopy which provide the deeper insight on metal binding on adsorbent [Nakkeerana and Selvarajua, 2017].

2.5.4 Brunauer–Emmett–Teller (BET) and Barrett–Joyner–Halenda (BJH)

Brunauer, Paul Hugh Emmett and Edward Teller proposed a theory to observe the surface area of a specimen which is commonly known as BET [Brunauer et al., 1938]. BET theory is associated with multilayer adsorption process and this is the extended work of Langmuir concept [Langmuir, 1918]. In BET theory, Langmuir assumptions are valid for each individual multilayer adsorption in equilibrium. The generalized linear form of BET equation for gas adsorption is expressed as follows:

$$\frac{1}{v\left[\left(\frac{P}{P_0}\right)-1\right]} = \frac{C-1}{v_m C}\left(\frac{P}{P_0}\right) + \frac{1}{v_m C} \qquad (2.1)$$

Where v and v_m represent the specific amount of gas and the adsorbed monolayer volume of gas respectively. P and P_0 are the equilibrium gas pressure and the saturation pressure respectively and c indicates the BET constant.

Monolayer adsorbed volume of gas (v_m) and BET constant (C) can be evaluated by using the intercept and slope of linear plot of equation (2.1) as follow:

$$C = slope/(intercept + 1) \quad (2.2)$$

$$v_m = 1/(slope + intercept) \quad (2.3)$$

The values of the surface area *S* (surface area per unit weight: unit $m^2\ g^{-1}$) can be observed by following equations (2.4):

$$S = \frac{v_m NA}{22{,}400\ x\ m} \quad (2.4)$$

Where *A* denotes the surface area of a single adsorbed gas molecule, *N* is Avogadro's number, *m* represents the mass of materials under observation and 22,400 indicates volume of one mole gas at the standard temperature and pressure (STP).

In order to determine the pore structure and the pore-size distribution of the raw material and metal loaded biomass, analytical techniques of Brunauer–Emmett–Teller (BET) and Barrett–Joyner–Halenda (BJH) are employed respectively [Xu et al., 2017].

2.5.4 Thermo Gravimetric Analysis (TGA)

Thermo gravimetric analysis (TGA) analysis provides the information about the change in weight loss with change in temperature. The decomposition of lignocellulosic matrix is categorized in different individual thermal degradation stages viz moisture evolution, hemicellulose, cellulose and lignin [Pakade et al., 2017]. The initial stage decomposition of biomass occur at about 100 ˚C which is attributed to moisture. According to Shinde and Singarvelu, (2014), the decomposition of lignonocellulosic matrix is given as follows: hemicellulose is degraded around 200 ºC to 350 ºC followed by cellulose around 305 ºC to 375 ºC and lignin around 250 ºC to 500 ºC

2.5.6 UV–Vis Spectrophotometer

UV–Vis spectrophotometer is employed to know the residual Cr(VI) concentration in aqueous solution. The quantification of the metal concentration in solution phase is carried out by using colorimetry process at 540 nm in acidic region which describe the purple color development after reaction complex of Cr(VI) with 1,5- diphenylcarbazide. However, purple colure does not developed for standard sample on complexation with 1,5 diphenylcarbazide which indicated the low concentration of Cr(VI). This method based on narrow range of metal concentration (0 to 0.8 mg L^{-1}) and it is very sensitive and fast method. Throughout the analysis, a light path of 1 cm cuvette made of Polymethyl methacrylate is used [Dong et al., 2011; Hachair and Hofmann, 2018].

2.6 Biosorption Process Studies in Batch and Column Mode

Frequently batch mode and continuous column processes are used by investigators for carrying out biosorption process. In fact, the selection of batch and columns process is depend on several parameters such as hydraulic flow, physical characteristics of the biosorbent(s), the types of target pollutant(s), space availability, and invested capital. Batch mode is used in biosorption process for optimization of several factors such as adsorbent dosage, contact time, pH of the medium, initial concentration of metal ions and agitation speed [Mahmood et al., 2017].

Batch mode investigation is used to optimize the operating parameters. Hence, continuous investigation is performed to know the practical application of prepared adsorbent at industrial scale. Column study makes the process more efficient to utilize the adsorbent capacity. Several investigators have reported the pollutant removal performance of biosorbents by using the up-flow packed bed which generally called as column reactor. Column reactor is more widely used due to more operation yield, simple, reproducible and

ease of scaling up procedure to industrial capacities. Packed bed is designed using batch experimental data and it is influenced by various parameters such as inlet flow rate, initial concentration and bed height. In addition, the effective application of column can be very well described by mathematical model and breakthrough curve [Bhaumik et al., 2013; Park et al., 2010].

2.7 Agricultural Waste Materials Used as Biosorbent for Removal of Cr(VI)

Activated carbon (AC) is considered as competitive and effective biosorbent for reduction of heavy metal form waste water at trace quantities. Owing to higher surface area, variable characteristics of surface chemistry, more porosity and high degree of surface activity, activated carbon appears to be more efficient biosorbent. However, the application of activated carbon for biosorption is not feasible due to high production cost [Panday et al., 1985; Dias et al., 2007]. Therefore several authors have done the investigation on development of low cost biosorbent from agricultural products and byproducts for removal of heavy metal from waste water [Dai et al., 2018]. Moreover, according to most of the researchers, low cost, availability, high regeneration capability, negligible release of sludge are the significant factor for selection of the better agriculture waste biosorbent [Nguyen et al., 2013]. The recent literature review based on several agriculture wastes as a biosorbent with or without treatment for removal of chromium is given below in detail.

Several researchers have performed adsorption work using agriculture waste in batch and continuous modes which are summarized below:

Kobya, (2004) studied the potential of activated carbon prepared from hazelnut shell to remove the Cr(VI) from waste water. Biosorption effect parameters like pH, initial Cr(VI) concentration and temperature were studied in batch system. Adsorption process was better

described by Langmuir isotherm and Pseudo-second-order model. Maximum adsorption capacity was 170 mg g^{-1} at pH 1.0 and 1000 mg L^{-1} of Cr (VI) solution. The thermodynamics result represented that adsorption was endothermic in nature.

Singh et al., (2005) studied the removal of hexavalent chromium from aqueous solution using novel biosorbent rice bran. The extent of adsorption was studied as a function of contact time, adsorbate concentration, pH of the medium and temperature. At lower pH 2.0, the rice bran sorbent showed maximum capability of removing Cr(VI) approximately 99.4% at initial concentration of 200 mg L^{-1} and at 20 °C temperature from aqueous synthetic solution. The pseudo-second-order and Langmuir isotherm models were fitted well with experimental data. The result of thermodynamics factors estimation reveals that adsorption was spontaneous and endothermic in nature.

Malkoc et al., (2006) studied the adsorption ability of waste pomace of olive oil factory (WPOOF) for adsorption of Cr(VI) from waste water in batch mode as well as in fixed bed column. The effect of several parameters like different flow rates and different inlet chromium (VI) concentrations were investigated in column studies. The maximum adsorption capacity and the longest breakthrough curve were observed in acidic range of solution at pH 2. Thermodynamics properties like standard enthalpy (ΔH°), free energy (ΔG°) and standard entropy (ΔS°) were studied to observe the feasibility of adsorption process. The results suggested that adsorption capacity was increased with decrease in flow rate and increase in initial Cr(VI) concentration. The experimental data obtained from inlet flow rate, initial concentration and bed height in continuous studies was analyzed by using Adams–Bohart model and the model parameters.

Dubey and Gopal, (2007) studied the adsorption of hexavalent chromium from contaminated water using two low cost adsorbents which were prepared by using groundnut husk. All the biosorption experiments were studied in batch process using with and without silver

impregnated groundnut husk. Biosorption of Cr(VI) was performed to test the several parameters such as adsorbent quantity, pH, contact time and agitation rate. The Freundlich model well described the adsorption process. The maximum adsorption capacity of chromium was calculated at pH 3 within 5 hours. Adsorption rate for chromium removal was high for chemically modified adsorbent than pure one. The results revealed that groundnut husk treated with silver exhibited better potential alternative biosorbent for chromium removal.

Garg et al., (2007) studied the potential of sugarcane bagasse, maize corn cob and jatropha oil cake biosorbents for removal of chromium by changing the various functions like pH, adsorbent dosage, and initial concentration of chromium (VI) in batch mode. Morphology and functional group of biosorbents were analyzed by SEM and FTIR measurements respectively. Biosorbents exhibited maximum adsorption capacity in acidic medium range at pH 2 with 250 rpm speed of orbital shaker and 60 minute contact time. Langmuir and Freundlich isotherm models were used to describe the adsorption process. The results revealed that the adsorption capacity performance was better for Jatropha oil cake than sugarcane bagasse and maize corn cob.

Nemr et al., (2007) studied the adsorption ability of Cr(VI) on pomegranate from waste water. Biosorption experiment was studied in batch system by varying several parameters like pH, sorbent concentration (2- 6 g L^{-1}), Cr (VI) concentration (25 and 50 mg L^{-1}), and contact time at room temperature. Langmuir isotherm model was employed to predict the maximum adsorption capacity of 10.59 mg g^{-1} at pH 1.0 of solution. The pseudo-second-order model better described the kinetics behavior of biosorption process.

Gao et al., (2008) studied the potential of adsorption capacity of rice straw to remove Cr (VI) from aqueous solution. The result suggested that the adsorption capacity was 3.15 mg g^{-1} at pH 2.0. The study showed that chromium removal rate was increased with increase in temperature and decrease in Cr(VI) concentration. In addition, Cr(VI) removal rate was

increased with decrease in straw size. Adsorption equilibrium was observed in about 48 hours at defined conditions. The result revealed that adsorption of chromium depends on protonation of biosorbent. It was further observed that the adsorption capacity of adsorbent by tartaric acid modified rice straw (TARS) and esterified rice straw (ERS) were more than pure form. Isotherm investigation showed that equilibrium sorption data were better followed by Langmuir model.

Gupta and Babu, (2009) studied the ability of activated tamarind seeds to remove the chromium (VI) from aqueous solutions. Tamarind seeds were treated with 98% w/w sulfuric acid followed by heating at 150 ˚C. Adsorption process was analyzed by various adsorption isotherms such as Langmuir, Freundlich, Redlich–Peterson, Koble–Corrigan, Tempkin and Dubinin–Radushkevich. Langmuir isotherm model was used to predict maximum adsorption capacity and it was 29.7 mg g^{-1} at the pH range of 1.12 to 1.46. Pseudo-second-order kinetics model was better fitted with experimental data with rate constant 2.605 x 10^{-3}, 0.818 x 10^{-3}, 0.557 x 10^{-3} and 0.811 x 10^{-3} g mg^{-1} min^{-1} for 50, 200, 300 and 400 mg L^{-1} of initial Cr(VI) concentration, respectively. Desorption studies showed that 95% of chromium was recovered from fresh activated tamarind seeds.

Marín et al., (2009) examined the potential of orange waste biomass for removal of Cr(VI) waste water. Biosorption experiment was conducted in batch and fixed bed columns to observe the adsorption capacity. Effect of several parameters like adsorbent dose, solution pH and particle size was studied. The percentage removal of Cr(VI) was high at higher adsorbent doses. Equilibrium of adsorption on orange waste was reached within 3 days. Adsorption capacity was increased from 0.57 mmol g^{-1} to 1.44 mmol g^{-1} as solution pH increased from 3 to 5 and it was observed by Sips model. The breakthrough curve was correctly described by BDST model for adsorption of Cr(VI). The sorption capacity was better in batch study than that in column adsorption process due to slow kinetics.

Jain et al., (2009) studied the ability of sunflower head (BSH) to remove the Cr(VI) from simulated waste water. Biosorption experiment was performed to examine the various optimum factors like contact time, pH of solution, adsorbent doses and initial metal concentration. Equilibrium of biosorption process was obtained within 120 minutes at optimized pH = 2.0. The percentage removal of Cr(VI) was decreased from 90.0 to 45.2 % as initial metal concentration increased from 10 to 70 mg L^{-1} and along with increase in adsorbent dose from 4.0 to 20.0 g L^{-1}. Experimental data was better explained by Langmuir isotherm as well as by pseudo-second-order kinetics model. The maximum adsorption capacity of adsorbent was 8.177 mg g^{-1}.

Baral et al., (2009) studied the potential of activated fresh water weed to remove the chromium from waste water in fixed bed column. They conducted experiments of biosorption by varying various parameters such as bed height and flow rate. The adsorption capacity was increased with decrease in bed height and flow rate of column. However with increase in initial metal concentration of solution, the adsorption capacity increases. Adsorption behavior and designing parameters of column was described by using several model like Adams–Bohart, Thomas and Yoon–Nelson and Bed Depth Service Time (BDST). In order to find out the best fit model, several statistical methods like Sum of the Square of the Error (SSE), Average Relative Error (ARE), Average Relative Standard Error (ARS), Sum of the Absolute Error (SAE), and regression coefficient were applied to investigate the prominent and unique characteristic features of the experiment.

Anandkumar and Mandal, (2009) studied the ability of activated carbon prepared from non-usable Bael fruit shell (BS) as a biosorbent to remove the Cr(VI) from waste water. The effect of various parameters like adsorbent dosage, agitation time, solute concentration and initial pH of solution were investigated in batch system. Maximum adsorption of chromium was 17.27 mg g^{-1} on Bael fruit shell within equilibrium time of 240 min and at optimum pH

2.0 of solution. The experimental data of adsorption process on Bale fruit shell fitted reasonably with both Langmuir as well as Freundlich model. Adsorption mechanism was well explained by Pseudo-second-order kinetics model. Before and after the adsorption, the adsorbent was characterized by various techniques like SEM, EDX and FTIR. Phosphoric acid treated adsorbent provided significant porosity on surface, which plays important role in adsorption of chromium. The adsorption result showed that the BSAC is an alternative and promising adsorbent for regulating the Cr(VI) in waste water.

Vinodhini and Das, (2010) evaluated the removal of Cr (VI) from water by Neem sawdust in a fixed bed column. This biosorption experiment was conducted by varying the several parameters like flow rate (5-15 ml min^{-1}) and bed depth (5-15 cm). Desorption study of adsorbent after biosorption was performed by using 2 N NaOH. Exhaustion time of breakthrough curve was decreased due to presence of co-ion solution. Biosorption process was performed in three cycles which represent approximately 3.75 L of tannery effluent was used in order to meet the regularity limit made by CPCB.

Venugopal and Mohanty, (2011) have investigated the biosorption potential of Parthenium (P. hysterophorus L.) to remove Cr(VI) from aqueous solution. An FTIR spectrum was used to record the functional groups like carboxyl, amine and alkane on biosorbent. The biosorption study was done by varying the parameters like biosorbent doses, contact time, pH, agitation speed, temperature and initial Cr(VI) concentration in batch system. The Langmuir and Freundlich isotherms model well describe the equilibrium data of biosorption. The maximum adsorption capacity was 24.5 mg g^{-1} and it was obtained at an optimum condition of pH 1.0, 200 rpm, 160 min equilibrium time, 0.1 g biomass dose and 20 $^{\circ}$C. The result of thermodynamic parameters represented that biosorption process was exothermic and spontaneous for 20 $^{\circ}$C to 60 $^{\circ}$C temperature range. The experimental data of kinetics of Cr(VI) biosorption was fitted well with the pseudo-second-order kinetics model.

Chen et al., (2012) performed the biosorption experiments in continuous fixed-bed column to examine the potential of modified corn stalk (MCS) as adsorbent to remove the Cr(VI) from aqueous solution. The biosorption process in column mode was tested by changing the several parameters like influent solution pH (2.66, 4.91 and 5.66), flow rate (5, 10 and 15 $mlmin^{-1}$), influent Cr(VI) concentrations (100, 200 and 300 mg L^{-1}) and bed depths (1.4, 2.2 and 2.9 cm). The decrease in flow rate and initial concentration with an increase in bed depth implies that the exhaustion time was increased. Adsorption process in fixed bed column was described by using Adams–Bohart, Thomas and Yoon–Nelson models. Thomas and Yoon–Nelson models fitted better with experimental data. Fixed bed column study indicates that MCS exhibited better alternative biosorbent for biosorption of Cr(VI).

Altun and Pehlivan, (2012) studied the potential of citric acid treated Walnut shell as a adsorbent to remove the Cr(VI) from waste water. The modification of walnut shell adsorbent was performed by using several factor like citric acid level (5-10 g), reaction time (0-24 h), and temperature (110-130 ˚C). Effect of adsorption studies were conducted under several variable conditions such as initial Cr(VI) concentration (0.1-1.0 mg L^{-1}), pH (2-9), contact time (10-240 min), adsorbent dose (0.02 - 0.20 g) and temperature. The maximum adsorption capacity was observed in acidic range (from pH 2 to pH 3) of solution. The equilibrium adsorption data was examined by several isotherms like the Langmuir, Freundlich and D–R isotherms. The Langmuir isotherm fitted well with experimental data compared to that of other models. The maximum adsorption capacity was 0.596 and 0.154 mmol g^{-1} for CA-WNS and untreated adsorbent respectively. Thermodynamics parameters result reveled that biosorption process was endothermic and spontaneous in nature. Chemically modified adsorbent CA-WNS showed good efficient and alternative adsorbent in removing the chromium from waste water.

Owalude et al., (2016) studied the uptake of Cr (VI) by modified and unmodified groundnut hull. Various parameters such as contact time, solution pH, temperature and adsorbate concentration that affect biosorption process were investigated. Scanning Electron Microscope (SEM) and Fourier Transform Infra-Red (FTIR) spectroscopy were used to analyze the morphology and presence of functional groups on biosorbents. Langmuir and the pseudo-second-order models showed better correlation with experimental data. The result revealed that adsorption capacity was better for modified groundnut hull than unmodified groundnut hull adsorbent.

Fawzy et al., (2016) studied the potential of date-palm-leaves (DPL) and broad-bean-shoots as biosorbent for the uptake of chromium from aqueous solution. FTIR, SEM, and EDAX analysis were taken to observe the complex nature of biosorbent. Langmuir and Freundlich isotherm reasonably fitted with experimental data. Adsorption kinetics is better explained by pseudo-second–order model. The maximum removal of Cr(VI) for DPL (98%) and BBS (95%) was obtained at several optimized parameters such as 100 mg L^{-1} of Cr(VI), 5 g L^{-1} biosorbent-dosages, 60 min contact-time and at pH 2 and 1 respectively.

Rai et al., (2016) studied the ability of H_3PO_4 treated mango fruit waste for removal of Cr(VI) from waste water. Activated carbon was prepared by treating with 40% H_3PO_4 followed by heating for 1 hour at 600 K in inert atmosphere. Morphology, surface area and functional groups of biosorbents were investigated by SEM, BET and FTIR techniques respectively. Several parameters like solution pH, Cr(VI) concentration, rate of agitation, solute dose, contact time and temperature were investigated in batch system. The Langmuir isotherm model was used to predict the maximum adsorption capacity and it was 7.8 mg g^{-1} at pH 2. Pseudo-second-order kinetics model described the mechanism of adsorption process better compared to other kinetics models.

Chwastowsk et al., (2017) studied the ability of Canadian Peat and coconut fiber for removal of chromium (VI) from waste water. Biosorbent was characterized by using various techniques like FTIR, SEM, EDX and BET. The maximum biosorption efficiency was 94% and 91% for coconut fiber and Canadian peat respectively. Several isotherm models like Freundlich, Temkin and Langmuir were used to describe the adsorption process. The kinetics of adsorption process was examined by various models like pseudo first-order, pseudo-second order and Webber-Morris kinetics. Several eluents were used to regenerate the adsorbent after adsorption. Approximately 53–65% of chromium ion elution was obtained. Regeneration results showed that the organic materials can be effectively reused for adsorption process. The obtained results indicated that the Canadian peat and coconut fiber can be employed as alternative biosorbent to remove the Cr(VI) from waste water.

Enniya et al., (2018) studied the potential of activated carbon prepared form apple peels (ACAP) to remove the Cr(VI) from waste water. The surface morphology and several functional groups were analyzed by SEM and FTIR respectively. Biosorption experiments were performed by changing several parameters like pH (2-7), initial Cr(VI) concentration (10–50 g L^{-1}mg L^{-1}) and temperature (10–40 ˚C) and adsorbent dose (0.025–0.15 g/50 mL). The maximum adsorption capacity was 36.01 mg g^{-1} at several optimum parameters like 50 mg L^{-1} Cr(VI) concentration, 0.05 g/50 mL adsorbent doses, 28 °C temperature and pH 2 of solution. Freundlich isotherm mode and pseudo-second-order kinetics models were fitted satisfactorily with experimental data. The thermodynamics results indicated that biosorption process was endothermic and spontaneous in nature.

Banerjee et al., (2018) studied the potential of walnut shell to remove the Cr(VI) from aqueous solution in column mode. Adsorbent was characterized by using several analytical analyzers such as FTIR, SEM and BET. Biosorption experiment was conducted at various optimized condition like low influent Cr(VI) concentration, low influent flow rate, and higher

bed depth. Adsorption behavior was investigated by using several kinetics models. Regeneration of adsorbent was performed by using several concentrations of NaOH to find the reusability characteristics of walnut shell.

Various biosorbents summarized in Table 2.1 are used in the treatment of Cr(VI).

Table 2.1: Summary of some agricultural materials as adsorbents used for removal of Cr (VI) ions from aqueous solution

Adsorbent	Solution pH	Maximum adsorption capacity (mg g^{-1})	References
Mango kernel activated carbon (MKAC)	2.0	7.8	Rai et al., (2016)
Rice husk carbon	2.0	47.62	Khan et al., (2016)
Hazelnut shell	2.0	17.7	Cimino et al., (2000)
Oat	2.0.	10.92	Torresdey et al., (2000)
Chrysophyllumalbidum (Sapotaceae) seed shells	3.0	84.31	Amuda et al., (2008)
Treated waste newspaper	3.0	59.88	Dehghani et al., (2016)
Ficusglomerata (Gular)	2	46.73	Rao and Rehman, (2010)
Modified walnut shells	2.0 and 3.0	7.98	Altun and Pehlivan, (2012)
Chemically modified Swieteniamahagoni Shells (SSMS , PSMS, RSMS)	2	47.61, 58.82 and 37.03	Rangabhashiyam and Selvaraju, (2015b)
Coconut coir	2	26.8	Gonzalez et al., (2008)
Rice husk carbon (RHC) and saw dust carbon (SDC)	2	48.31 and 53.48	Bansal et al., (2009)
Chemically Syzygiumjambolanum nut	2	39.81	Muthukumaran and Beulah, (2010)
Neem sawdust	2	58.82	Vinodhini and Das, (2010)

Table 2.1: *(Continued)*

Adsorbent	Solution pH	Maximum adsorption capacity (mg g^{-1})	References
Melaleuca diosmifolia leaf	2	62.5	Kuppusamy et al., (2016)
Tobacco-leaf	1	113.2	Chen et al., (2009)
Mangrove leaf powder	2.0	60.24	Sathish et al., (2015)
Boiled sunflower head	2	7.9	Jain et al., (2009)
Peanut shell (P. Shell),	2	4.32, 3.66 and 4.48	Ahmad et al., (2017)
Activated carbon derived from wood apple shell using H_2SO_4	1.8	151.51	Doke and Khan, (2012)
Prepared activated carbon from fox nutshell using $ZnCl_2$	2.0	43.45	Kumar and Jena, (2017)
Sugarcane bagasse	2.0	13.40	Sharma and Forster, (1994)
Fox nutshell by chemical activation with H_3PO_4	2.0	74.95	Kumar and Jena, (2017)
Adsorption abilities of the chestnut shell and prepared carbon with H_3PO_4	2.0	4.44 and 33	Niazi et al., (2018)
Bio-composite of mango (MKBC)	3	320.07	Akram et al., (2017)
HCl acid-activated banana peel (AABP) and organo montmorillonite	4	15.1 and 6.67	Ashraf et al., (2017)

2.8 Gap in Existing Research

Based on literature review, it is well understood that disposal of heavy metal in waste water from several industries activities is a growing concern for environment because they are highly soluble in aquatic environment. Heavy metal causes severe health hazardous, if they are consumed beyond the permission limit [Nguyen et al., 2013; Barakat, 2011]. Therefore, several researchers proposed adsorption technique, which is the most effective and versatile technique, for the removal of chromium toxic metal from waste water [Burakov et al., 2018]. However, economical treatment of heavy metal containing waste water is regarded as major criteria. Based on literature, it is noted that most of the reported low cost adsorbent showed the lower capacity of adsorbent for Cr(VI) removal. In addition, limited studies have been reported regarding biosorption studies in continuous column. Most of the adsorption studies reported about batch system using low cost adsorbents for purification of waste water. Besides, the desorption process of adsorbent make the adsorption process more economical. However, the recycling of the adsorbent after regeneration of metal loaded adsorbent was not addressed by many. Thus, the biosorption process still requires investigation of extensively available, effective agricultural waste as biosorbent and further modification of adsorbent for practical application.

2.9 Scope and Objectives

The main aim of the present study is to prepare a low cost adsorbent from the naturally available agriculture waste material which can be utilized as a adsorbent for the removal of Cr(VI) from synthetic solution. For this, the adsorption properties of the biosorbents, Water Caltrop Shell (*Trapa Natans*) and Dtura (*Datura Stramonium) fruit* are to be investigated with and without chemical modification so as to employ them for controlling the extent of Cr(VI) in waste water.

In order to meet the above goal, the following objectives are to be carried out

- To evaluate the optimum operation parameters such as pH, equilibrium time, initial metal ion concentration, particle size, temperature, biosorbent dose, shaking speed and biosorbent concentration in batch mode experiment and to determine the maximum uptake capacity of biosorbents
- To characterize the several properties of biosorbent before and after biosorption like surface morphology, functional groups and elemental mapping, specific surface area using FESEM, FTIR, EDX, TGA and BET analyzer respectively
- To describe the adsorption process of each adsorbents by using some commonly used adsorption isotherms and kinetic models through linear and non-linear modeling
- To evaluate the thermodynamic parameters of each biosorbent, in order to ascertain the feasibility of biosorption process
- To investigate the ability of the biosorbent in fixed bed column studies and to ascertain the optimum parameters like column bed height, flow rate and biosorbent quantity
- To investigate the desorption properties of biosorbent in order to find the reusability of biosorbent

MATERIALS AND METHODS

Chapter-3
Materials and Methods

3.1 Reagents and Preparation of Stock Solution

In this research, all the chemicals used in the experimental process were of analytical grade and these were purchased from Hi-Media and Merck. In this study, a stock solution (1000 mg L^{-1}) (shown in Fig. 3.1) of Cr(VI) was obtained by dissolving 2.82 g of potassium dichromate ($K_2Cr_2O_7$) in 1000 mL of distilled water. A appropriate dilution factor with distilled water was used to make desired concentration of Cr(VI) solution. Cr(VI) solutions pH were tuned by using 0.1 M NaOH and 0.1 M HCl.

Fig. 3.1: Photograph of 1000 PPM Cr(VI) stock solution

3.2 Adsorbent Preparation

Water caltrop (*Trapa Natans*) shell and Datura *(Datura Stramonium)* fruit were used for the preparation of raw and chemical activated carbon adsorbents.

3.2.1 Preparation of Raw Biosorbents

Water caltrop shell *(Trapa Natans*) and Datura *(Datura Stramonium)* fruit (shown in Fig. 3.2) were collected from local area in Guwahati, Assam (India) and this biomass are easily available as an agriculture material. The biomass was washed properly using distilled water and subsequently dried in oven at 48 °C for 48 hour. The resulting materials were crushed using mixer grinder and followed by sieving to get the desired adsorbent size and subsequently it stored in air tight container for further experiments as needed.

3.2.2 Chemical Treatment of Biosorbent

Some portions of grounded biomass (Water caltrop (*Trapa Natans*) shell and Datura (*Datura Stramonium*) fruit) were subjected to chemical treatment in order to improve the biosorption capacity of biosorbent. Activated carbon from these biosorbents was prepared by using two chemicals such as H_2SO_4 and H_3PO_4 (shown in Fig. 3.3).

Fig. 3.2: Schematic diagram of biosorbent preparation

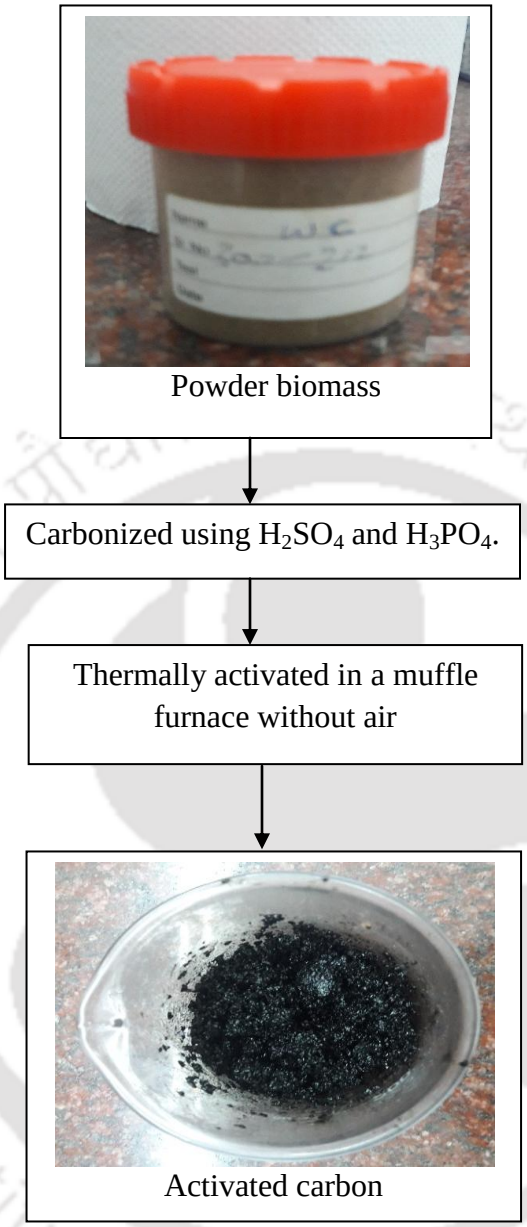

Fig. 3.3: Schematic diagram of activated carbon derived from biomass

3.2.2.1 Sulphuric Treatment

Sulphuric acid treatment of biomass powder was performed by following methodology: The biomass power was mixed with 98% Sulfuric acid in the ratio of 1:2 w/v (biomass: acid) and kept in muffle furnace at 150 °C for 24 hour in order to get the carbonized form of biosorbents. The obtained carbonized materials were subjected to washing with distilled water and then soaked in 1% sodium bicarbonate solution overnight in order to remove the acid. The resulting carbonized materials were further washed with distilled water and kept in oven at 105 °C for 24 hour. The resulting adsorbents are represented as sulphuric treated activated carbon [Rangabhashiyam and Selvaraju, 2015b; Nakkeeran and Selvaraju, 2017].

3.2.2.2 Phosphoric Treatment

Phosphoric acid treatment was carried out by dissolving the given biomass in 88% ortho-phosphoric acid solution in the ratio of 1:2.5 w/v (biomass: acid). And then residual is dried at 110 °C for 2–3 hour. The dried samples were kept in muffle furnace at 400 °C for 1.5 hour in order to convert the biomass into the carbonized form. The obtained carbonized materials were soaked in 1% sodium bicarbonate solution to remove the residual acid left on the adsorbents. Subsequently, the resulting carbonized materials were washed thoroughly with distilled water and then these were dried in oven at 105 °C for 24 hour. The resulting adsorbents are indicated as phosphoric treated activated carbon [Rangabhashiyam and Selvaraju, 2015b; Nakkeeran and Selvaraju, 2017]

.

3.3 Determination of Point of Zero Charge (pH_{pzc})

The point of zero charge is defined as the pH point at which the adsorbent surface possesses zero electrical charge density i.e. it describes the condition that the positive charges on the adsorbent surface equal to the negative charges. The information about the pH_{pzc} of adsorbent surface allows hypothesizing the interaction of metal ion in solution with ionized functional group on the adsorbent surface. When the solution pH is lower than the pH_{pzc} value, the surface becomes protonated while at pH value more than pH_{pzc}, the surface becomes negatively charged.

The determination of PZC of biomass was performed as follows: A 40 ml of 0.1 M KNO_3 solution of different pH values from 1 to 12 were made and the initial pH value is designated as pH_0. 0.1 g of biosorbent was dissolved in 0.1 M KNO_3 solution and after that it kept in orbital shaker at 120 rpm for 24 hour. The final solution pH (pH_f) was measured by using digital pH-meter (make: Sartorious and model: AG,PB 11, Bengaluru, Karnataka, India). The difference between pH_0 and pH_f was plotted against pH_0. The pH_{PZC} was referred as intersection point of difference in pH (pH_0 - pH_f) curve with initial pH axis [Rangabhashiyam and Selvaraju, 2015a].

3.4 Characterization of Adsorbent

The biosorbent characterization is carried out to investigate the several characteristic of prepared adsorbent using various technologies. The elemental composition in weight percent and surface morphology were carried out with EDS (Make: Zeiss, Model: Sigma, Germany) and FESEM (Make: Zeiss, Model: Sigma, Jena, Germany)) systems respectively. In order to observe the morphology and elemental composition with FESEM and EDS, powdered adsorbent must be

conductive in nature. This is carried out by coating a conductive layer with a thin layer (1.5 – 3.0 nm) of gold. After that, the adsorbent was mounted on a special holder like steel stab.

CHNS (Eurovector EA3000) technology was performed to get the information about the composition of biomass. The results obtained as follows: WC shell contains *N* = 3.09%, *C* = 46.14%, *H* = 6.69%, and *S* = 0 % and DS fruit contains *N* = 1.91 %, *C* = 44.66 %, *H* = 5.92 %, and *S* = 0% (The percentage is expressed in weight %). FTIR (Fourier Transform infrared) spectroscopy (Model: IRAffinity-1; Make: M/s Shimadzu, Chiyoda-ku, Tokyo, Japan) was performed in the range of 4000 to 500 cm^{-1} to study the functional groups present on the adsorbent surface and in this analysis, the sample was mixed with dried KBr (weight ratio of 1:20, sample to KBr). The surface area of adsorbent is another important factor which was observed by using Brunauer-Emmet-Teller (BET) surface analyser (Model: Tristar II; Make: M/s Micromeritics, Norcross, GA, USA) through nitrogen adsorption technique at 77.15 K. Prior to analysis, the prepared adsorbent was made to degas at 120 ˚C overnight under high vacuum. The thermal stability of the prepared adsorbent was characterized by Thermo-Gravimetric analysis (TGA) (Make: Netzsch, Model: STA449F3A00 Jupiter, Wittelsbacherstr 42, and 95100 Selb, Germany). The experiment was performed under Nitrogen atmosphere at a given flow rate and degradation temperature of adsorbent was observed from room temperature to 600 °C with a heating rate of 10 °C min^{-1}.

3.5 Adsorption Mode

3.5.1 Batch Experiment

Equilibrium experiments were performed to study the influence of several parameters such as temperature, contact time, adsorbent dosage, agitation speed and pH for removal of Cr(VI) ions from waste water in batch mode (shown in Fig. 3.4). Batch experiments were carried out by adding required amount of adsorbent in 50 ml working solution at desired contact time, temperature and pH of solution. The several Cr(VI) concentration solutions were prepared from stock solution using distilled water. 0.1 mol L^{-1} NaOH and 0.1 mol L^{-1} HCl was used to adjust the pH of solution using pH meter instrument (Make: Sartorious, Model: AG,PB 11, Bengaluru, Karnataka, India) was used to measure the pH of solution. The equilibrium time of experiments was measured by taking out the sample at regular intervals of time from orbital shaker. After reaching the equilibrium, the aqueous phase solutions were filtered through whatman 42 filter paper. The filtrate solution was used to measure the amount of Cr(VI) by using UV-Vis spectrophotometer (Make: Gene Quant, Model: 1300, GE, Holliston, MA, USA) at 540 nm. The measuring of Cr(VI) amount in solution are based on complex formation of Cr(VI) with 1,5-diphenylcarbazide in acidic medium. The adsorption capacity and removal percentage of Cr(VI) were determined according to the following equations:

$$q = \frac{(C_0 - C_e)\,V}{m} \tag{3.1}$$

$$\%\ \text{Rempoval of Cr(VI)} = \left(\frac{C_0 - C_e}{m}\right) X\ 100 \tag{3.2}$$

Where q represents the adsorption capacity (mg g^{-1}), C_0 and C_e denotes the initial and equilibrium concentration of Cr(VI) (mg L^{-1}) in solution, m is the weight of adsorbent and V is the volume of Cr(VI) solution (L).

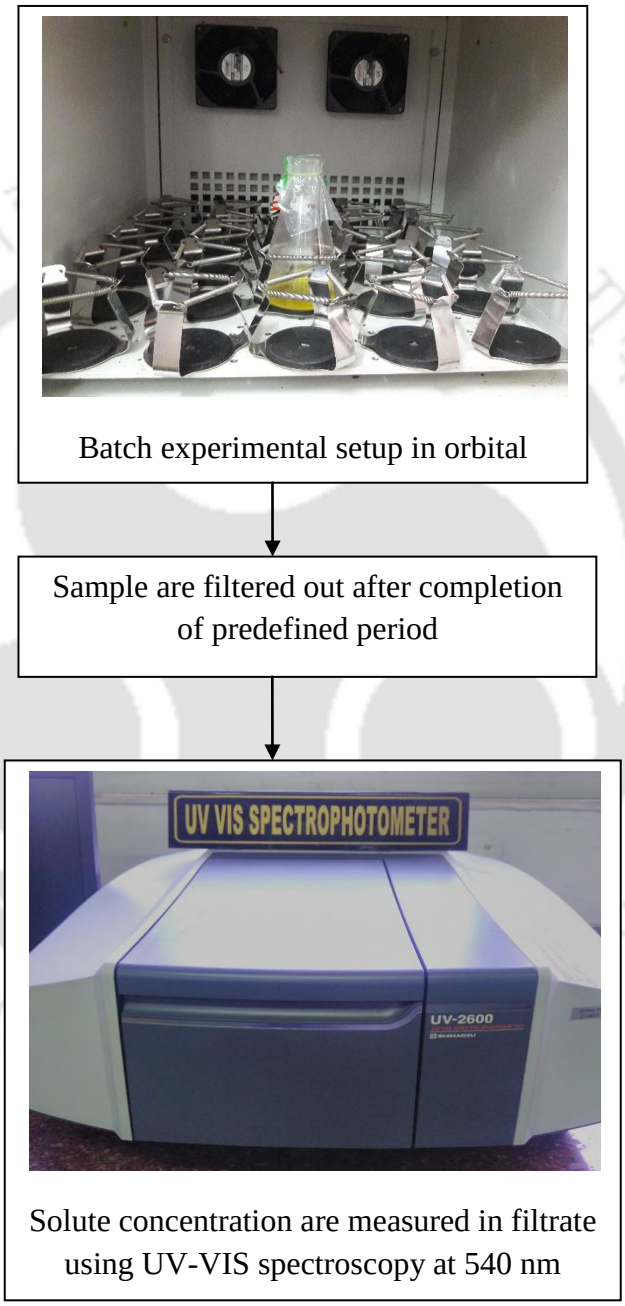

Fig. 3.4: Schematic diagram of batch experiment adsorption process setup

3.5.2 Column Experiments

Column operation allows one to get more practical relevance of adsorbent in pilot scale water treatment. The column study was performed in lab scale design column as shown in Fig. 3.5 Fixed bed column is employed with 2 cm inner diameter and 15 cm height. The fixed bed column is packed with desired amount of adsorbent to produce the required bed height in between the glass wool. In order to provide the uniform distribution of solution, the glass beads are used on the top and bottom section of glass wool in column. The desired Cr(VI) concentration solution was allowed to pass through the column in an up flow direction at a required bed height and flow rate. The flow rate was controlled by a peristaltic pump. The effluent was collected from the exit of column at predetermined time interval. Continuous experiment was performed at optimum pH 2 which was determined from batch experiments. In the column study, the effect of various parameters such as bed height, inlet flow rate and inlet metal ion concentration were carried out to understand the removal of Cr(VI) in continuous mode. 1, 5 diphenyl-carbazide was mixed to the Cr(VI) solution to produce the Cr(VI) complex which was used to determine the Cr(VI) concentration in solution by UV-Vis Spectrophotometer at 540 nm.

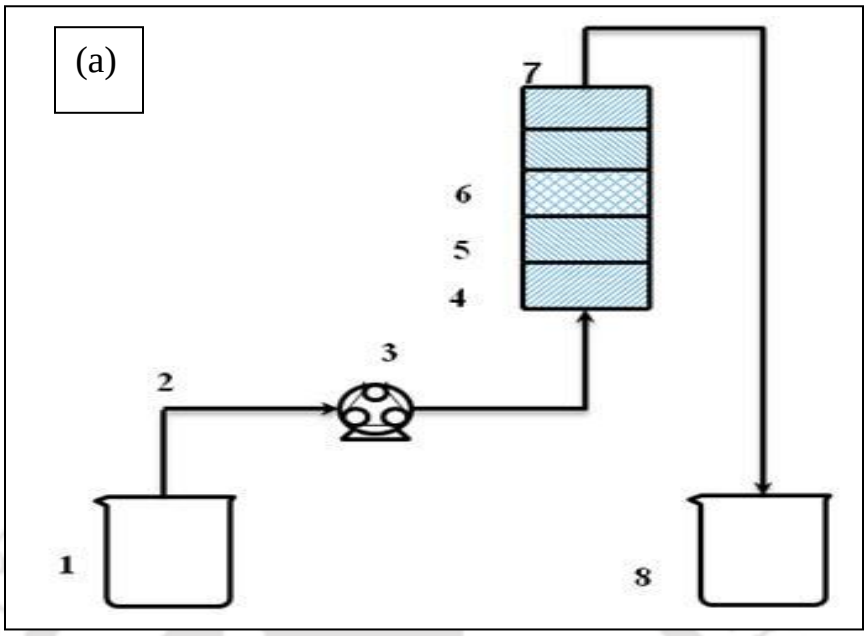

1. Synthetic solution of Cr(VI), 2. Silicon tube, 3. Peristaltic pump, 4. Glass beads, 5. Glass wool, 6. Adsorbents bed (Activated carbon), 7. Column, 8. Effluents

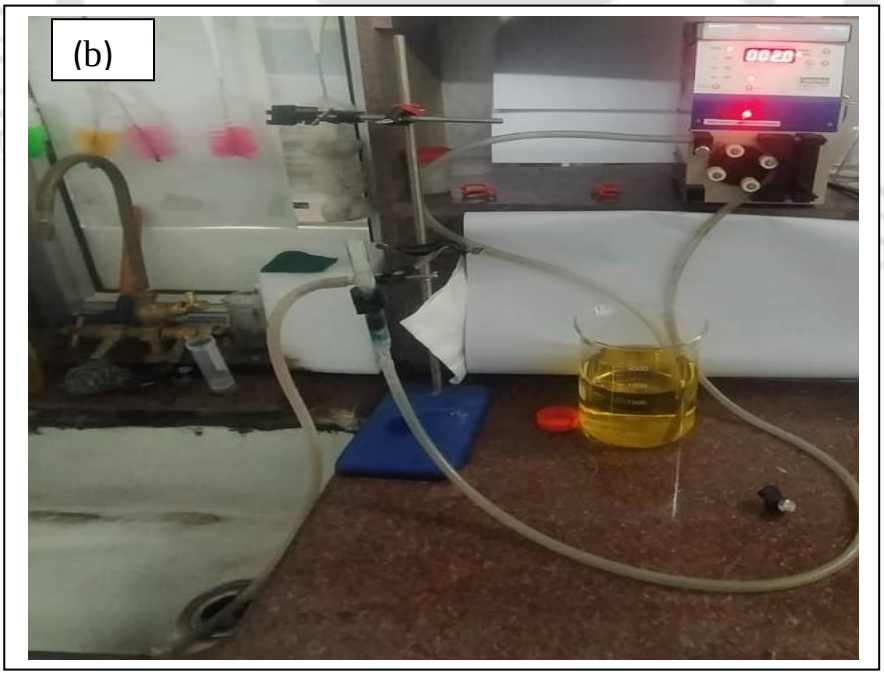

Fig. 3.5: (a) Schematic diagram and (b) photograph depicts the fixed bed column for continuous adsorption process

3.5.2.1 Column Performance Analysis

The performance of fixed bed column is predicted by breakthrough curve. The typical shape of breakthrough curve shown in Fig. 3.6 which depicts the column utilization at given condition [Afroze et al., 2016]. The shape of curve and appearance of breakthrough time are important characteristics to determine the operation and dynamic response of fixed bed column. Breakthrough time is the time at which adsorbed species are detected in the column effluent (approximately when solute concentration in effluent reaches C_t = 0.05 to 0.1 % C_0). Breakthrough point provide the knowledge about the maximum allowable solute concentration ($C_t = C_b$) for industrial practice application (lab scale treated synthetic solution shown in Fig. 3.7). The column is operated until the concentration of effluent became 95% of initial concentration and this point is known as column exhaustion point.

The breakthrough curves can be obtained by plotting the ratio of concentration (C_t/C_0) against time (t) or treated volume. Where C_t and C_0 are the outlet and inlet Cr(VI) concentration (mg L^{-1}) of column .

The maximum adsorbed quantity of metal ion in column for a desired inlet concentration can be obtained by following equations:

$$q_{total} = \frac{Q\,A}{1000} = \frac{Q}{1000}\int_{t_0}^{t_{total}} C_{ad}\,dt = \frac{Q}{1000}\int_{t_0}^{t_{tota\,l}} (C_0 - C_t)\,dt \qquad (3.3)$$

Where A is the area above the breakthrough curve, C_{ad} is adsorbed metal ion concentration, Q is volumetric flow rate and t_{total} is the total time flow.

Equilibrium adsorption capacity can be observed by following expression:

$$q_{e(\exp)} = \frac{q_{total}}{M} \quad (3.4)$$

Where, M is the total mass of biosorbent inside the column, $q_{e(exp)}$ is the experimental adsorption capacity (mg g^{-1}) and q_{total} is capacity of the column capacity in (mg). The total Cr(VI) introduced into the column can be calculated by the following equations:

$$m_{total} = \frac{C_0 Q t_{total}}{1000} \quad (3.5)$$

Where m_{total} is amount of Cr(VI) passed into the column. Percentage removal of Cr(VI) ions can be estimated by using the following equation.

$$Y\ (\%) = \frac{q_{total}}{m_{total}}\ X\ 100 \quad (3.6)$$

The total volume passed through the column, V_{eff} (mL), can be observed by the following equations:

$$V_{eff} = Q t_{total} \quad (3.7)$$

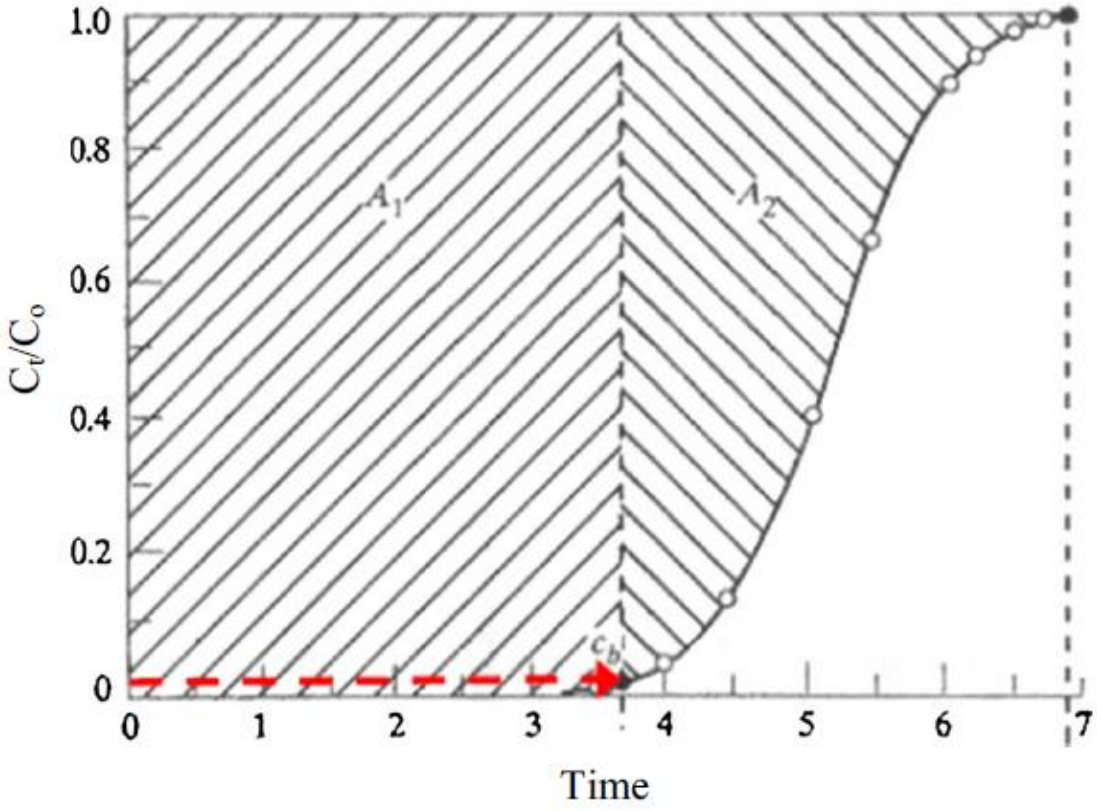

Fig. 3.6: Typical breakthrough curve (Afroze et al., 2016)

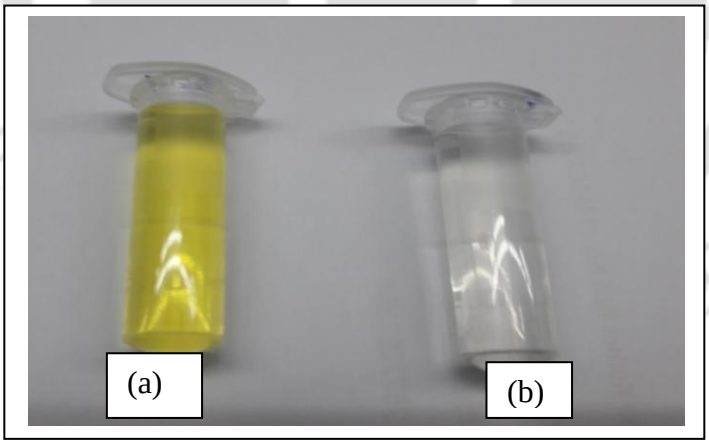

Fig. 3.7: (a) Photograph of untreated sample and (b) treated effluent at breakthrough point

3.5.2.2 Mathematical Modeling of Column Data

The modeling of biosorption breakthrough curve is required to understand the design parameters as well as to predict the breakthrough curve behavior and performance of fixed bed column. Experimental data obtained from the column are fitted to the several models such as Adams-Bohart model, Thomas model, Yoon-Nelson model and Bed Depth Service Time model. In addition, these studies are used to analyze the breakthrough curve observed at various condition such as inlet influent Cr(VI) concentrations, biosorbent bed heights, and influent flow rates which can be applied to scale-up purpose.

3.5.2.2.1 Thomas Model

Thomas model is most widely used in describing the behavior of breakthrough curve in column bed. This model predicts the maximum adsorption capacity of adsorbent as well as yield of column. This model assumes, the inner and external diffusion are absent in the process of adsorption [Thomas, 1944]. The linear form of Thomas model equation is stated as:

$$\ln\left(\frac{C_0}{C_t} - 1\right) = \frac{K_{TH}\, q_0\, W}{Q} - K_{TH}\, C_0 t \qquad (3.8)$$

Where K_{Th} (ml (mg. Min)$^{-1}$) is represented as the rate constant; W (mg) indicates the weight of adsorbent; C_o (mg L^{-1}) is the inlet concentration of Cr(VI) and C_t (mg L^{-1}) is the outlet concentration at the time interval t min. The q_0 (mg g^{-1}) and Q (mL min^{-1}) represent the adsorption capacity and flow rate respectively. The linear plot of $\ln(C_0 / C_t - 1)$ vs. t allows us to calculate the different parameters of Thomas model at a given flow rate condition.

3.5.2.2.2 Yoon – Nelson Model

Yoon-Nelson model is an established simple model and this model assumes that probability of adsorption rate for each adsorbate molecule decreases is proportional to likelihood of adsorption of adsorbate and the probability of unabsorbed molecule mean adsorbate breakthrough mean [Yoon and Nelson, 1984]. The linearized form expression of this model is given by:

$$\ln\left(\frac{C_t}{C_0 - C_t}\right) = K_{YN}\, t - K_{YN}\, \tau \qquad (3.9)$$

Where K_{YN} (min^{-1}) is the rate constant, τ (min) indicates the time needed to achieve 50 % of adsorbate breakthrough, and t represents the time. The plot between ln (C_t/ (C_0-C_t)) and t gives a straight line which are used to get the slope K_{YN} and intercept (τ) of this model.

3.5.2.2.3 Adams-Bohart Model

The Adams-Bohart model relies on the theory of surface reaction and it assumes that equilibrium is not instantaneous. Therefore, the rate of sorption is directly related to residual capacity of the adsorbent and concentration of adsorbate. This model is extensively used to describe the initial part of breakthrough curve [Bohart and Admas, 1920]. This model obeys the following expression:

$$\ln\left(\frac{C_t}{C_0}\right) = K_{AB}\, C_0\, t - K_{AB}\, N_{AB}\left(\frac{Z}{u}\right) \qquad (3.10)$$

Where K_{AB} denotes the kinetic constant ($L(mg,min)^{-1}$), N_{AB} represents the saturation concentration in mg L^{-1}, u (cm min^{-1}) represents the linear flow rate which is observed by

dividing the flow rate by the column section area , Z is the bed depth of column, C_0 is the initial concentration and C_t is the effluent concentration at time t. Characteristic parameters of this model can be observed from the linear plot of ln(Ct/Co) as a function of t at given condition.

3.5.2.2.4 Bed Depth Service Time (BDST) Model

The BDST model is most widely implied to explain the bed capacity in column studies at given condition. Initially this model was suggested by Bohart and Adams, however latter it was modified by Hutchins. It is simple model based on some assumption such as adsorption rate is controlled by surface reaction between the residual capacity of the adsorbent and adsorbate. Moreover, this model ignores the external film resistance as well as internal mass transfer resistance i.e. the adsorption is exposed on the surface of adsorbent [Hutchins, 1973]. This model is used to describe the linear relationship between the bed height and service time. It is expressed by given below equation:

$$t = \left(\frac{N_0 Z}{C_0\, u}\right) - \left(\frac{1}{C_0 K_a}\right) \ln\left(\frac{C_0}{C_b} - 1\right) \qquad (3.11)$$

Where t represents the service time (min), N_0 represents adsorption capacity (mg L^{-1}), Z represents the bed height of column (cm), K_a represents the adsorption rate constant (L (mg. min)$^{-1}$), C_0 and C_b represents the inlet metal concentration (mg L^{-1}) and breakthrough effluent concentration (mgL^{-1}) respectively, u is the linear flow velocity of solution feed (cm min^{-1}). A plot of service time at breakthrough against time t yield a straight line which are used to calculate the K_a and N_0 parameters value of BDST model [Simate and Ndlovu, 2015].

The results obtained from batch and continuous studies are discussed in next chapter.

RESULTS AND DISCUSSION

CHAPTER - 4

Chapter- 4

Removal of Cr(VI) from Synthetic Solutions Using Water Caltrop Shell (*Trapa Natans*) as a Low-Cost Biosorbents

4. Results and Discussion

In the present study, the adsorption potential of Water caltrop shell is tested in batch mode. The results observed from batch adsorption experiments and characterizations of adsorbents before and after adsorption are described in the following section.

4.1 Characterization of Biosorbent

The FESEM image of unused biosorbent indicates that the biosorbent surface is highly irregular, porous, and rough in nature as shown in Fig. 4.1(a). After chromium biosorption, the surface and pores are covered with Cr(VI) as shown in Fig. 4.1(b). The PZC (pH $_{PZC}$), which was estimated from the plot of Δ pH vs. pH_0 (Refer Fig. 4.2), was found to be 6.2 for WC shell. It reveals that the surface of biosorbent was positive below pH 6.2 and negative above pH 6.2. The results obtained from EDX analysis are presented in Fig. 4.3(a-b). It is clear that the useful groups such as O–H and –COOH are present on the biosorbent as evident by the presence of C and O peaks. The appearance of Chromium peaks in EDX spectrum of biosorbent after biosorption confirms the chromium biosorption. Fig. 4.4 shows the FT-IR spectrum of WC shell in the range of 500–4000 cm^{-1} both before and after biosorption. The appearance of several peaks in FT-IR spectrum were attributed to the presence of various functional groups (carbonyl, carboxyl, hydroxyl, amide, etc.) on WC shell as summarized in Table 4.1 [Srivastava et al., 2006]. These functional

groups are mainly responsible for binding the Cr(VI) ions from the aqueous solution on to the surface of WC shell. The significant change in the peak position was observed for some of the functional groups (such as carboxyl, hydroxyl, amide, etc.) owing to its highly active participation in biosorption process. Also, the small yet significant changes in FT-IR spectra peak after biosorption confirm the binding of metal with functional groups as reported by other researchers [Wojciechowska, 1999; Ilyas et al., 2013]. In addition, after biosorption, the absorption peaks around 912.46 and 1039.90 indicated the existences of Cr=O, Cr–O stretching which confirm the Cr(VI) attachment on functional groups of biosorbents surface. The BET surface area of biosorbent of particle size 0.150 mm was found as 464.937 m^2 g^{-1} and the BET isotherm is shown in Fig. 4.5. The WC shell showed wider pore size distribution such as 1.7-2.0 nm and 3.8-4 nm which signified microporous and mesoporous, respectively. Fig. 4.6 showed the TGA results of biosorbents both before and after biosorption to determine the change in weight with change in temperature. The results showed that the weight loss of WC biosorbent divided into three stages in the interval of 28-600 °C. The first-stage weight loss below 200 °C represents loss of moisture and volatile compound. The second- and third-stage weight loss between 200-350 °C and 350-600 °C were attributed to loss of cellulose and lignin, respectively. As from Fig. 4.6, it is observed that the weight loss of biosorbent sample after biosorption was less in comparison to biosorbent sample before biosorption which indicated the Cr(VI) binding on biosorbent [Liu et al., 2017].

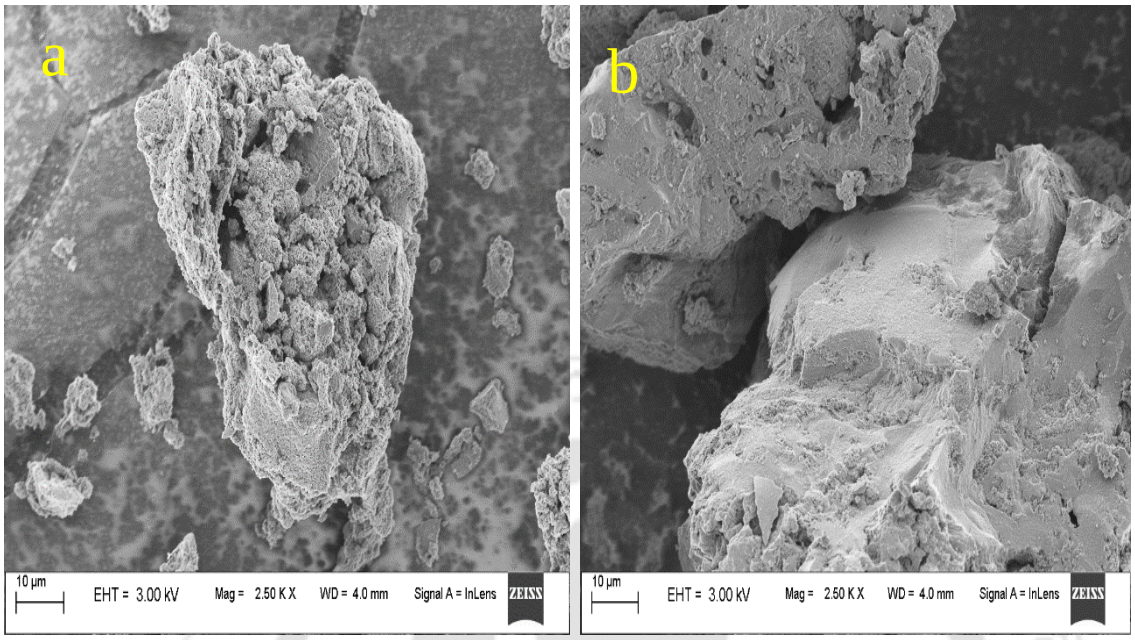

Fig. 4.1: FESEM micrograph images of WC shell (a) before Cr(VI) biosorption and (b) after Cr(VI) biosorption

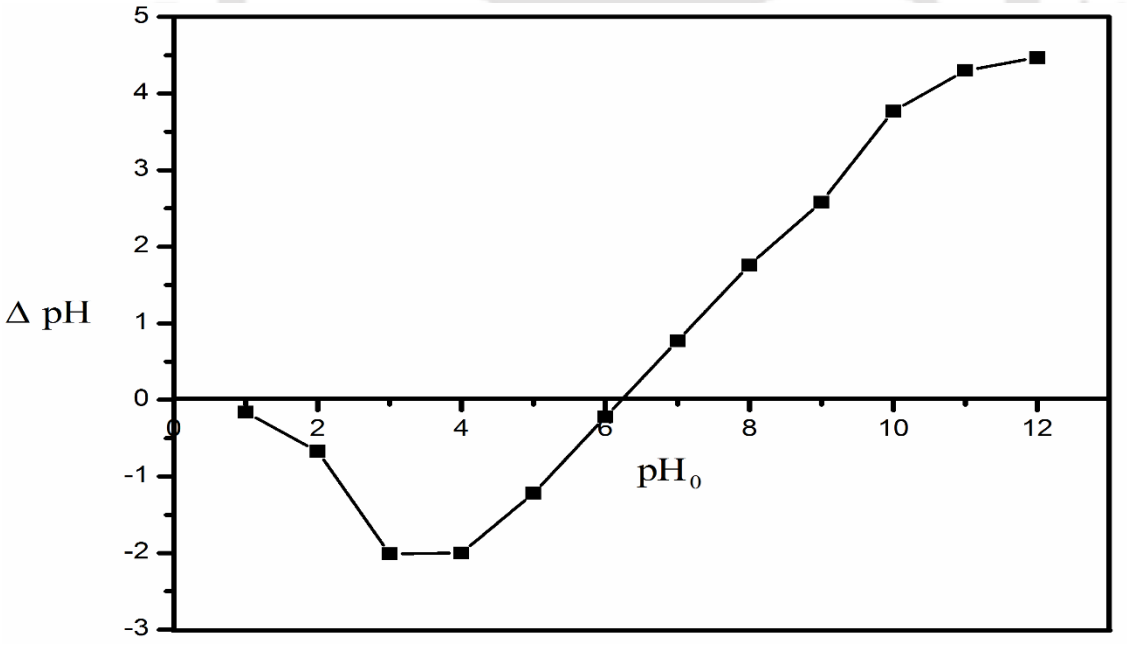

Fig. 4.2: PZC of WC shell surface, ΔpH (pH_0 - pH_f) vs. pH_0

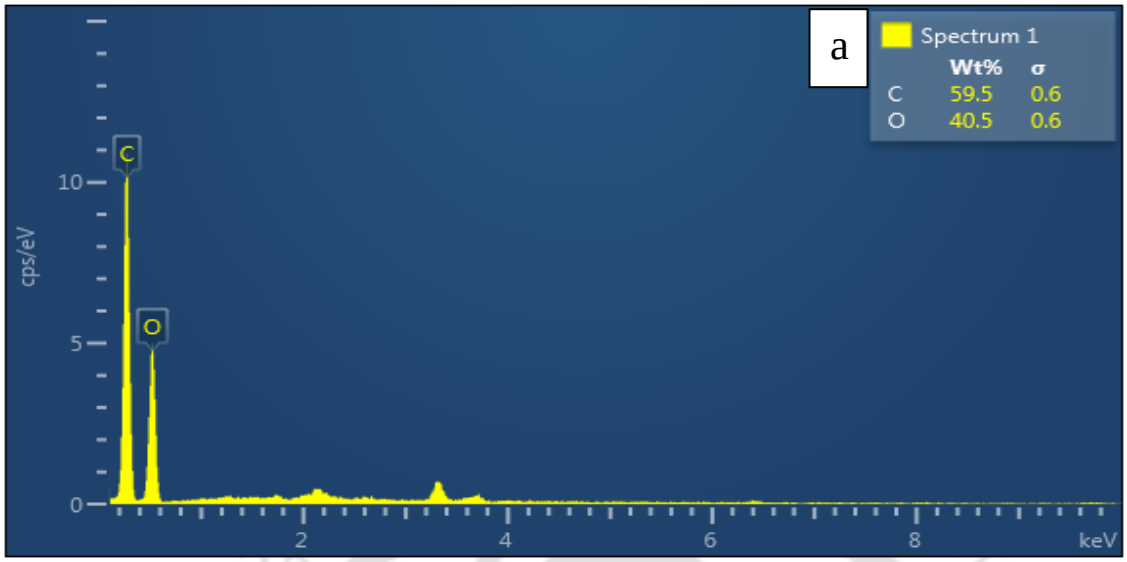

Fig. 4.3: (a) EDX images of WC shell before Cr(VI) Biosorption

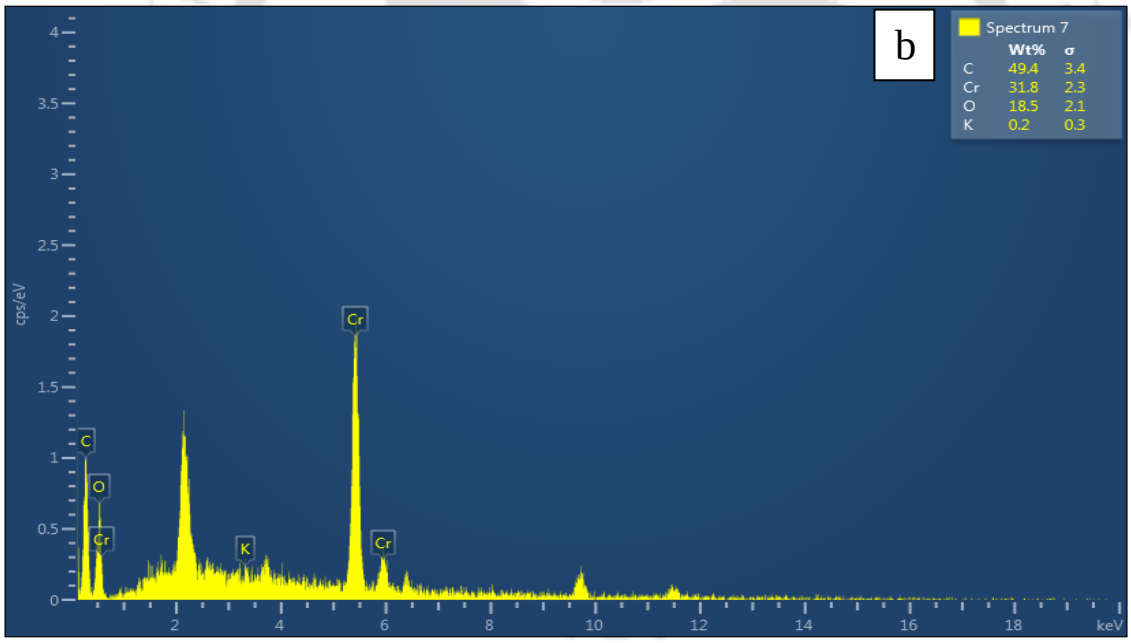

Fig. 4.3: (b) EDX images of WC shell after Cr(VI) loaded

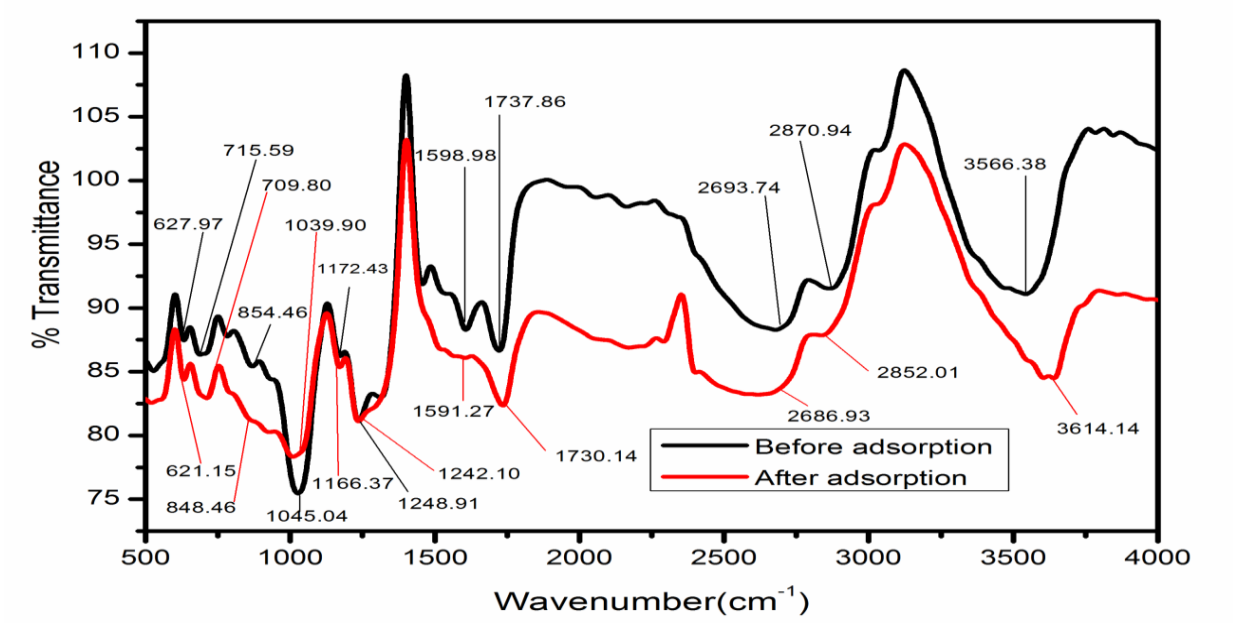

Fig. 4.4: FTIR spectra of WC shell (a) before biosorption and (b) after biosorption

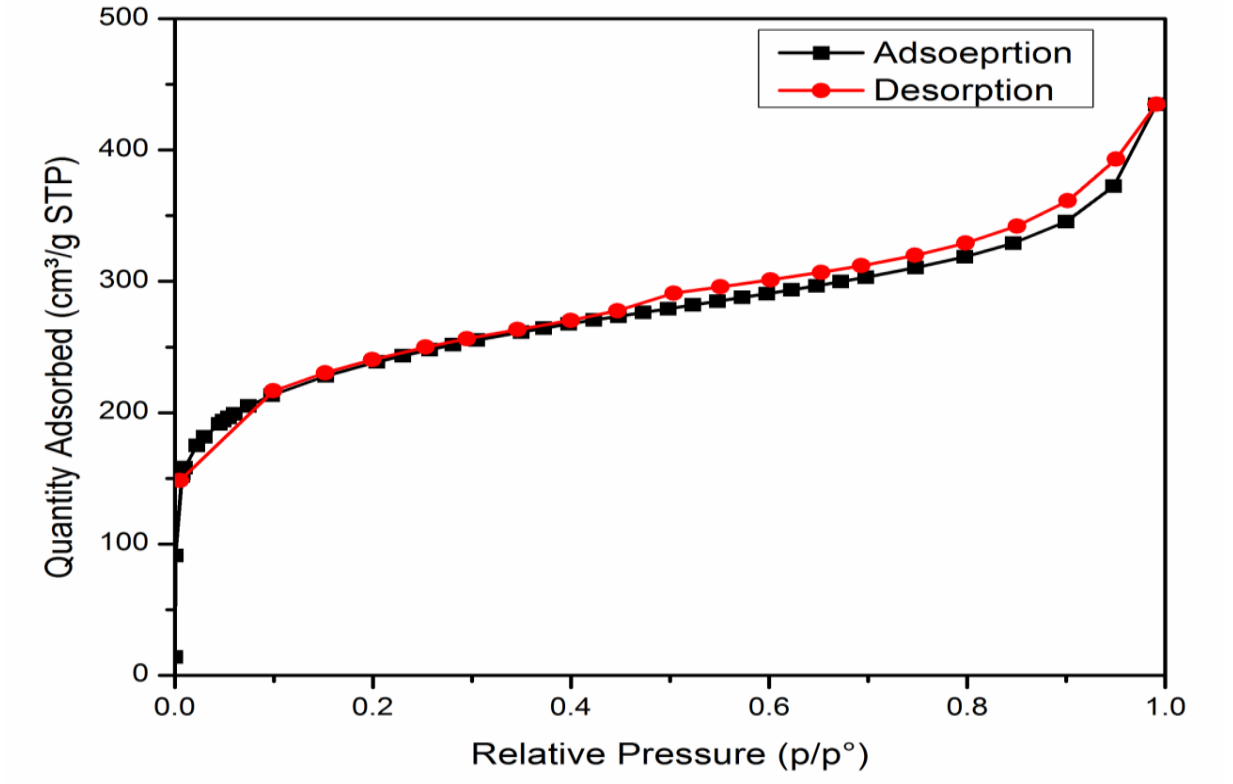

Fig. 4.5: N_2 adsorption and desorption BET isotherm of WC shell

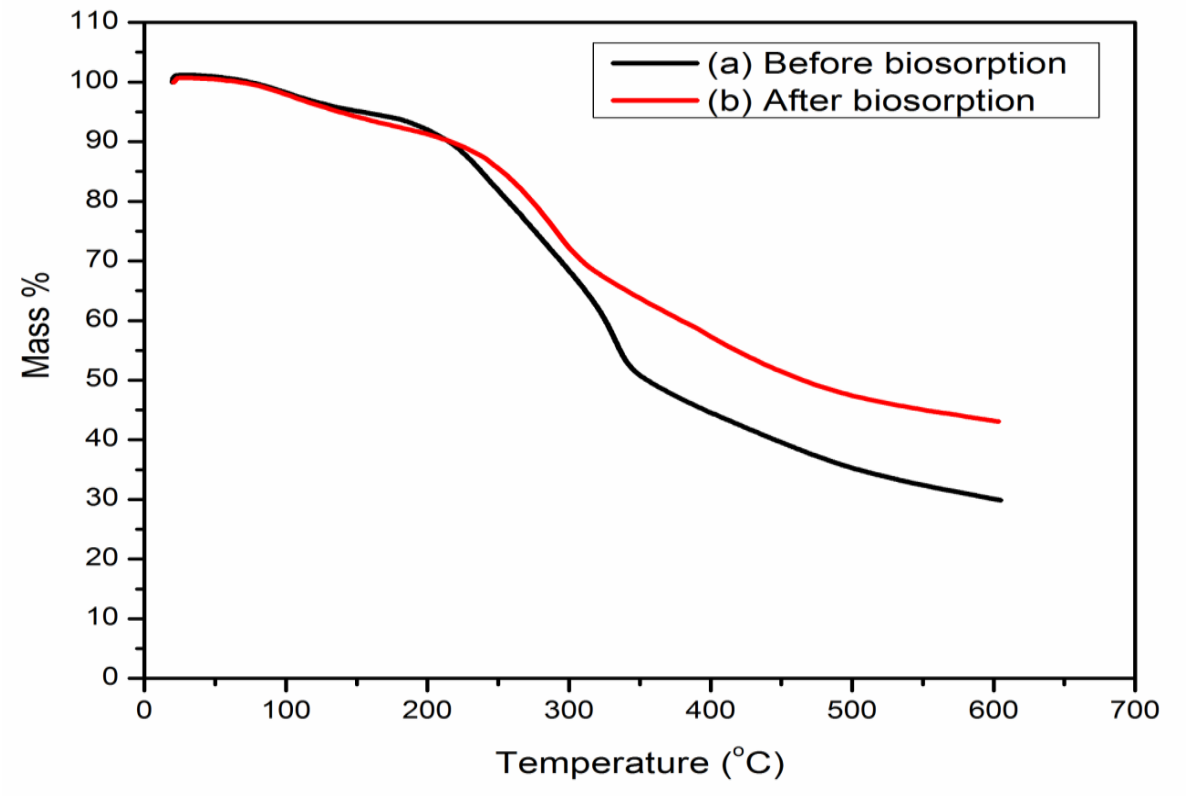

Fig. 4.6: TGA results of biosorbent WC shell before (a) and after (b) biosorption of Cr(VI)

Table 4.1: Functional groups analysis of WC shell before and after Cr(VI) biosorption by FT-IR measurements

Functional groups	Wave number (cm^{-1})	
	Before biosorption	**After biosorption**
–C≡C–H , C–H bond , alkynes	715.59	709.80
alkyl halides, after biosorption Cr=O stretching mode,	854.46	912.46
C–O stretch , alcohols, carboxylic acids, esters, ethers , after biosorption Cr-O stretching	1045.97	1039.90
($–CH_2X$) , alkyl halides	1172.43	1166.37
C–N stretch , aliphatic amines	1242.10	1248.91
C–C stretch (in–ring) , aromatics	1591.27	1598.98
C=O stretch, esters, saturated aliphatic	1737.86	1730.14
C–H stretch, alkanes	2693.74	2686.93
C–H stretch, aromatics	2870.94	2852.01
O–H stretch, free hydroxyl , alcohols, phenols	3566.38	3614.14

4.3 Studies of Batch Biosorption

Biosorption studies were employed to investigate the impact of various parameters such as pH (2-11), agitation speed (20-180), temperature (303-333 K), and biosorbent doses (0.2-5 g L^{-1}) on the biosorption of Cr(VI) from aqueous solution onto the WC shell. Experiments were conducted in batch mode using 250 mL stopper conical flasks containing 50 mL of test solution. To equilibrate the system, flask was shaken for 60 min at 28°C in thermostatic orbital shaker at 100 rpm to provide sufficient time for metal ions to get adsorbed onto the biosorbent. Then, the content of flask was filtered using 41 Whatman paper. The filtrate was analyzed by UV-visible spectrophotometer for determining the Cr(VI) concentration using 1, 5-diphenylcarbazide in acid medium. 1, 5-diphenylcarbazide forms a purple color complex selectively with Cr(VI) which is identified by peak at 540 nm. All the studies were conducted at 303 K unless otherwise mentioned.

4.3.1 Influence of pH on Biosorption

To observe the influence of pH on the removal of Cr(VI) from aqueous solution, a series of adsorption experiments were conducted by varying the pH value of Cr(VI) aqueous solution (2-11) at room temperature and keeping other parameters constant (1 g L^{-1} biosorbent dose, 60 min equilibration time and 100 rpm agitation speed). The contact time was also varied from 20 -100 min for each pH value and the results obtained are shown in Fig. 4.7.

It is clearly seen from this figure that the maximum biosorption capacity of 50 mg g^{-1} was observed at pH 2 and the value decreases with further increase in pH value. The similar trend was reported in the literature for various other biosorbents [Hasan et al., 2008; Rangabhashiyam and Selvaraju, 2015b]. This result can be described by several phenomenon's as follows:

Generally the Cr(VI) exists in different forms ions such as chromate (CrO_4^{2-}), dichromate ($Cr_2O_7^{2-}$) and bichromates ($HCrO_4^-$) depending on pH value of the solution and is negatively charged at all pH values. At lower pH values of the solution, $HCrO_4^-$ complex ion is predominated while at higher pH values of the solution, $Cr_2O_7^{2-}$ and CrO_4^{2-} complex ions are predominated on biosorbent surface. Further, the biomass surface become negatively charged in basic medium values (> 6.2) and positively charged in acidic medium values due to deprotonation and protonation respectively. It is obvious from Fig. 4.7 that biosorption capacity decreases with increase in pH values of the solution, which is attributed to the increased electrostatic repulsion force among CrO_4^{2-}, $Cr_2O_7^{2-}$ and OH^- ions on depronated biosorbent surface. In addition it can be speculated that in basic medium OH^- ions is available in abundant amount on the biosorbent surface due to it's less size. Therefore OH^- ions hinder the diffusion of CrO_4^{2-} and $Cr_2O_7^{2-}$ ions and subsequently it resulted in less biosorption of Cr(VI) at higher pH values. Biosorption capacity was increased with decrease in pH value of the solution and it was maximum at pH 2 of Cr(VI) solution as shown in Fig. 4.7. The enhanced biosorption was mainly due to the driving force of electrostatic attraction between negatively charged chromate ion and positively charged biosorbent surface. In addition, the phenomenon of high biosorption capacity of Cr(VI) at low pH was attributed to the release and exchange of H^+ ion from functional group such as carboxyl groups, $-NH_2$ groups onto the biosorbents surface. It can be revealed that numerous proton is required to promote the rate of reaction, as per the following reduction reactions of Cr(VI) ions.

$$H_2CrO_4 \leftrightarrow H^+ + HCrO^-_4 \quad (4.1)$$

$$HCrO_4^- \leftrightarrow CrO_4^{2-} + H^+ \quad (4.2)$$

$$2HCrO_4^- \leftrightarrow Cr_2O_7^{2-} + H_2O \quad (4.3)$$

Therefore from this result, pH 2 was chosen for further batch experiments [Fawzy et al., 2016; Jobby et al., 2018].

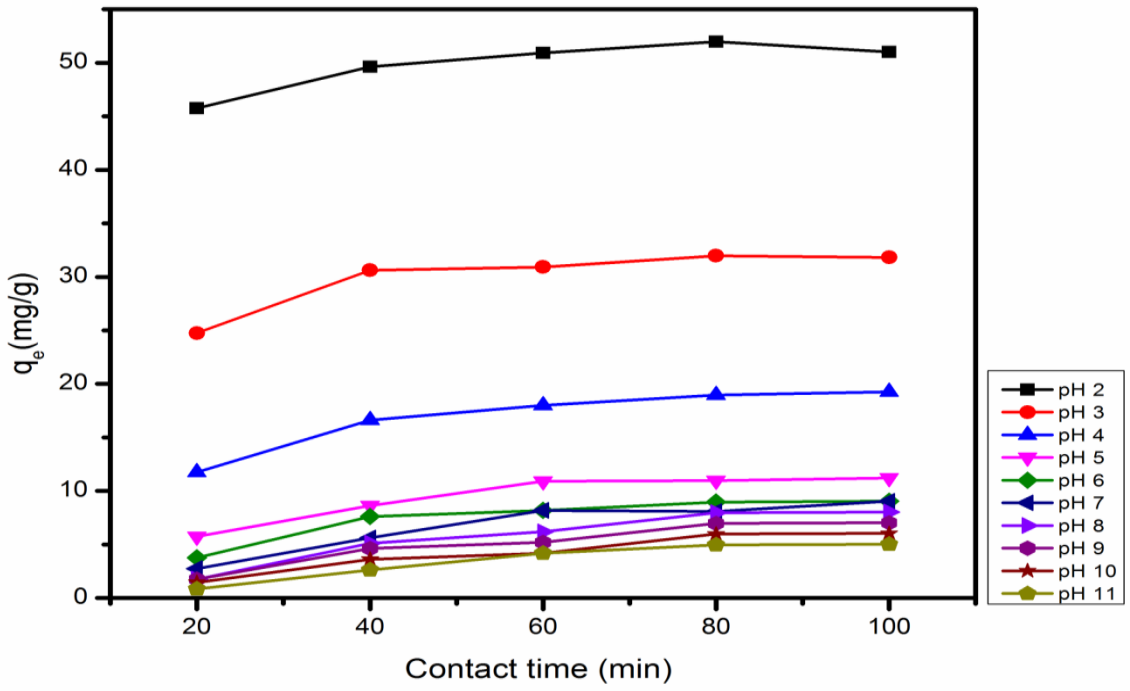

Fig. 4.7: Plot of biosorption capacity of WC shell versus contact time at different pH

4.3.2 Influence of Water Caltrop Size and Dosage

Fig. 4.8 shows the effect of biosorbent size (< 0.150 mm, 0.300 -0.400 mm, > 0.600 mm>) on biosorption capacity investigated at pH 2, 60 min equilibration time and 1g L^{-1} biosorbent dose. As expected, the biosorption capacity decreases from 49.40 to 38.07 mg g^{-1} with increase in particle size of biosorbent. As biosorption is a surface phenomenon, the more surface area is available at lower particle size for the Cr(VI) to bind at the active sites of biosorbent [Saranya et al., 2017]. Thus, further experiments were carried out with < 0.150 mm particle size of biosorbent. The influence of biosorbent dosages on Cr(VI) ion biosorption capacity was also

examined by changing the dosage from 0.2 to 5 g L^{-1} of biosorbent at initial metal ion concentration of 100 ppm, pH 2.0 and agitation speed of 100 rpm. The results are plotted in Fig. 4.9 which shows that increase in biosorbent dosage increases the percentage of biosorption of Cr(VI) removal from 11.88 to 99.8 while decreases the biosorption capacity from 59.4 to 17.2 mg g^{-1}. Increase in biosorbent dosage would normally result in increase of number of active sites which subsequently increases the % Cr(VI) removal. Similar observation was reported for Cr(VI) removal using rose waste as biosorbent [Iftikhar et al., 2009].

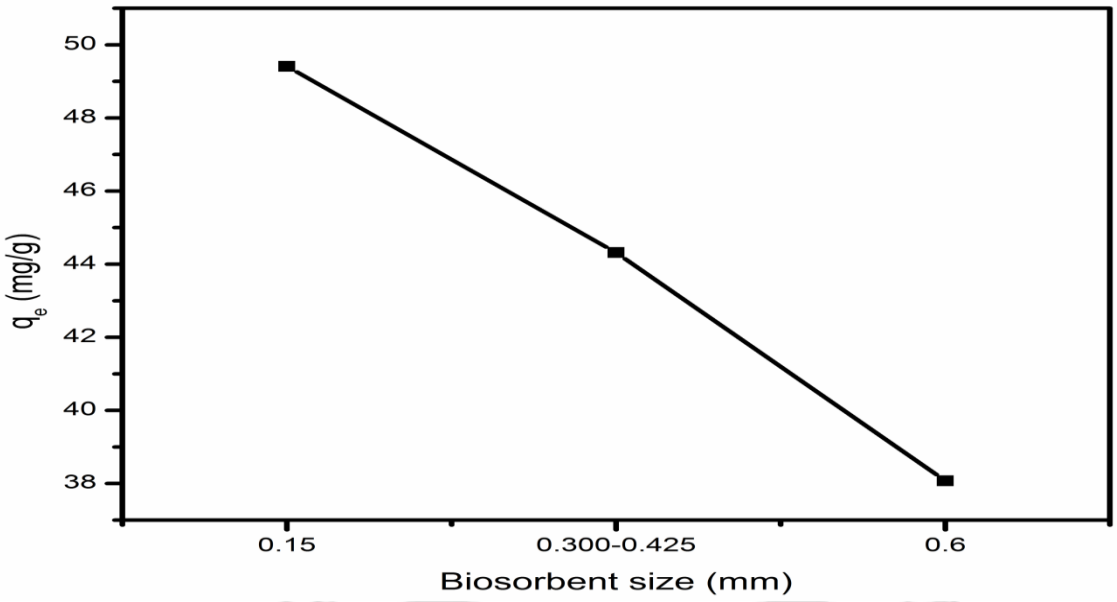

Fig. 4.8: Plot of biosorption capacity of WC shell for Cr(VI) versus the different size of the WC shell

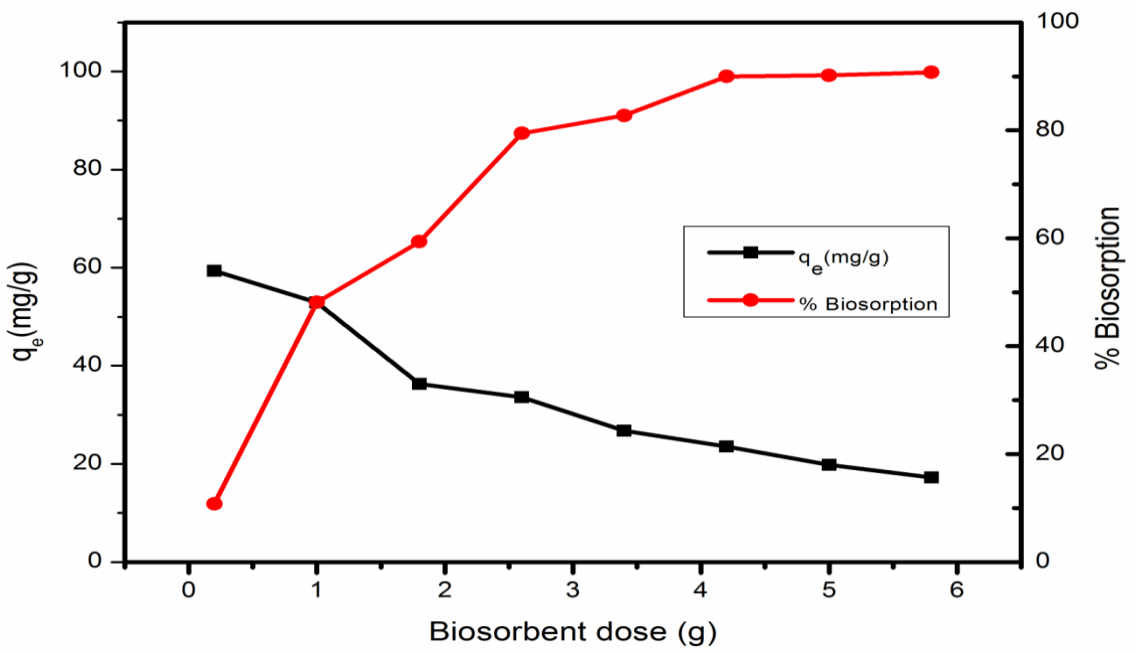

Fig. 4.9: Plot of biosorption capacity and percentage biosorption of Cr(VI) In biosorbent dosages

4.3.3 Influence of Agitation Speed, Initial Cr(VI) Concentration and Contact Time

The impact of agitation speed was studied by varying the agitation speed from 20 to 180 rpm at optimum pH 2.0, 1 g L^{-1} biosorbent dosage and initial metal ion concentration of 100 ppm. The biosorption capacity shows maxima (45.04 mg g^{-1}) at the agitation speed of 100 rpm as shown in Fig. 4.10. This is attributed to the fact that the increase in agitation speed increases the exposure of active sites to the metal ions via increasing the metal ions diffusion rate for sequestration and hence, increases the uptake capacity. However, increasing agitation speed beyond certain value would provide less contact time for the metal ions to bind to the biosorbent surface and as a consequence, the uptake capacity decreases [Rangabhashiyam and Selvaraju, 2015b].

Both the initial metal ion concentration in aqueous solution and batch time also play a significant role in determining the biosorption capacity. Hence, the influence of initial Cr(VI) ion concentration (100, 200, 300, 400 and 500 mg L^{-1}) and contact time (20 - 180 minute) were studied at 1.0 g L^{-1} biosorbent dosage, pH 2.0 and 100 rpm agitation speed. The observed results are depicted in Fig. 4.11 which reveals that the biosorption capacity was increases with increases contact time and then attains the steady state value after 60 minutes. Also, the steady state value is strongly influenced by the initial metal ion concentration as evident from Fig. 4.9. Higher the initial metal ion concentration (500 ppm), higher the steady state value attained (88.65 mg g^{-1}). The increase in biosorption capacity with initial metal ion concentration is likely due to its increased number of collisions with biosorbent active sites [Tewari et al., 2005; Tsamo et al., 2018].

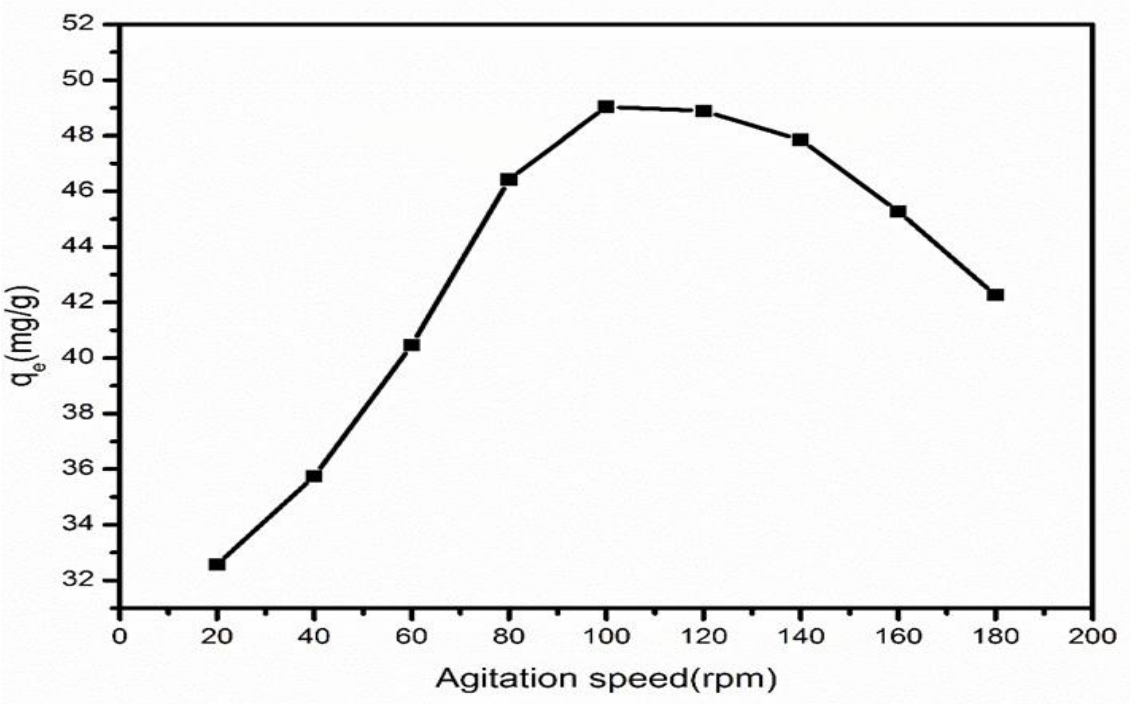

Fig. 4.10: Influence of agitation rate in biosorption capacity of WC shell

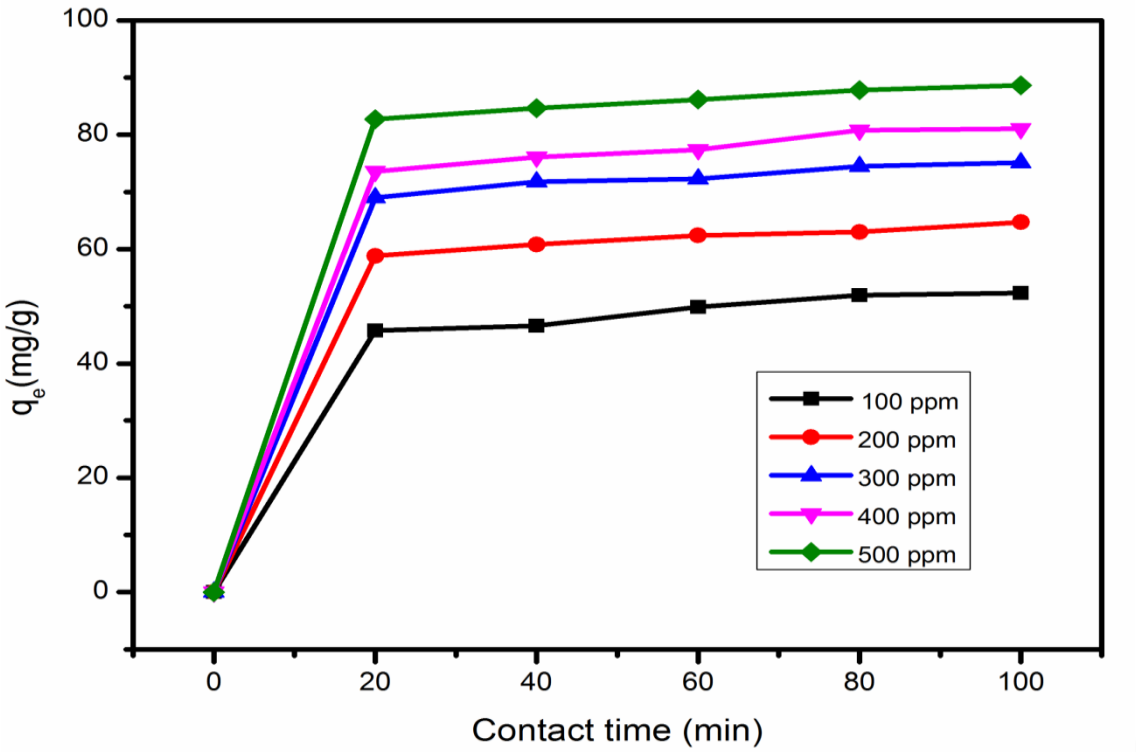

Fig. 4.11: Biosorption capacity and contact time for various initial Cr(VI) concentration

4.3.4 Influence of Temperature

The influence of temperature (303 K, 313 K, 323 K and 333 K) for different solution concentrations (100, 200, 300, 400 and 500 mg L^{-1}) was investigated at pH 2.0, 1 g L^{-1} biosorbent dose and 100 rpm agitation speed. The increase in temperature results in increase of biosorption capacity as shown in Fig. 4.12. This is likely due to the increase in mobility of the Cr(VI) ions towards biosorbent at higher temperature. In addition, the activation of surface and increase of biosorbent pore size at high temperature also favor the increase of biosorption capacity [Nakkeeran and Selvaraju, 2017].

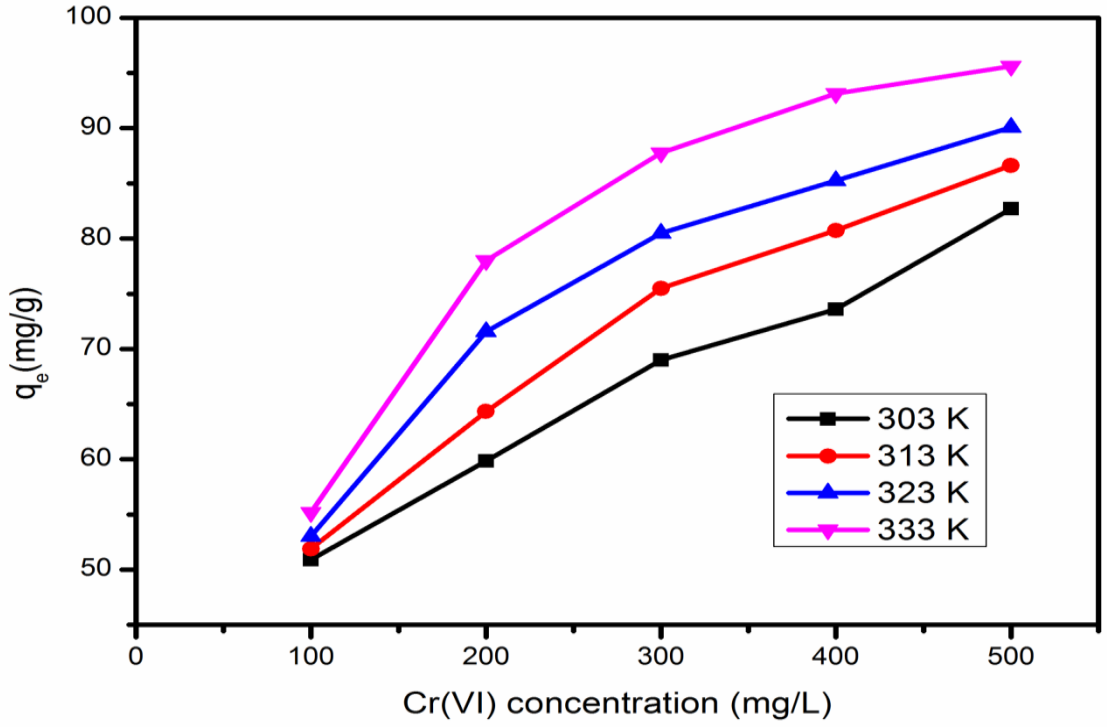

Fig. 4.12: Effect of temperature on biosorption capacity of WC shell at different initial Cr(VI) concentration

4.4 Biosorption Isotherm

Adsorption isotherm model could be employed to understand the adsorption phenomenon occurring in solid- liquid system. In the current study, various two parameter adsorption isotherm models such as Langmuir, Freundlich and Dubinin–Radushkevich were considered to understand the equilibrium data obtained from batch studiesat 303 K. The isotherm constants were estimated by employing linear regression analysis and the best fit was identified using the value of coefficients of determination (R^2) [Dąbrowski et al., 2001].

4.4.1 The Langmuir Isotherm Model

As per Langmuir theory, the adsorption is restricted to monolayer coverage of biosorbent molecules on homogeneous biosorbent surface and feature of this with expression are given in chapter-1. The values of Q_0 and b were estimated by fitting the experimental data in the Langmuir isotherm model (Refer Fig. 4.13) and the obtained values along with coefficient of determination R^2 is reported in Table 4.2. The very high R^2 value (0.989) suggests that the adsorption of Cr(VI) ions on WC shell could be well explained by Langmuir isotherm model. Besides, the lower value of b (0.0172) indicates the higher affinity of Cr(VI) metal ion towards biosorbent surface. Further, the dimensionless separation (or equilibrium) factor (R_L) was estimated by the following equation.

$$R_L = {}^{1}/_{1 + bC_i} \qquad (4.4)$$

Where C_i indicates the initial concentration (mg L^{-1}) of Cr(VI) metal ion and the value b (L mg^{-1}) can be obtained from Langmuir equation. In general, the magnitude of R_L indicates the ease of biosorption i.e. the biosorption is adverse if R_L>1, linear if R_L=1, favorable if $0<R_L<1$ and irreversible if $R_L=0$ [Khan et al., 2016]. The estimated values are reported in Table 4.3 and the values (0.11-0.37) indicate that the biosorption of Cr(VI) on WC shell is more favorable for all the initial metal ion concentrations being considered in this study.

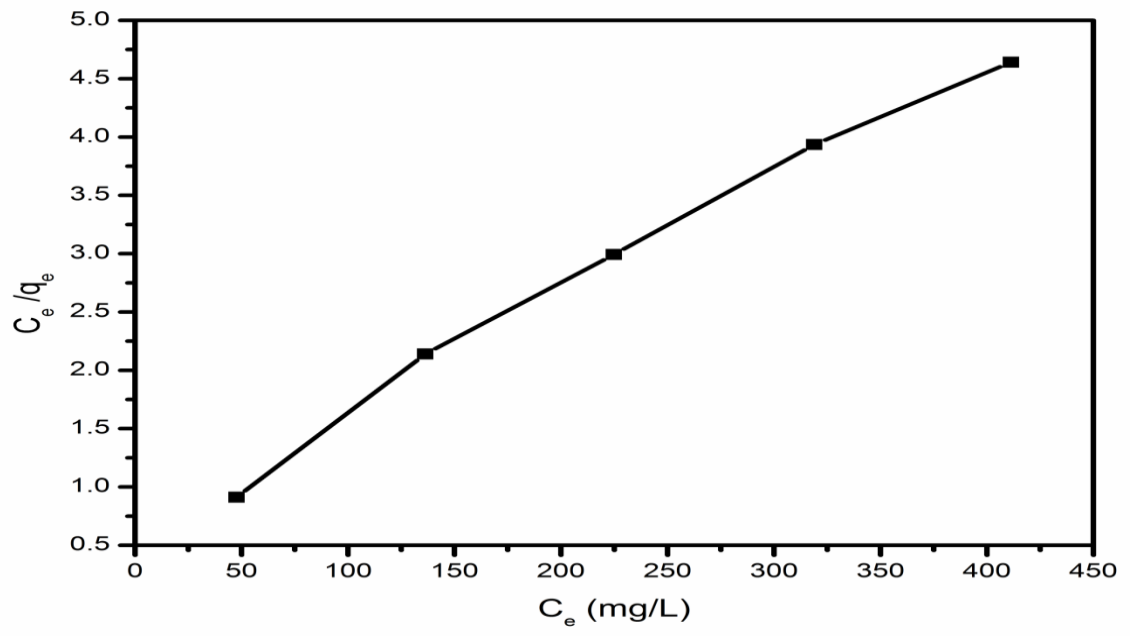

Fig. 4.13: Langmuir model isotherm for experimental data of biosorption on WC shell

4.4.2 Freundlich Isotherm Model

Unlike Langmuir model, Freundlich isotherm model considers multilayer formation of biosorbate molecules on heterogeneous surface [Freundlich and Helle, 1939]. Empirical equation of this model is given in chapter-1. The estimated values of K_f and n_f from the linear regression analysis of equilibrium data (Refer Fig. 4.14) are shown in Table 4.2. The value of empirical parameter (0.243), which lies in between 0.1 and 1, is indicating the fact that the biosorption of Cr(VI) ion on water caltrop shell is favorable. The R^2 value obtained for Freundlich isotherm model was high (0.986). However, it is still less in compared to Langmuir isotherm model. Similar result was reported in the literature for other biosorbents [Mansour et al., 2011].

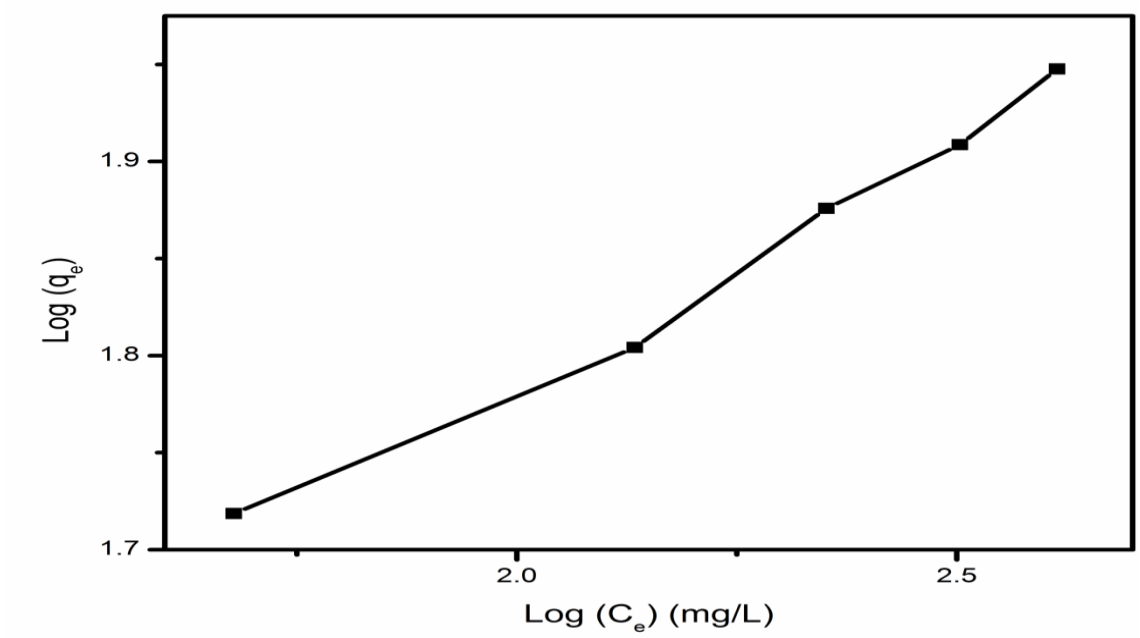

Fig. 4.14: Freundlich model isotherm for experimental data of biosorption on WC shell

4.4.3 Dubinin–Radushkevich Model

The nature of biosorption (physical or chemical) could by identified by using Dubinin–Radushkevich (D–R) model [Bansal et al., 2009; Chowdhury et al., 2011]. The detailed about this model is explained in chapter-1.

From the plot of $ln\, q_e$ vs. ϵ^2 , the values of $Q_{m,DR}$ and K_{DR} were obtained and results are reported in Table 4.2. Further, mean free biosorption energy (E, KJ mol^{-1}) was calculated from K_{DR} by the following equation

$$E = \frac{1}{\sqrt{2K_{DR}}} \qquad (4.5)$$

The '*E'* value indicates the nature of biosorption; The predominant mechanism is physical when $1< E<8$ KJ mol^{-1}, chemical when $E > 16$ KJ mol^{-1} and ion exchange when $8 < E <16$ KJ mol^{-1} [Saha et al., 2010]. In the present study the mean free energy of biosorption value was determined as 1.697 KJ mol^{-1} for the biosorption of Cr(VI) on WC shell which reveals that biosorption process occurs via physical adsorption. However, low R^2 value indicates that the removal of Cr(VI) by WC shell could not be explained by D-R model adequately.

The isotherm models were also tested for various temperatures and the results are summarized in Table 4.2. It is very clear that R^2 value is higher for Langmuir isotherm models at all the temperatures.

Table 4.2: Biosorption isotherm constants of various models obtained through linear regression analysis for Cr(VI) removal by WC shell

Temperature (K)	**Langmuir isotherm**			**Freundlich isotherm**			**Dubinin Radushkevich**			
	Q_0 (mg/g)	b (L/mg)	R^2	K_f $(mg^{1-1/n}L^{1/n}/g)$	n_f	R^2	Q_m (mg/g)	K_{DR} (mol^2/J^2)	E (KJ/mol)	R^2
293	89.28	0.018	0.992	19.53	4.56	0.978	73.10	0.036	3.716	0.741
303	98.04	0.017	0.989	19.98	4.10	0.986	81.81	0.174	1.696	0.852
313	104.166	0.015	0.990	18.74	3.78	0.985	82.49	0.036	3.373	0.762
323	104.17	0.162	0.994	18.33	3.64	0.994	85.65	0.036	3.371	0.820
333	107.53	0.017	0.996	19.52	3.65	0.993	90.55	0.032	3.971	0.845

Table 4.3: Langmuir separation factor for Cr(VI) removal by WC shell

Initial Cr(VI) concentration (mg L^{-1})	100	200	300	400	500
$R_L$value	0.37	0.23	0.17	0.13	0.11

4.5 Biosorption Kinetics

Various kinetics models such as pseudo-second-order, pseudo-first-order and intra-particle diffusion kinetic models were tested to determine the kinetics of biosorption of Cr(VI) on WC biomass.

4.5.1 Pseudo -First - Order Model

The pseudo–first- order expression is employed to explain the mechanism of adsorption process and detail about this are discussed in chapter-1. Using the plot of $\log(q_e - q_t)$ vs. t of pseudo-first-order expression (Figure is not shown), the values of k_1 and q_e were calculated and tabulated in Table 4.4. It is clear from this table that the discrepancy between experimental and calculated data is huge and R^2 value is lower than other. Therefore, the kinetics of biosorption of Cr(VI) on WC shell is not explained by the pseudo-first-order kinetics. Similar result is reported for adsorption of Cr(VI) on other biosorbents such as chemically modified Strychnine tree fruit shell [Ahmad et al., 2017] .

4.5.2 Pseudo –Second-Order Model

The detail about the pseudo-second-order model is explained in chpter-1. From the slope and intercept of plot of $\frac{t}{q_t}$ vs. t (shown in Fig. 4.15), the k_2 and $q_{e(cal)}$ values were calculated and tabulated in Table 4.4. It is clear that the biosorption capacity calculated through this model matches well with the experimental data. Also, higher R^2 value (0.9985) suggests that the Pseudo-second-order model could be employed to explain the biosorption mechanism of Cr(VI) removal from aqueous solution using WC shell as biosorbent because determination coefficient is higher than other model. As per this model, the biosorption occurs by chemical reaction via the

exchange or sharing of valence electrons between the biosorbent and Cr(VI) ions [Barkakati et al., 2010].

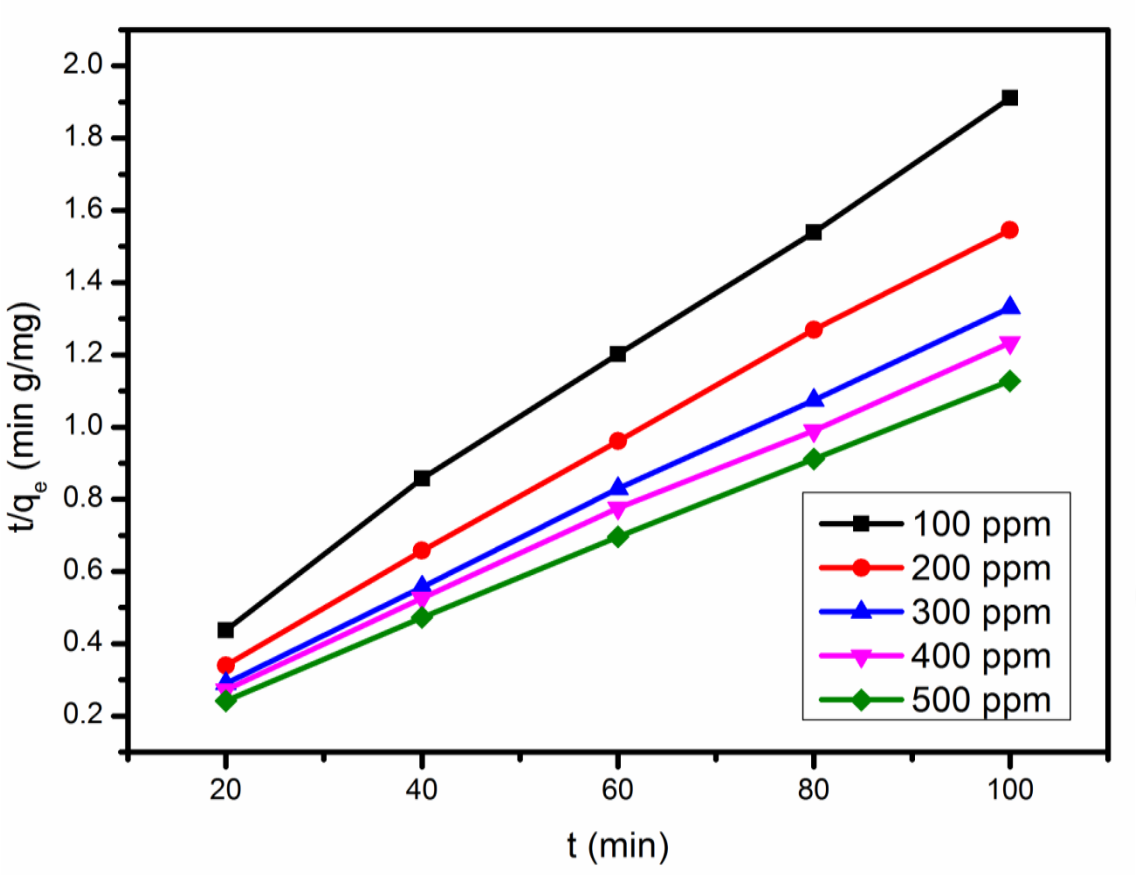

Fig. 4.15: Pseudo-second-order kinetic plots at various initial Cr(VI) concentrations

4.5.3 Intraparticle Diffusion Model

Weber Morris suggested that the intraparticle diffusion model can be used to analyze kinetic data in order to understand the diffusion effects [Weber and Morris, 1963].

In detail the general form of Weber's diffusion model is expressed in chapter -1. The information about the boundary layer thickness could be obtained from the intercept *C*. The biosorption mechanism can follow the intraparticle diffusion process when the plot q_t vs. $t_{1/2}$ is linear with a

slope k_d. However, Fig. 4.16 demonstrates that the plot is non - linear at lower concentrations (100-200 ppm) and linear at higher concentrations (300-500 ppm). It reveals the involvement of more than one process in biosorption of Cr(VI) ions on water caltrop shell at lower concentrations i.e. intraparticle diffusion process is taking place at initial stage and film biosorption is taking place at second stage. Moreover, Table 4.4 reveals that the value of *C* increases with initial metal ion concentration, which is attributed to the increase in boundary layer thickness. It suggests that the surface biosorption of Cr(VI) ions on biosorbent is the major rate-controlling step [Doke and Khan, 2017].

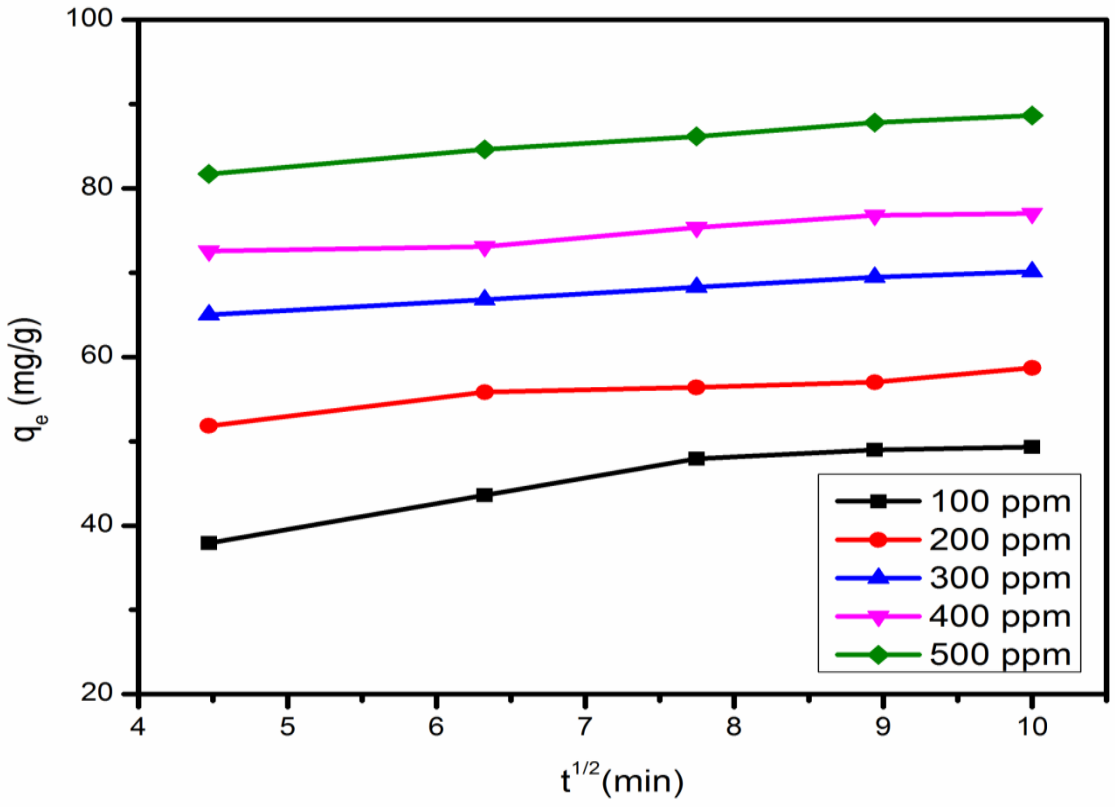

Fig. 4.16: Intraparticle diffusion model plots for the biosorption of Cr(VI) by WC shell

Table 4.4: Kinetic rate constants observed for biosorption of Cr(VI) onto WC shell

Cr(VI) Conc. (mg/L)	q_e(exp) (mg/g)	Pseudo-first-order			Pseudo-second-order			Intraparticle diffusion		
		k_1 (min^{-1})	q_e(cal) (mg/g)	R^2	k_2 (g/mg/min)	q_e(cal) (mg/g)	R^2	k_{id} (mg / g / $min^{½}$)	C (mg/g)	R^2
100.000	52.311	0.049	26.903	0.852	0.003	54.945	0.999	1.342	39.255	0.939
200.000	64.703	0.021	8.894	0.991	0.005	66.225	0.999	1.019	54.318	0.987
300.000	75.140	0.034	13.543	0.879	0.005	76.923	1.000	1.096	64.325	0.968
400.000	81.037	0.055	36.216	0.766	0.000	84.034	0.999	1.432	67.047	0.959
500.000	88.645	0.032	12.993	0.937	0.005	90.090	1.000	1.099	77.760	0.996

4.6 Thermodynamic Parameters

The detail about thermodynamic parameters such as enthalpy (ΔH°), and entropy (ΔS°) and Gibbs free energy change (ΔG) and equation are given in chapter-1. The Values of ΔS^{o} and ΔH^{0} were calculated using the intercept and slope of the plot $\ln K_C$ vs $1/T$ (figure not shown) and the results are reported in Table 4.5. The negative value of ΔG^{o} indicates that biosorption of Cr(VI) on WC shell is spontaneous at lower concentration of metals ions in aqueous solution while positive value of ΔH^{0} reveals the endothermic nature of Cr(VI) biosorption process. The value obtained for ΔS^{o} was positive that showed sorbet ions are unstable on the surface of biosorbent. The positive ΔS^{o} value is attributed to the increase in degree of freedom. These types of biosorption behavior were observed by other researchers [Agarwal et al., 2006; Zhang et al., 2010].

Table 4.5: Thermodynamic parameters evaluated for Cr(VI) biosorption on WC shell at initial metal ion concentration of 100 mgL^{-1}

Initial Cr(VI) concentrations (mg/L)	**Temperature (K)**	***Kc***	**ΔG° (kJ/mol)**	**ΔH° (kJ/mol)**	**ΔS° (kJ/Kmol)**
100 ppm	303	1.097	-0.233	2.897	0.010
	313	1.123	-0.301		
	323	1.128	-0.324		
	333	1.230	-0.574		

4.7 Regeneration Study

The reusability of the biosorbents provides the information about potential of biosorbents for commercial consideration. For the investigation of repeated biosorption - desorption, five cycles were performed at 1g L^{-1} dosage, initial concentration of 100 ppm Cr(VI), 0.1 N HCl and other parameter were also kept constant. The surface of biosorbent covered with H^+ ion after regeneration of Cr(VI) loaded biosorbent. The reusability study shows that the biosorption capacity was decreased with consecutive number of regeneration cycle such as 52.77 (1^{st} cycle), 41.55 (2^{nd} cycle), 29.68 (3^{rd} cycle), 23.24 (4^{th} cycle), 20.87 (5^{th} cycle) for elimination of Cr(VI). The decreasing phenomenon of biosorption capacity of repeated biosorbent can be attributed to the changes on the surface of biosorbent and some of the Cr(VI) being held in the pore of biosorbents [Bansal et al., 2009; Dehghani et al., 2016].

4.8 Cost Estimation

Cost analysis is an important criterion in selecting a suitable biosorbent for the removal of Cr(VI) from waste water at commercial scale. The cost of commercially available activated carbon, which is used for removing heavy metals from waste water, is about ranging from $1500 to 2000 /tons in India [Saha et al., 2010; Arul et al., 2016]. However, WC shell suggested in this work is available at free of cost. 1 kg of WC is required to treat 1 m^3 of Cr(VI) solution or 2 kg of WC is required to remove 0.05 kg of Cr(VI) from the waste water solution. The total cost required to remove the Cr(VI) from waste water (which includes the expense of chemical and electrical energy for preparation of biosorbent) was observed to be approximately $ 93.39 /ton. This indicates that WC shell expense for removal of Cr(VI) is lower than the commercially

available activated carbon. Thus, it is suggested that WC shell could be used as low cost biosorbent to remove Cr(VI) from waste water.

4.9 Comparison of the Present Study with Literature

Comparison of maximum biosorption capacity Q_0 (mg g^{-1}) of WC shell with those of some other biosorbents stated in the literature is given in Table 4.6. From this comparison, WC shell was found to be effective and better than many biosorbents reported in the literature for chromium removal from aqueous solution.

Table 4.6: Comparison of biosorption capacities of various biosorbents with WC shell for Cr(VI) removal

Biosorbent	Maximum adsorption capacity (mg g^{-1})	pH	References
Caryota Urens	100	2	[Rangabhashiyam and Selvaraju, 2015a]
Boiled rice husk	8.5 2	2	[Bansal et al., 2008]
Palm pressed fibers	15.0	2	[Tan et al., 1993]
Maize bran	312.52	2	[Hasan et al., 2008]
Green Moringa leaves	33.9	2	[Timbo et al., 2017]
Neem sawdust	58.82	2	[Vinodhini and Das, 2010]
Mangrove leaves	8.87	4.5–5.5	[Elangovan et al., 2008]
Parthenium hysterophorus weed	24.5	1.0	[Venugopal and Mohanty, 2011]
Peanut shell	4.32	2-3	[Ilyas et al., 2013]
Sunflower head	8.177	2	[Jain et al., 2009]
Ocimumamericanum L. seed pods	83.3	1.5	[Levan et al., 2009]
Eucalyptus bark	45	2	[Sarin and Pant, 2006]
Carbonized Buckwheat straw	55.19	1	[Chen et al., 2014]
Coconut coir	6.3	2	[Gonzalez et al., 2008]
Rice straw	3.2	2	[Gao, et al., 2008]
Pomegranate husk	10.59	1	[Nemr, 2007]
Water caltrop shell	**98.04**	**2**	**Present study**

4.10 Conclusion

WC shell is suggested as a potential biosorbent to remove the Cr(VI) from aqueous solutions. The characterization of biosorbent both before and after biosorption reveal the fact that various functional groups such as hydroxyl, carboxyl, carbonyl and amine group on the biosorbent are taking part in biosorption of Cr(VI) ions. The extensive batch studies showed that the maximum uptake capacity of 98.04 mg g^{-1} could be achieved at optimum conditions of pH 2, temperature 303K, agitation speed 100 rpm, and dosage 1.0 g L^{-1}.

The equilibrium data obtained from the batch studies is analyzed with several isotherms and kinetic models. The analysis suggest that Langmuir adsorption isotherm model could be employed to describe the biosorption of Cr(VI) on WC shell. Similarly, the kinetics follows the pseudo-second-order kinetic model which indicates the involvement of chemical rate controlling step in the biosorption process. Thermodynamic analysis confirms that the biosorption is feasible, spontaneous and endothermic in nature. The suggested biosorbent showed better performance in term of biosorption capacity compared to various biosorbents recommended in the literature for Cr(VI) from the aqueous solution.

RESULTS AND DISCUSSION

CHAPTER - 5

Chapter-5
Kinetic and Thermodynamic Studies on Biosorption of Cr(VI) on Raw and Chemically Modified Datura *(Datura Stramonium)* Fruit

5. Results and Discussion

In the present study, the Datura *(Datura Stramonium)* fruit were activated by using H_3PO_4 and H_2SO_4. The efficiency of raw and acid activated Datura *(Datura Stramonium)* fruit were evaluated for removal of Cr(VI) from waste water by conducting equilibrium batch experiments. The results observed from batch adsorption experiments are explained in the following section.

5.1 Characterization of Raw and Carbonized Activated Datura *(Datura Stramonium)*

FESEM was performed to analyze morphology of the biosorbent and the results are shown in Fig. 5.1. The FESEM micrograph of RDSF shown in Fig. 5.1a which revealed that fibers are agglomerated with less pores and less rough surface. The morphology of PDSF (Fig. 5.1b) revealed the difference in size and shape of pores, and fiber, due to the removal of volatile gases. The SDSF morphology in Fig. 5.1c shows that pores are open due to the removal of viscous compound. The FESEM morphologies (Fig. 5.1d-f) after Cr(VI) adsorption show that the biosorbent surface became smooth due to filling up of Cr(VI) metal ions in pores. Energy dispersive X-ray (EDX) studies of biosorbent sample were carried out before and after biosorption in order to support the information obtained from FESEM and the results are shown in Fig. 5.2. The EDX spectra exhibit *C* and *O* peaks on the biosorbents surface before

biosorption as shown in Fig. 5.2 (a, b and c). The EDX spectra showed a new peak after biosorption of Cr(VI) (refer to Fig. 5.2 (d, e and f)) which suggests that it is a characteristic signal of Cr(VI) ion. FTIR spectra were carried out to obtain an information about the functional groups which involved in binding of Cr(VI) ions. The deviation in vibration frequency was used to predict the same. FTIR spectrum of biosorbents showed a number of absorption peaks (unloaded and loaded Cr(VI)) in the range 400 – 4000 cm^{-1} which suggest the complex nature of biosorbents. FTIR spectra of RDSF biosorbent (before and after biosorption) display several absorption peaks as shown in Fig. 5.3a. The absorption peaks of unloaded biosorbent assigned at 3655.10, 2893.71, 1737.27, 1523.76, and 1258.86 were shifted to 3566.38, 2884.71, 1728.23, 1513.32, and 1251.63 respectively after biosorption of Cr(VI). These absorption peaks represent O–H stretch, C–O stretch, C–H stretch, C=C, and C=O stretch which contributed to the binding of Cr(VI) ions onto the biosorbent surface. FTIR spectrum of SDSF biosorbent (before and after biosorption) indicates that there is a considerable change in band of functional groups as shown in Fig. 5.3b. FTIR spectrum peaks after biosorption in contrast to before biosorption were moved from 3556.20, 1637.63, 1359.69, 1229.29, and 760 to 3529.60, 1511.66, 1341.70, 1226.45, and 751.66 respectively. These adsorption peaks correspond to O–H stretch, N–O stretch, C=O stretch, and C–O functional groups which contributed in binding of Cr(VI) ions with the biosorbent surface. Similarly, FTIR spectrum of Cr(VI)-loaded PDSF biosorbents reveals the shifting of absorption peaks from 3619.39, 3081.64, 1737.22, 1535.33, and 778.65 to 3584.40, 3064.63, 1710.23, 1502.54, and 751.66 respectively. These absorption peaks represent the functional group such as O–H stretch, C=C stretch, =C–H stretch, and C=O stretch as shown in Fig. 5.3c. The changes in FTIR spectrum from unloaded to loaded Cr(VI) of biosorbents are indicating the fact that the functional groups are indulged in biosorption of Cr(VI).

Similar results were presented by other researchers to assess the biosorption of Cr(VI) through functional groups [Singha and Naiya 2011; Jain et al. 2009].

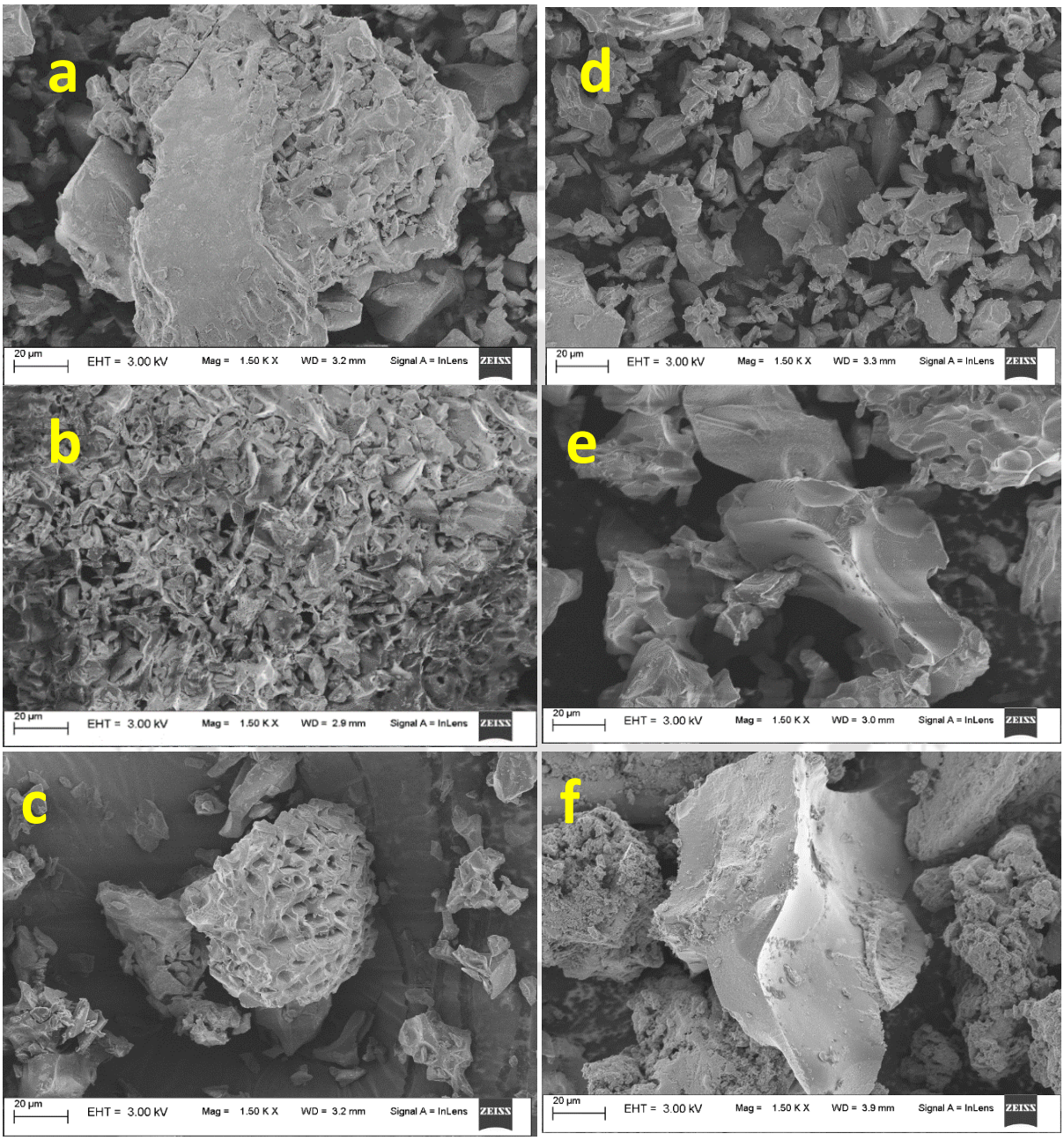

Fig. 5.1: Scanning electron micrographs of RDSF (a, d), PDSF (b, e) and SDSF (c, f), before and after biosorption

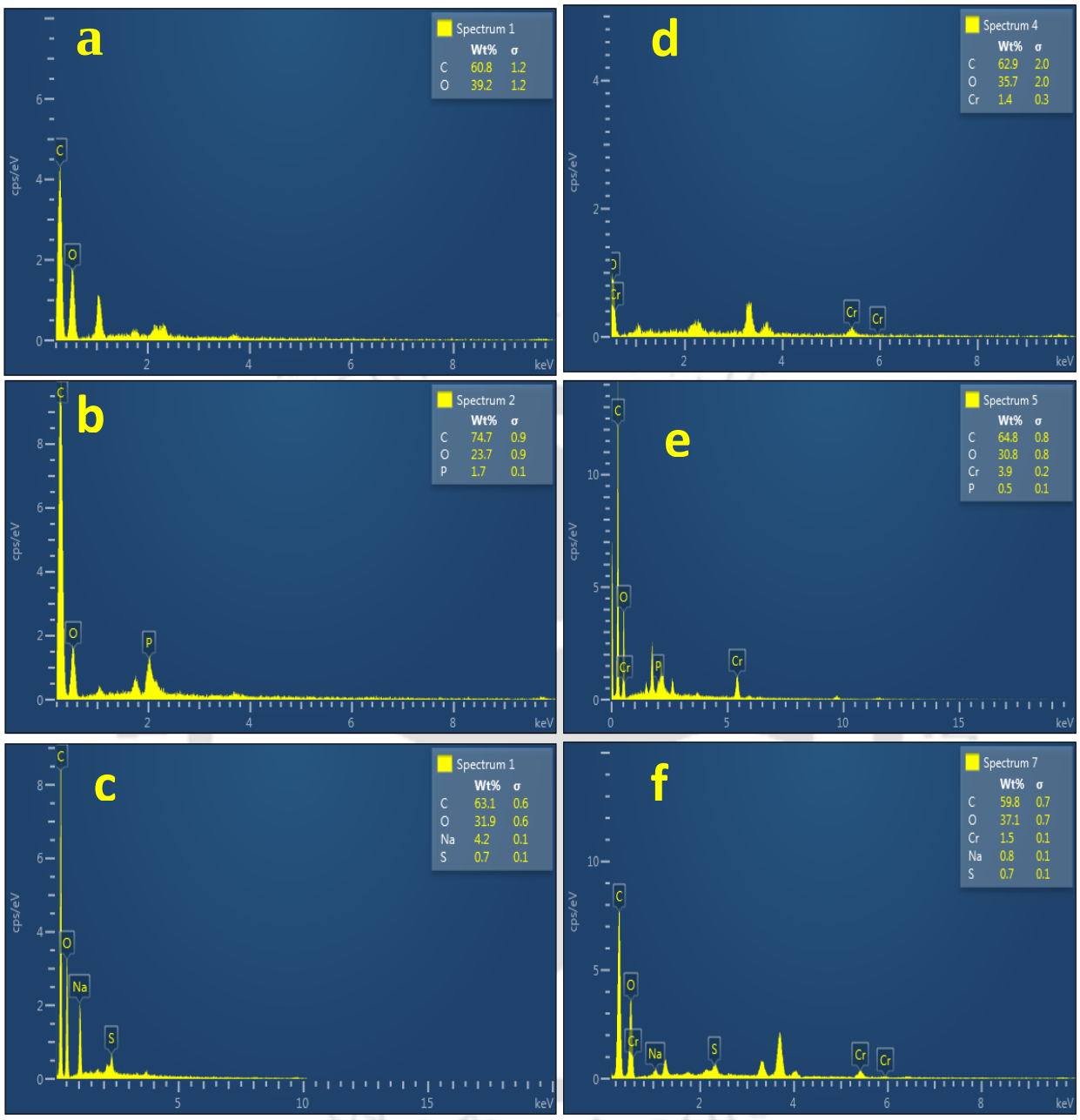

Fig. 5.2: EDX image of RDSF (a, d), PDSF (b, e) and SDSF (c, f), before and after biosorption

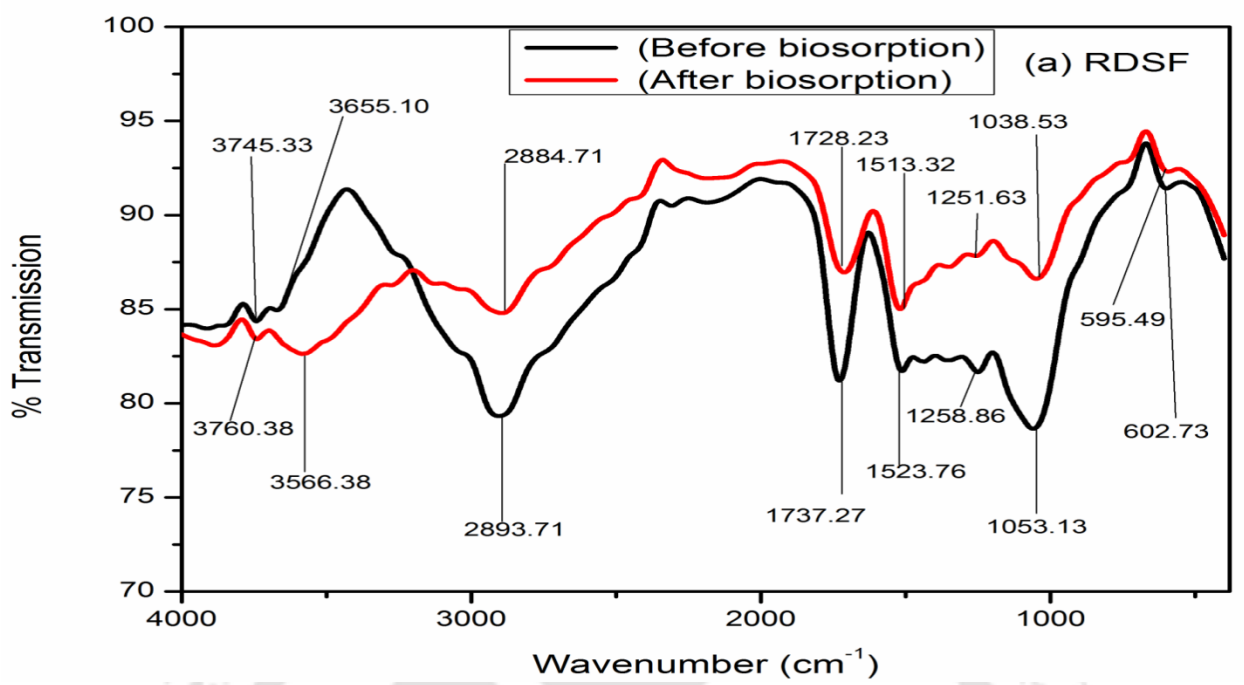

Fig. 5.3: (a) FTIR spectrum of unloaded and metal-loaded on RDSF biosorbent

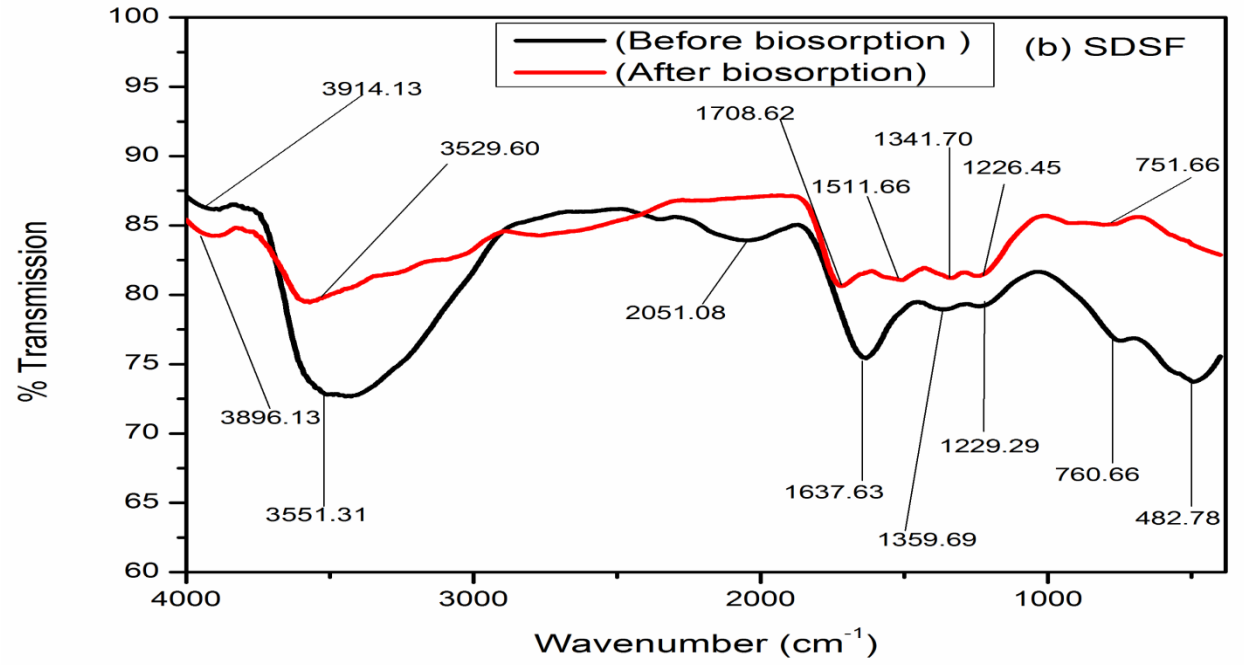

Fig. 5.3: (b) FTIR spectrum of unloaded and metal-loaded on SDSF biosorbent

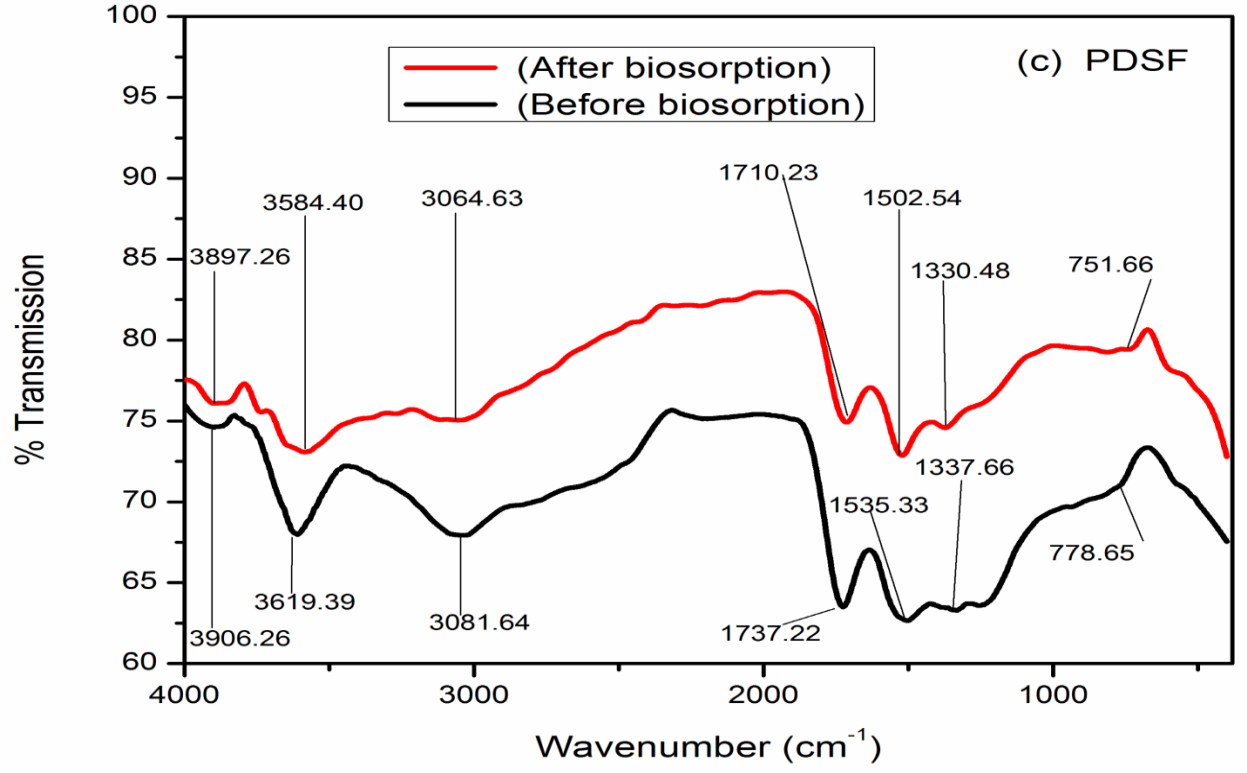

Fig. 5.3: (c) FTIR spectrum of unloaded and metal-loaded on PDSF biosorbent

5.2 Influences of pH

The pH value of the aqueous medium plays an important role in biosorption of Cr(VI) by the biosorbents' surface. In the present study, biosorption experiments were conducted over a wide range of pH from 2 to 9, keeping other parameters as constant. It is revealed from Fig. 5.4 that uptake capacity of Cr(VI) on RDSF, SDSF and PDSF biosorbents increases as the pH of the sorbent solution decreases. The estimated biosorption capacity of Cr(VI) was 44.64 mg g^{-1}, 50.72 mg g^{-1}, and 50.42 mg g^{-1} on RDSF, PDSF and SDSF respectively at pH 2 of the aqueous medium. Biosorption phenomenon of Cr(VI) on RDSF, SDSF and PDSF can be described by changes in polarity of the biosorbents' surface due to variation in pH of metal solution. The biomass attains positive charge due to lower pH and gradually gets deprotonated as the pH of the

solution rises. Cr(VI) occurs in different ionic forms in the aqueous solution such as chromate (CrO_4^{2-}), dichromate ($Cr_2O_7^{2-}$) and hydro chromates ($HCrO_4^-$) depending upon the pH value of the aqueous medium. $HCrO4^-$ ions dominate among all the chromate ions at low pH values while CrO_4^{2-} ions dominate towards the higher pH values of the aqueous medium. Biomass gets protonated at lower pH of solution and therefore more biosorption of Cr(VI) takes place at this pH range, due to the electrostatic force of attraction between $HCrO_4^-$ ions and protonated biosorbent surface. At higher pH, the concentration of OH^- increases and therefore biosorption capacity of the biosorbents drop due to the electrostatic force of repulsion between the CrO_4^{2-} and OH^- ions, which causes hindrance in path of chromate ion binding on the active sites of the biosorbent [Rangabhashiyam and Selvaraju 2015a; Blazquez et al., 2009].

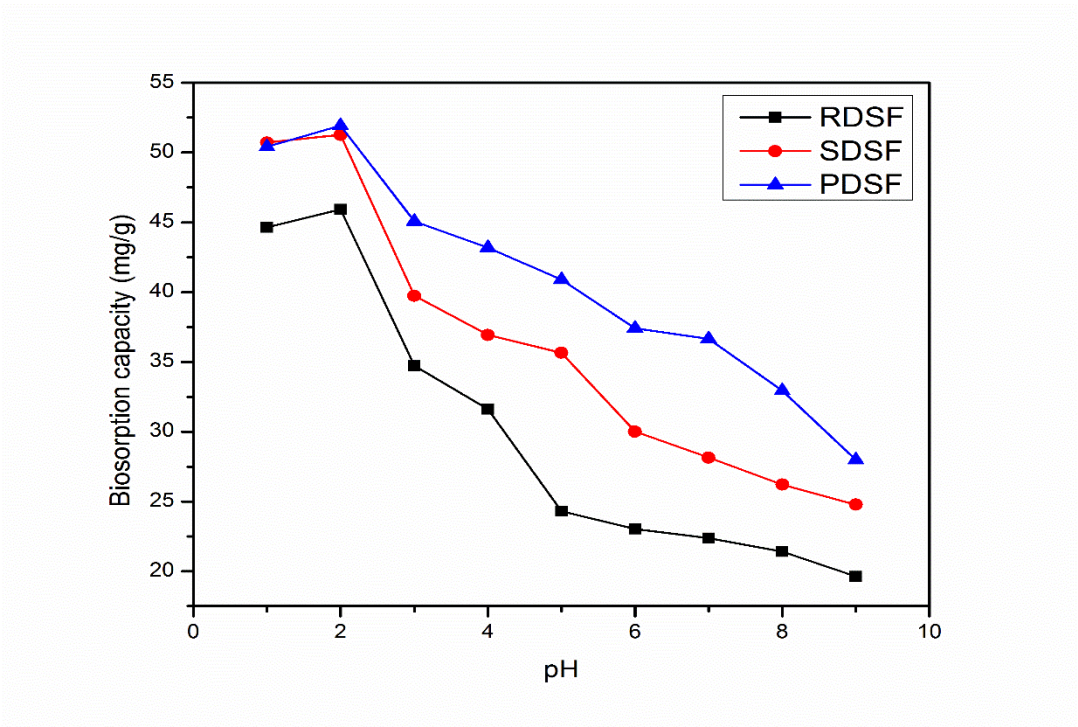

Fig. 5.4: Effect of pH on biosorption capacity of Cr(VI) at optimum dosage of RDSF, SDSF and PDSF biosorbents

5.3 Effect of Temperature

The effect of temperature (303 K to 333 K) was studied by changing the initial Cr(VI) concentration (100 mg L^{-1} to 300 mg L^{-1}), with 0.2 g L^{-1} of biosorbent dosage and maintained the solution pH at 2. The mixture of biosorbent and Cr(VI) solution were kept in an orbital shaker at 100 rpm for 60 min. The results obtained are shown in Fig. 5.5 which denotes that the maximum biosorption capacity was observed at temperature 333 K for all the three (RDSF, SDSF, and PDSF) biosorbents. The maximum adsorption of Cr(VI) at higher temperature is attributed to the increase in mobility of chromium ions within the adsorbents pore network. In addition, enhancement in the biosorption of Cr(VI) phenomenon at higher temperature can also be described by the creation of some new biosorption sites owing to the cracking of bond between molecules of the biosorbents [Singh et al., 2005].

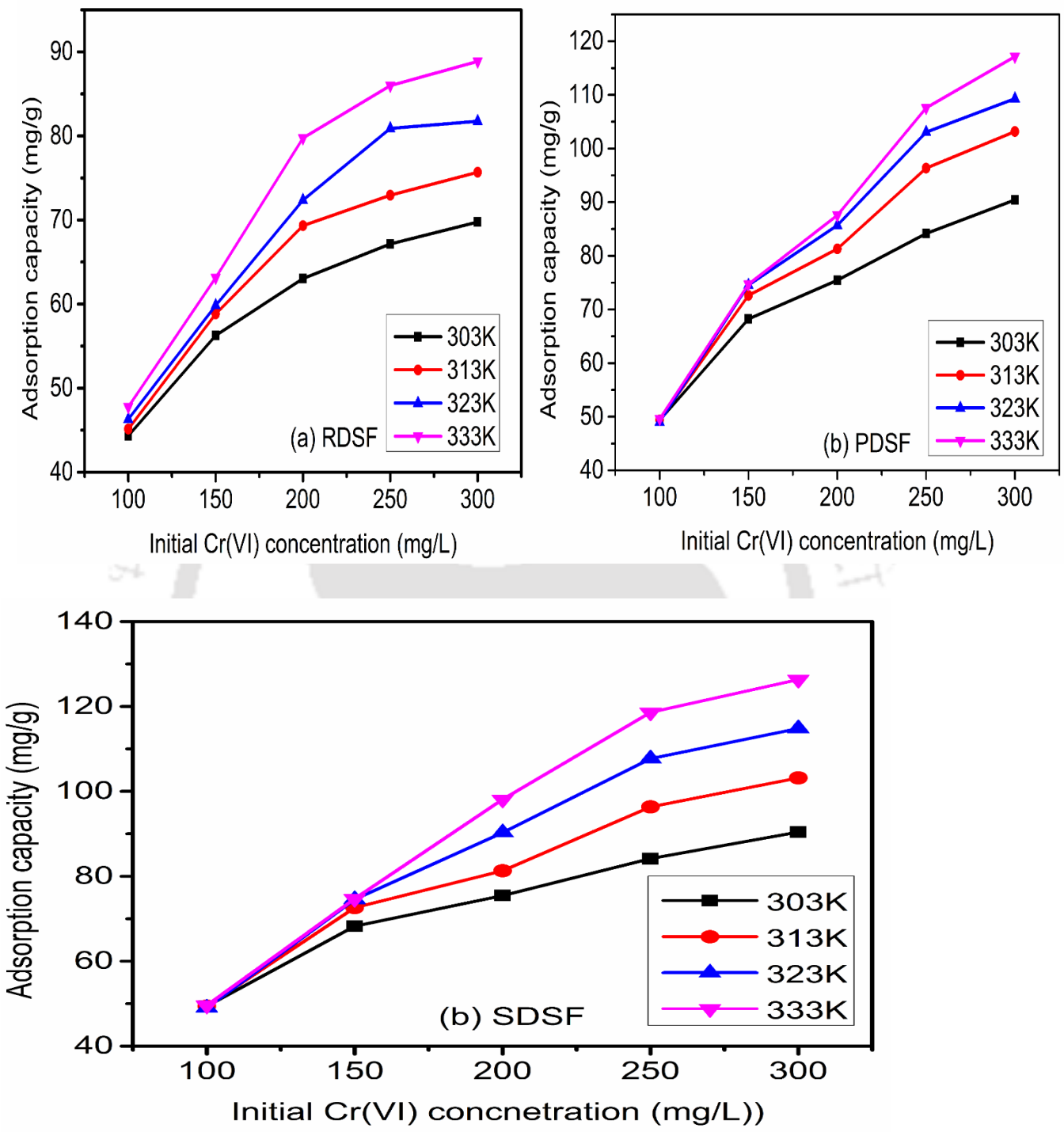

Fig. 5.5: Effect of temperature and initial Cr(VI) ion concentration on adsorption capacity of RDSF, SDSF and PDSF biosorbents

5.4 Effect of Adsorbent Doses

The impact of biosorbent dosage (0.2 to 5 g L^{-1}) on Cr(VI) biosorption was investigated at room temperature while the other parameters such as agitation speed (100 rpm), contact time (60 min), pH (2), and hexavalent chromium concentration (100 mg L^{-1}) were kept constant. The results obtained are shown in Fig. 5.6 which confirm that the biosorption capacity decreases whereas the percentage elimination of Cr(VI) increases from 31.49 to 66.92%, 32.12 to 94.67%, and 30.28 to 84.67% for RDSF, SDSF, and PDSF biosorbents, respectively, with an increase in biosorbent dosage. The percentage elimination of Cr(VI) increases (refer to Fig. 5.6) from 31.49 to 66.92%, 32.12 to 94.67%, and 30.28 to 84.67% for RDSF, SDSF, and PDSF biosorbents respectively. These results are attributed to the increased surface area as well as increased number of binding sites with increased in biosorbent dosage. However, the uptake of hexavalent chromium from solution is decreased from 69.73 to 29.46, 80.30 to 49.34, and 75.70 to 46.34 mg g^{-1} on RDSF, PDSF, and SDSF biosorbents respectively. This is likely due to the aggregation of biosorbent particles and unsaturated sites on biosorbent. Consequently, the active sites are deprived from being bind by metal ions [Albadarin et al., 2012; Khoubestani et al., 2015].

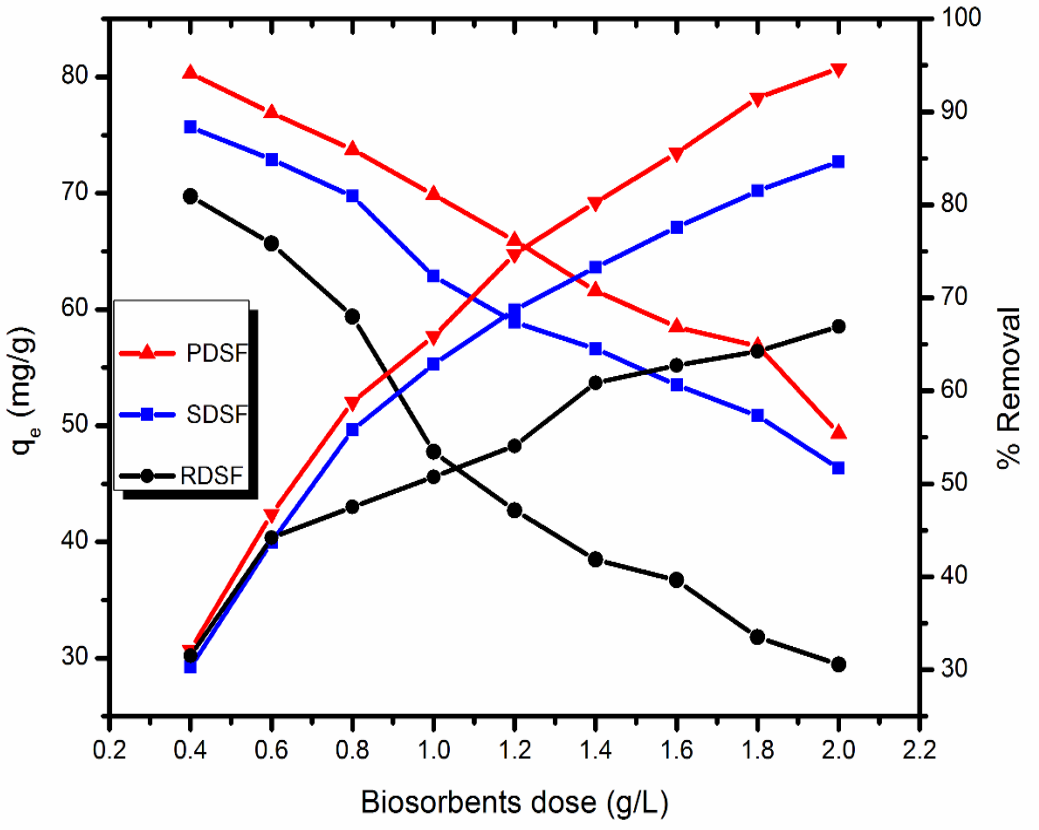

Fig. 5.6: Effect of biosorption capacity and the percentage Cr(VI) removal at 100 mg L^{-1} initial Cr(VI) concentration by different dosages of RDSF, SDSF and PDSF biosorbents

5.5 Impact of Initial Cr(VI) Ion Concentration and Interaction Time

Both interaction time and initial Cr(VI) concentration are significant factors in determining the hexavalent Chromium elimination through biosorption process. The elimination of Cr(VI) from simulated solution was done with different initial concentrations (100 ppm 150 ppm 250 ppm and 300 ppm) of biosorbate and with various contact time (from 20 min to 140 min) at optimized condition i.e. biosorbents dosage (1 g L^{-1}), pH (2), 100 rpm agitation speed and at room temperature. The results obtained are shown in Fig. 5.7. As shown in this plot the biosorption

capacity increases steeply with an increase in initial concentration of Cr(VI). Eventually, the adsorption capacity attained the equilibrium value with further increase in contact time. As the initial concentration increased from 100 to 300 ppm, the adsorption capacity is increased from 44.34 to 69.76, 47.55 to 94.79, and 49.39 to 90.43 mg g^{-1} for RDSF, PDSF and SDSF respectively. This is likely due to the greater driving force (concentration gradient of Cr(VI) ions between the simulated solution of Cr(VI) and the adsorbent surface) at higher Cr(VI) concentrations. It is also attributed to more collisions between the adsorbate and adsorbent. At equilibrium, all the active sites are occupied by Cr(VI) ions [Singha and Das, 2011].

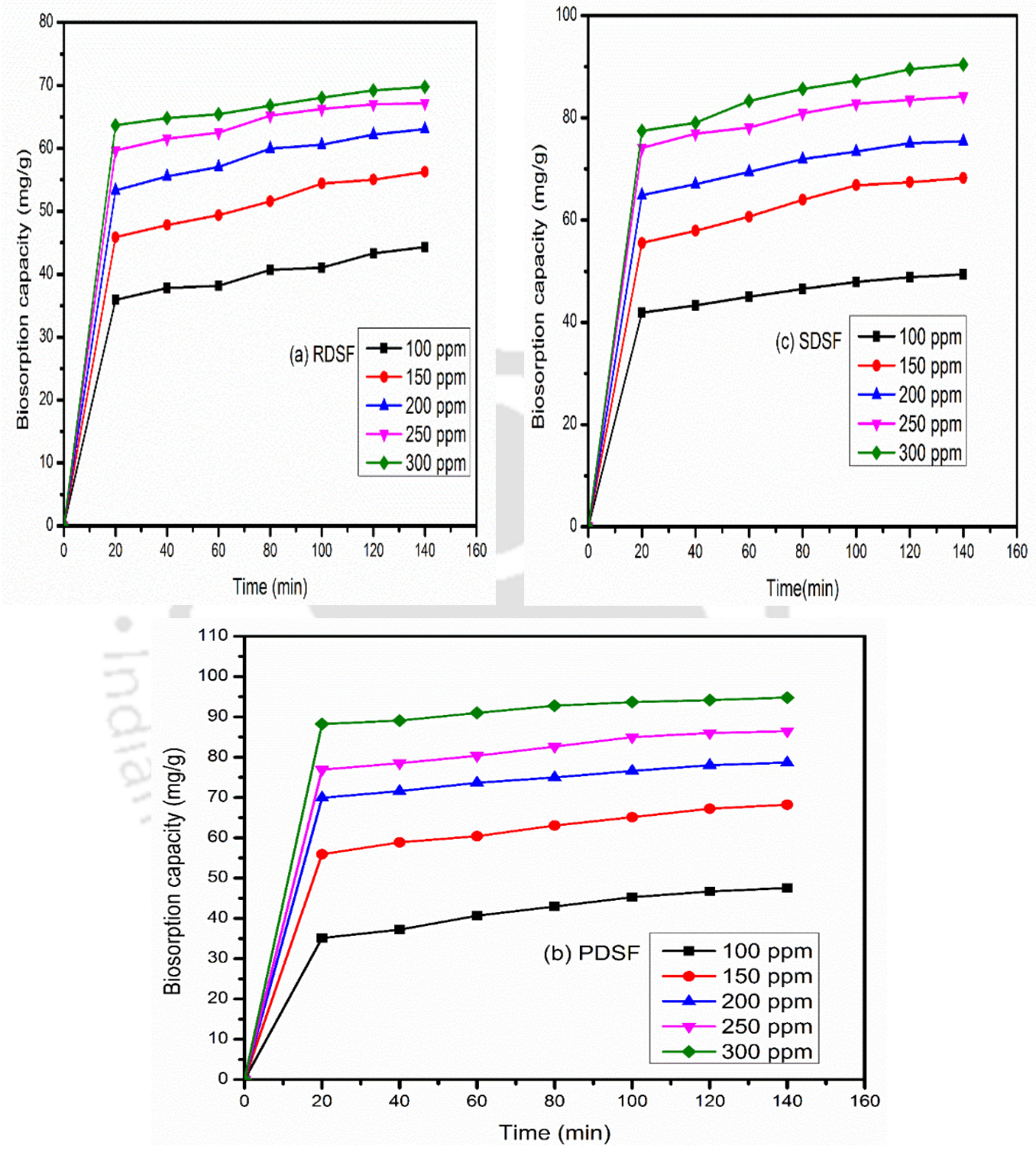

Fig. 5.7: Effect of contact time on biosorption capacity of Cr(VI) for RDSF, SDSF and PDSF biosorbents

5.6 Modeling of Equilibrium Data Using Isotherm, Sorption Kinetic Model

Generally model parameters are more frequently estimated by linear regression method. However, non-linear regression analysis gives more reliable results [Chen et al., 2008]. Thus, in the present study, both non-linear and linear regression analyses were employed to evaluate the model parameters values (isotherm and kinetics model equation). Besides, error calculation analysis was performed to quantify the difference between the experimental data and the predicted by the model.

5.6.1 Nonlinear Regression Analysis

Nonlinear regression analysis was performed using the original form of kinetics and isotherm model equations. The best fit model parameters were extracted using an optimization technique. The main objective function of the optimization is to minimize the χ^2 value. The optimization was carried out by using solver add-in in Microsoft excel application.

$$\chi 2 = \sum_{i=1}^{m} \left(\frac{Q_i - q_i}{q_i} \right)^2 \qquad (5.1)$$

Where Q_i is the experimentally observed adsorbed concentration, q_i is the predicted amount of adsorbed on adsorbent and m represents the number of observations carried out in experiment process [Chen et al., 2008].

5.6.2 Isotherm Studies

Adsorption isotherms are used to examine the equilibrium characteristics of the biosorption phenomenon between the sorbate molecules adsorbed per unit mass of biosorbent. In the present investigation, various isotherm models such as Langmuir, Freundlich, and Dubinin–Radushkevich were selected to understand the biosorption process on the biosorbent's surface. In each isotherm model, the initial metal ion concentration and the contact time was varied while the other parameters viz. biomass load, temperature, and pH were kept constant [Singha and Das, 2011; Nasseh et al., 2017].

5.6.2.1 Langmuir Isotherm Model

In order to understand the adsorption phenomenon over homogeneous surface, Langmuir isotherm model was used, which postulates that there, is no interaction among the sorbate molecules [Langmuir, 1918]. Non-linear and linear form mathematical expression of the Langmuir adsorption isotherm are represented in chapter-1 and it is applied for the equilibrium adsorption data. The intercept and slope of plot *Ce/qe* against *Ce* (refer to Fig. 5.8) were used to evaluate the values of *b* and Q_0. The values of determination coefficient (R^2) and isotherm model are stated in Table 5.1. The calculated determination coefficient (R^2) data for all the three biosorbents (RDSF, PDSF and SDSF) were close to 1 which indicated better agreement with Langmuir isotherm model. The significant characteristics parameters of Langmuir isotherm can be expressed in terms of separation factor, R_L. The dimensionless expression is already discussed in equation 1.7. R_L values provide the information about the nature of adsorption process to be either unfavorable if $R_L > 1$, linear if $R_L = 1$, favorable if $0 < R_L < 1$, and irreversible if $R_L = 0$ [Dehghani et al., 2016; Gupta et al., 2010; Sharma and Forster, 1994].

In the present study, it is clear from Table 5.1 that the observed R_L values are less than unity and more than zero (0) onto RDSF, SDSF and PDSF biosorbents and validate that the Langmuir isotherm is favorable for adsorption.

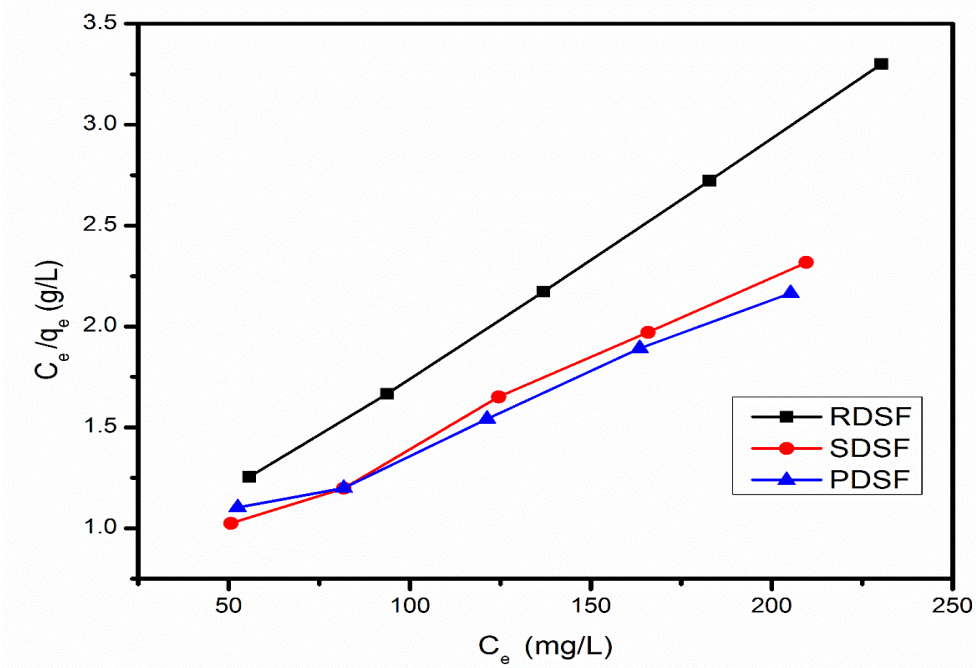

Fig. 5.8: Langmuir isotherm plots for Cr(VI) adsorption onto the RDSF, SDSF and PDSF biosorbents

5.6.2.2 Freundlich Isotherm Model

The Freundlich isotherm was employed to determine the multilayer sorption of the sorbate molecules over heterogeneous surfaces [Freundlich and Heller, 1939]. The linear and non linear forms of mathematical expressions are given in Chapter-1. The value of n_f greater than 1 indicates the higher intensity of adsorption. The plot of *log* q_e versus *Ce* was used to evaluate n_f and K_f. In this study, the values of Freundlich constant parameter "n_f" was found to be as 3.137, 2.451, and 1.950 for RDSF, SDSF, and PDSF biosorbents respectively. Therefore, the values of "n_f" suggest that the biosorption process is favorable under the studied conditions.

5.6.2.3 Energy of Sorption by Dubinin–Radushkevich Model

The characteristics of the sorption curve which is associated with porosity of the adsorbent were studied by using Dubinin–Radushkevich (D-R) model [Dada et al., 2012].

The detailed about the mathematical expression are discussed in equations 1.10, 1.11, 1.12 and 1.13. $Q_{(m,DR)}$ and K_{DR} constant can be obtained from the plot of lnq_e against $\in^{\wedge 2}$ using the linear equation of D-R isotherm and the values are stated in Table 5.1. The values of mean energy of Cr(VI) biosorption were calculated as 0.05, 0.05, and 0.041 kJ mol^{-1} on RDSF, SDSF, and PDSF biosorbents respectively. The mean free energy obtained for all three studied adsorbent was less than 8 kJ mol^{-1} which suggested that the adsorption followed physisorption process. Determined R^2 values of Freundlich and Dubinin–Radushkevich (D-R) model for RDSF, SDSF, and PDSF biosorbents are less than those of Langmuir isotherm R^2 value as shown in Table 5.1. These results suggested that the D-R isotherm model was least agreeable with observed experimental values. Similar result was also reported in the literature [Khan et al., 2016; Pandey et al., 2010].

5.6.2.4 Isotherm Analysis by Non-Linear Regression Approach

The simulated data obtained for different adsorption isotherm models from non-linear regression analysis are shown in Fig. 5.9 and the best-fit isotherm parameters are presented in Table 5.2. It is clearly evident that χ^2 value is minimum for Langmuir adsorption isotherm. Thus, both linear (high R^2 value) and non-linear (low χ^2 value) regression analysis suggest that Langmuir isotherm model could explain the adsorption process better in comparison to other isotherm models. Similar finding is reported in other literature as well [Apiratikul and Pavasant, 2008].

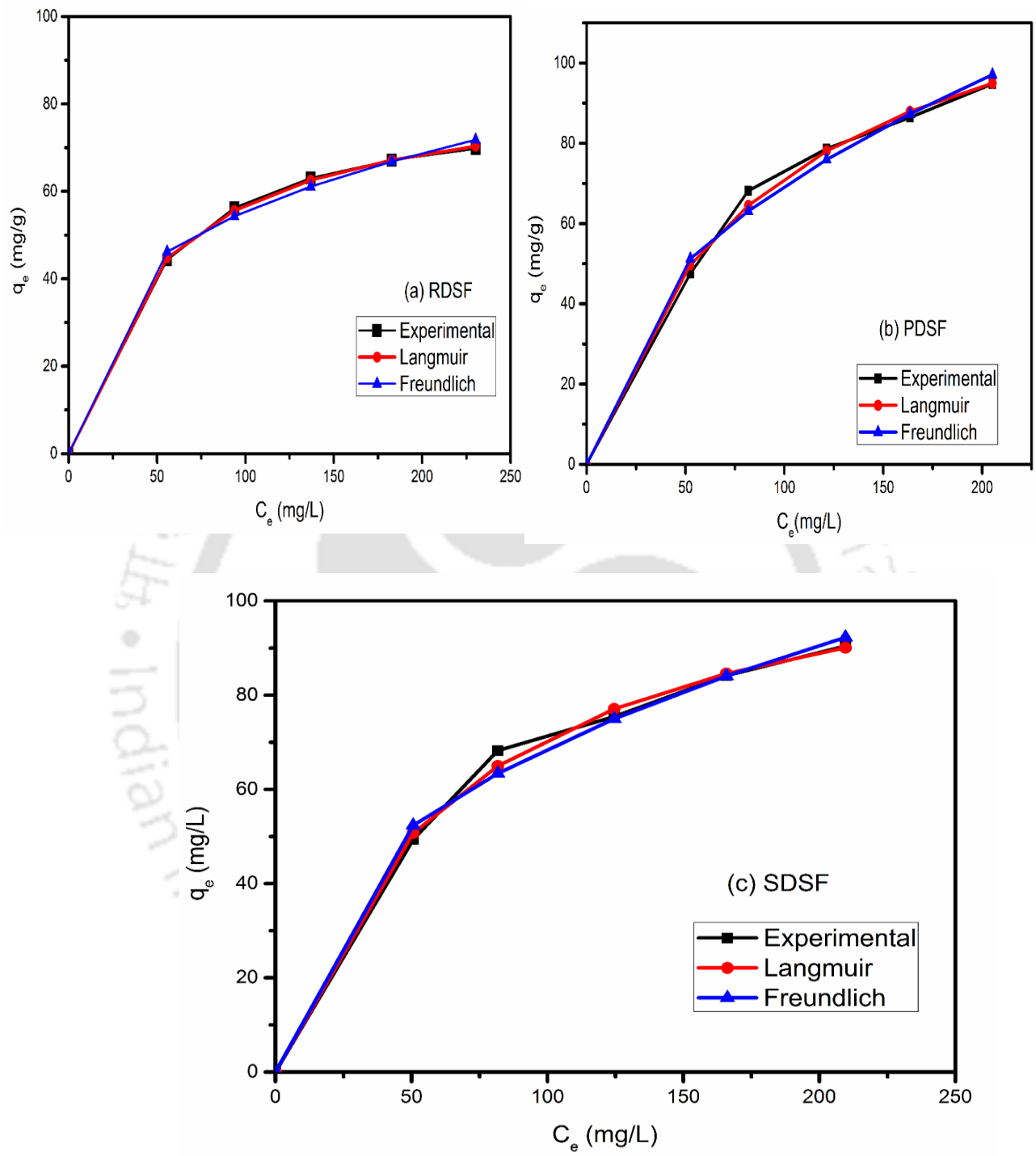

Fig. 5.9: Isotherm model curves fitted by non-linear regression analysis for Cr(VI) biosorption on RDSF, SDSF and PDSF biosorbents

Table 5.1: Biosorption isotherm constants obtained for various models obtained through linear regression analysis for Cr(VI) removal by RDSF, SDSF and PDSF biosorbents

Isotherm model	Parameters	RDSF	SDSF	PDSF
Langmuir	$Q_0\ (mg/g)$	84.745	119.05	135.0
	$b\ (L/g)$	0.020	0.014	0.011
	R^2	0.999	0.995	0.993
	R_L	0.329	0.406	0.471
Freundlich	$K_f\ (mg^{1-1/n}L^{1/n}/g)$	12.752	6.415	10.493
	n_f	3.137	2.451	1.950
	R^2	0.964	0.958	0.958
Dubinin - Radushkevich	$Q_m\ (mg/g)$	69.296	93.232	88.243
	$K_{DR}(mol^2/J^2)$	0.0002	0.0003	0.0002
	$E\ (KJ/mol)$	0.05	0.05	0.041
	R^2	0.971	0.977	0.964

Table 5.2: Langmuir and Freundlich isotherm parameters along with Chi-square value as observed by the error analysis method

Isotherm model	Parameters	RDSF	SDSF	PDSF
Langmuir	$Q_0\ (mg/g)$	85.916	119.632	138.074
	$b\ (L/g)$	0.020	0.015	0.011
	$\chi 2$	0.020	0.231	0.326
Freundlich	$K_f\ (mg^{1-1/n}L^{1/n}/g)$	13.245	10.954	8.029
	$1/n_f$	0.311	0.399	0.468
	$\chi 2$	0.266	0.564	0.828

5.6.3 Adsorption Kinetics

The mechanism and the rate-controlling steps of adsorption process over a series of contact time for different initial Cr(VI) concentrations was studied by adsorption kinetic models. Various kinetics models (pseudo-first-order, intraparticle diffusion model, and pseudo-second-order kinetics models) were selected to study the adsorption mechanism and the fittings of these models are shown in Fig. 5.10.

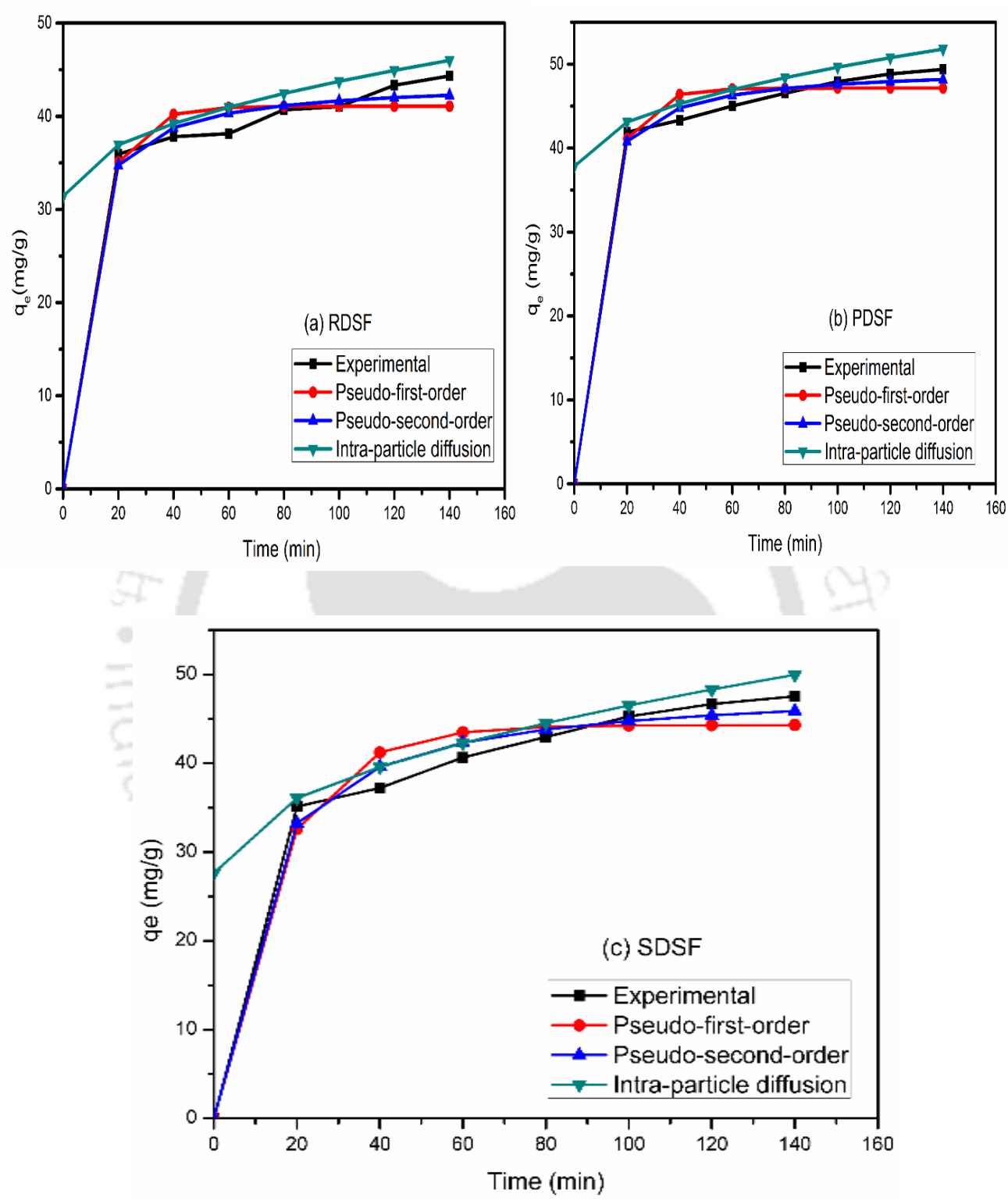

Fig. 5.10: Kinetics model curves fitted by non-linear approach for Cr(VI) biosorption onto RDSF, SDSF and PDSF biosorbents

5.6.3.1 Pseudo-First-Order Kinetics

Lagergren, (1898) proposed the pseudo-first-order model assuming that the rate of change in concentration of the reactants with time is directly proportional to gradient of solute in solution. The linear form empirical equation of pseudo-first-order is already explained in chapter-1.

The values of equilibrium metal concentration $q_{e(cal)}$, rate constant k_1, and coefficient of determination (R^2) can be obtained by plotting $log\ (q_e - q_t)$ against t (time). R^2 values of pseudo-first-order are presented in Table 5.3 which infer poor correlation coefficient for Cr(VI) adsorption. From Table 5.3, it can be indicated that calculated $q_{e(cal)}$ values were least fit with the experimental q_e values compared to other kinetic models.

5.6.3.2 Pseudo-Second-Order Kinetics

This model was proposed to study the chemical sorption mechanism by Ho and McKay [Ho and McKay, 1999]. The pseudo-second-order empirical equation is already discussed in chapter-1 and equation 1.16 and 1.17. The correlation coefficient R, and the calculated biosorption capacity at time t and at equilibrium, i.e., q_t and q_e respectively are listed in Table 5.3. The plot of t/q_t vs t is shown in Fig. 5.11 for the biosorption of Cr(VI) species onto the surface of RDSF, SDSF, and PDSF. Table 5.3 suggests that the R^2 value of pseudo-first-order is fitting poorly to the experimental data than the pseudo-second-order kinetics (closer to 1). Moreover, the predicated values of biosorption capacity at equilibrium mimic the experimental values. Therefore, it can be concluded that biosorption of Cr(VI) onto RDSF, SDSF, and PDSF is explained better by pseudo-second-order kinetics and chemisorptions may be the rate controlling step in biosorption which possibly occurred via electron exchange [Gonzalez et al., 2008].

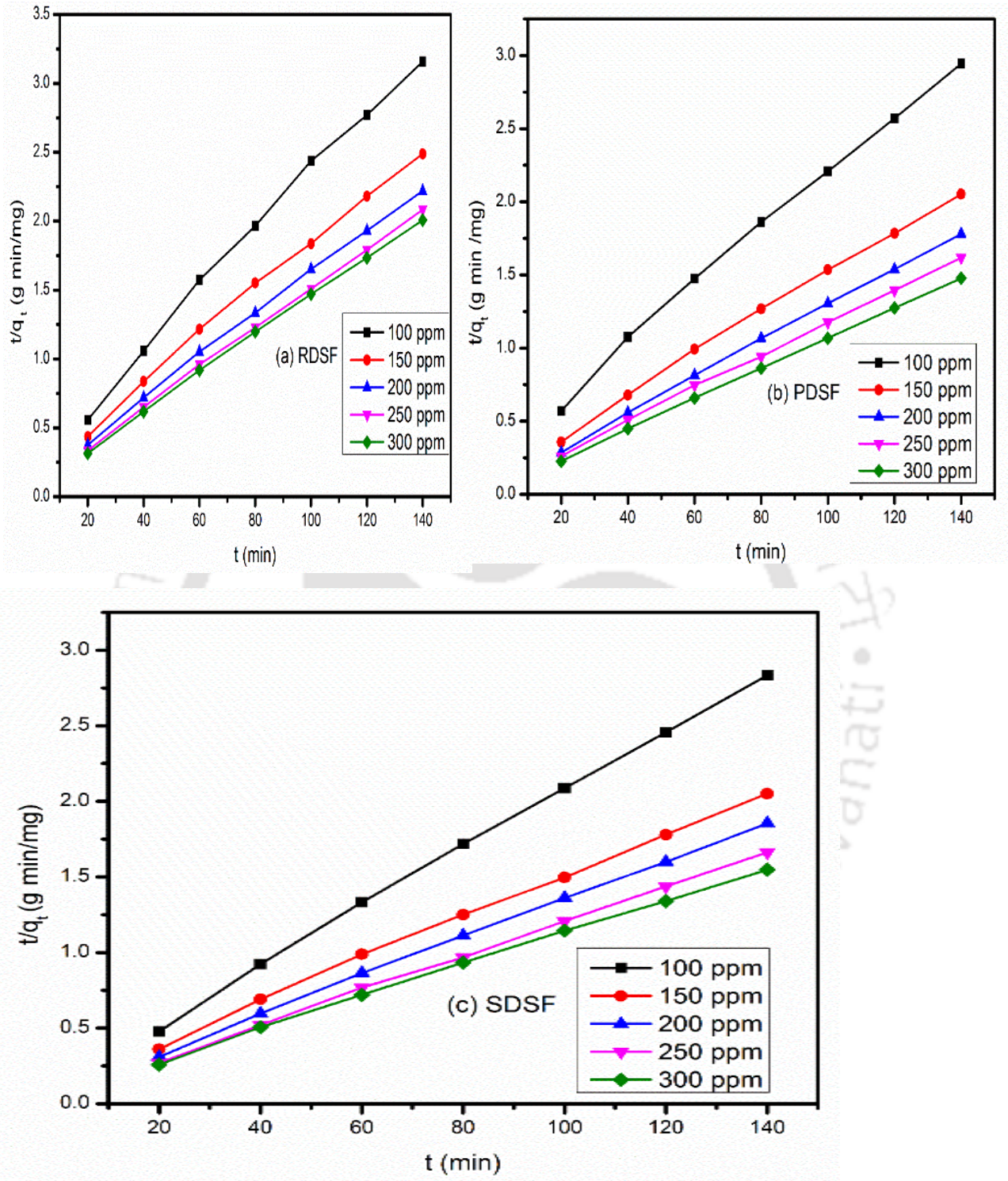

Fig. 5.11: Pseudo-second-order plots for adsorption of Cr(VI) onto the RDSF, SDSF and PDSF biosorbents

5.6.3.3 Intraparticle Diffusion Model

To understand the mass transfer mechanism onto the surface of RDSF, SDSF, and PDSF, intraparticle diffusion model was used. The mathematical expression of this model is described in chapter-1. The plot q_t against $\sqrt{t}$ was used to observe the data of K_{id} and C, which are represented in Table 5.3. It can be inferred from the results that the value of C increases as initial concentration of Cr(VI) ion increases. It is likely due to the increase in boundary layer thickness. The dual nature of the plot (Fig. 5.12) was credited to the adsorption phenomenon. If the plot q_t against $\sqrt{t}$ passes via origin, then it indicates that intraparticle diffusion process is the rate regulatory step in biosorption process; otherwise, it implies that some other mechanism also will be involved. In fact, the plot obtained is multi linear, indicating that biosorption of Cr(VI) is affected by more than one process. The first stage of graph suggested that an external mass transfer to the surface of absorbent from liquid solution is the rate determining step, whereas the second stage indicated pore diffusion or intraparticle diffusion is the rate controlling mechanism.

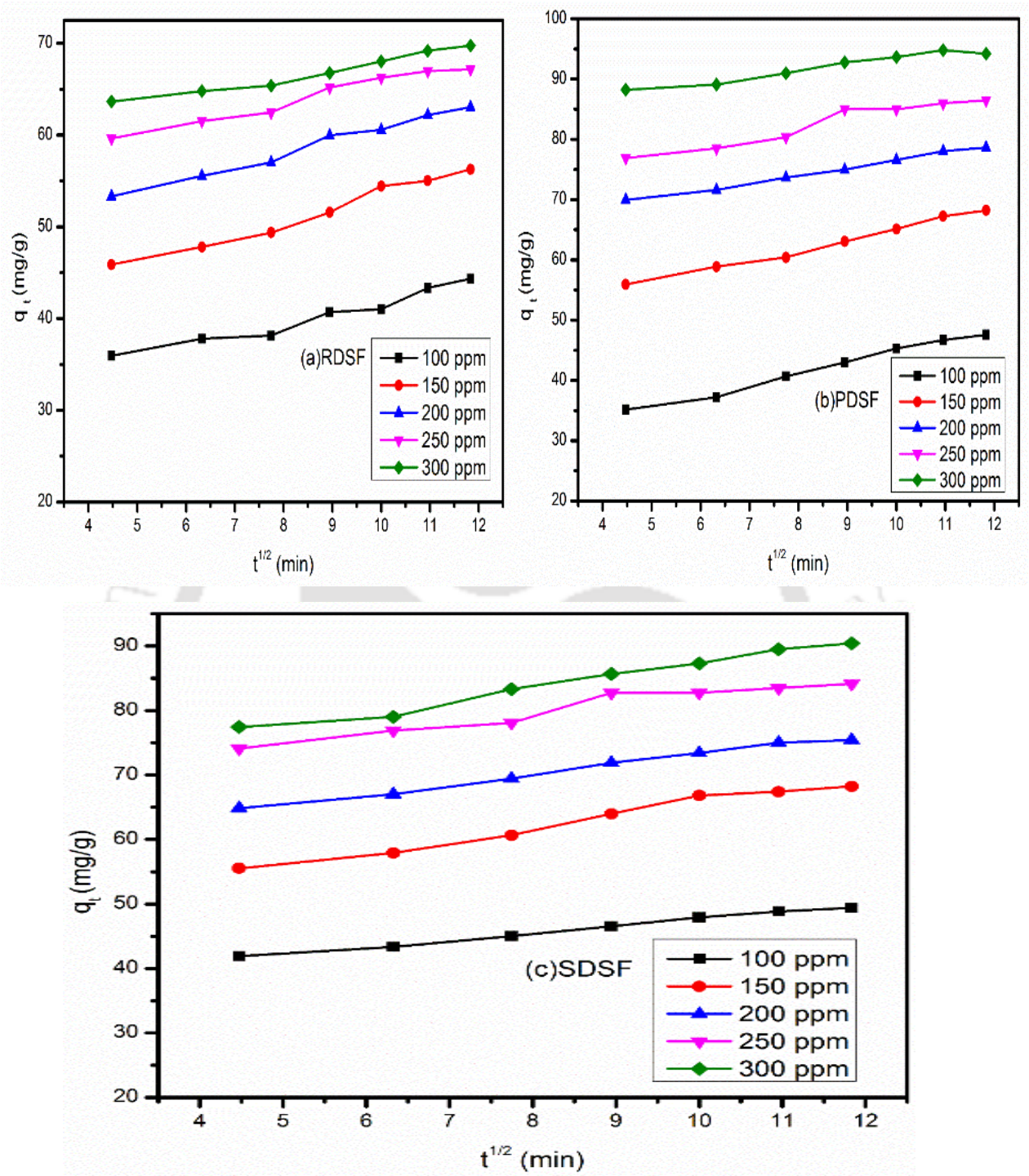

Fig. 5.12: Intraparticle diffusion model plots for the biosorption of Cr(VI) by RDSF, PDSF and SDSF biosorbents

5.6.3.4 Kinetic Model Analysis by Non-Linear Regression Analysis

Kinetic parameters were also evaluated by nonlinear regression analysis. The determined kinetic parameters values are summarized in Table 5.4. From Tables 5.3 and 5.4, it can be revealed that the values of R^2 and χ^2 of pseudo-second-order model are higher and lower respectively than the other kinetic models used in this study. In addition, the theoretical q_e values evaluated by pseudo-second order are closer to experimental values. Hence, both these observations implied that the adsorption of Cr(VI) on biosorbent is better described by pseudo-second-order model. These findings also suggested that the chemisorptions process may be the rate-limiting step and similar conclusions were observed by other researchers also [Bansal et al., 2009; Muthukumaran and Beulah, 2011].

Table 5.3: Estimated kinetic parameters for biosorption of Cr(VI) onto the raw and chemically modified Datura *(Datura Stramonium)* fruit surface

Sample	Cr(VI) Conc. (mg/L)	q_e (exp) (mg/g)	Pseudo first order			Pseudo-second-order			Intraparticle diffusion		
			k_1 (min^{-1})	$q_{e\ (cal)}$ (mg/g)	R^2	k_2 (g/mg/min)	$q_{e(cal)}$ (mg/g)	R^2	k_{id} (mg / g / min½)	C (mg/g)	R^2
RDSF	100	44.34	0.019	15.24	0.902	0.002	46.3	0.995	1.143	30.34	0.956
	150	56.26	0.022	13.53	0.93	0.002	59.17	0.997	1.492	38.63	0.978
	200	63.04	0.023	18.81	0.931	0.002	65.36	0.998	1.37	47.03	0.987
	250	67.16	0.035	24.22	0.896	0.003	69.44	0.999	1.116	54.56	0.968
	300	69.76	0.022	12.62	0.867	0.004	71.43	0.999	0.869	59.32	0.972
PDSF	100	49.39	0.025	16.33	0.931	0.003	51.28	0.998	1.081	36.83	0.992
	150	68.24	0.028	31.2	0.939	0.002	71.94	0.998	1.889	46.68	0.977
	200	75.44	0.03	27.93	0.883	0.002	78.13	0.999	1.542	57.74	0.99
	250	84.15	0.028	22.8	0.942	0.002	89.29	0.994	1.794	65.75	0.818
	300	90.43	0.025	28.48	0.912	0.002	94.34	0.999	0.114	75.54	0.97
SDSF	100	47.55	0.026	27.68	0.937	0.001	51.55	0.996	1.08	26.44	0.988
	150	68.2	0.023	25.36	0.893	0.002	71.43	0.997	1.721	47.87	0.991
	200	78.66	0.024	18.61	0.901	0.003	80.65	0.999	1.243	64.07	0.994
	250	86.45	0.029	25.83	0.895	0.002	92.59	0.99	1.95	67.06	0.714
	300	94.79	0.024	13.71	0.968	0.004	96.15	0.999	0.951	83.71	0.949

Table 5.4: Kinetic parameters determination using non-linear regression analysis

Sample	Cr(VI) Conc. (mg/L)	$q_{e\ (exp)}$ (mg/g)	Pseudo first order			Pseudo-second-order			Intraparticle diffusion		
			k_1 (min^{-1})	$q_{e(cal)}$ (mg/g)	χ^2	k_2 (g/mg/min)	$q_{e(cal)}$ (mg/g)	χ^2	k_{id} (mg / g / $min^{½}$)	C (mg/g)	χ^2
RDSF	100	44.34	0.096	41.08	0.738	0.004	43.833	0.340	1.143	30.34	0.667
PDSF		49.39	0.103	47.15	0.490	0.005	49.67	0.172	1.180	37.84	0.516
SDSF		47.55	0.067	44.31	1.208	0.002	49.01	0.440	1.888	27.64	0.511

5.7 Adsorption Thermodynamics

The thermodynamic studies were performed to understand the feasibility and thermal effect on biosorption process onto the surfaces of RDSF, SDSF and PDSF. Van't Hoff and Gibb's Helmholtz equations were used to analyze the thermodynamic process of biosorption [Pandey et al., 2010]. Thermodynamic mathematical expressions are already discussed in equation 1.19, 1.20 and 1.21. Calculated values of ΔG^0, ΔS^0, and ΔH^0 for the current study are represented in Table 5.5. Negative values of ΔG^0 indicated that biosorption process was spontaneous and favorable with the increase in temperature. The possible reason could be the faster diffusion of Cr(VI) ions from bulk solution phase to biosorbent at higher temperatures. ΔH^0 and ΔS^0 values (refer Table 5.5) were observed from the values of slope and intercept of lnK_C vs $1/T$ plot and it suggested that biosorption was endothermic and highly arbitrary in nature at the liquid–solid interface [Hasan et al., 2008; Rangabhashiyam and Selvaraju, 2015a, 2015b].

5.8 Determination of Activation Energy

The temperature dependence activation energy of adsorption was determined by the linear form of Arrhenius equation and it is expressed by the following equation [Argun and Dursun, 2008]

$$LnK_2 = \ln A - \frac{E_a}{RT} \tag{5.2}$$

Where K_2 denotes the rate constant of pseudo-second order model (g mg^{-1} min^{-1}), A indicates the Arrhenius factor, E_a represents the activation energy, T represents the solution temperature (K), and R is a gas constant (8.314 J mol^{-1} K^{-1}). The activation energy provides information about the type of adsorption process, i.e., whether it is chemical or physical [Argun and Dursun, 2008; Mahmoud, 2015].

It is also reported that the physisorption process normally requires less energy (0-40 kJ mol^{-1}) comparing to chemisorptions (40-800 kJ mol^{-1}) since the force involved between adsorbate and adsorbent is weak and the process rapidly attained the equilibrium. The activation energy is estimated from the slope of $ln\ K_2$ vs $1/T$ plot (Fig. not shown). The calculated activation energy values for sorption are found to be 0.192, 7.632, and 7.794 kJ mol^{-1} for RDSF, SDSF, and PDSF respectively which confirm that adsorption on the studied biosorbent is physical in nature.

In addition, it is evident from Table 5.1 that the mean free energy estimated by using Dubinin–Radushkevich model is also less than 8 kJ mol^{-1} which confirms that the adsorption is occurred by physical process in nature on adsorbents surface [Gupta et al., 2010].

Table 5.5: Thermodynamic parameters for biosorption of Cr (VI) onto the raw and chemically modified Datura *(Datura Stramonium)* fruit

Initial Cr concentration (mg/L)	Temp. (K)	RDSF				PDSF				SDSF			
		K_c	ΔG° (kJ/mol)	ΔH° (kJ/mol)	ΔS° (kJ/Kmol)	K_c	ΔG° (kJ/mol)	ΔH° (kJ/mol)	ΔS° (kJ/Kmol)	K_c	ΔG° (kJ/mol)	ΔH° (kJ/mol)	ΔS° (kJ/Kmol)
100 ppm	303	0.796	-0.249	1.680	0.004	0.975	-0.026	0.037	0.002	0.906	-0.107	0.864	0.031
	313	0.822	-0.220			0.976	-0.026			0.937	-0.073		
	323	0.862	-0.172			0.961	-0.045			0.947	-0.062		
	333	0.915	-0.106			0.984	-0.018			0.977	-0.027		
150 ppm	303	0.600	-0.558	2.194	0.005	0.834	-0.197	2.104	0.006	0.833	-0.198	2.155	0.006
	313	0.645	-0.495			0.938	-0.072			0.889	-0.133		
	323	0.663	-0.477			0.987	-0.014			0.977	-0.027		
	333	0.727	-0.383			0.992	-0.009			0.983	-0.020		
200 ppm	303	0.460	-0.848	4.229	0.011	0.605	-0.548	5.728	0.017	0.648	-0.474	3.437	0.009
	313	0.530	-0.716			0.684	-0.427			0.685	-0.426		
	323	0.567	-0.661			0.822	-0.336			0.758	-0.323		
	333	0.663	-0.493			0.963	-0.300			0.860	-0.181		
250 ppm	303	0.367	-1.095	4.435	0.011	0.507	-0.742	4.785	0.013	0.528	-0.697	5.070	0.014
	313	0.412	-1.002			0.627	-0.527			0.614	-0.549		
	323	0.478	-0.860			0.701	-0.413			0.716	-0.388		
	333	0.524	-0.776			0.755	-0.337			0.798	-0.270		
300 ppm	303	0.303	-1.306	3.967	0.008	0.431	-0.919	4.714	0.012	0.462	-0.844	4.207	0.011
	313	0.337	-1.227			0.524	-0.729			0.530	-0.715		
	323	0.374	-1.145			0.580	-0.633			0.585	-0.625		
	333	0.420	-1.040			0.640	-0.535			0.657	-0.505		

5.9 Desorption

Desorption studies reveal information about biosorbent's potential to be regenerated and reused for commercial scale application. One molar of HCl was used for the desorption of Cr(VI) from biosorbents. For this study, three consecutive adsorption–desorption cycles were performed. Protons (H^+) ions from HCl solution displaces the chelated Cr(VI) metal ion from the biosorbent's surface during regeneration process. The regeneration results revealed (shown in Fig. 5.13) a percentage reduction in adsorption capacity for each step of regeneration cycle such as the following: from 71.12% (1st cycle), 62.45% (2nd cycle), to 42.34% (3rd cycle) for PDSF; from 64.43% (1st cycle), 51.01% (2nd cycle), to 29.87% (3rd cycle) for SDSF; and from 52.54% (1st cycle), 34.70% (2nd cycle), to 12.09% (3rd cycle) for RDSF biosorbents. This is likely due to the structural changes of biosorbents' surface with the binding of Cr(VI) ions [Muthukumaran and Beulah, 2011; Pourfadakari et al., 2017].

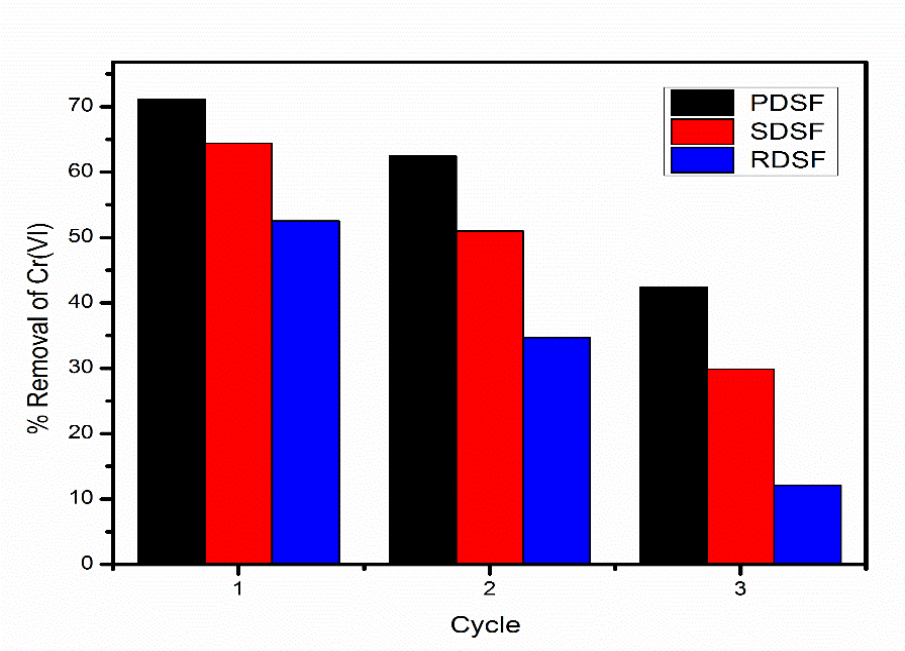

Fig. 5.13: Desorption of Cr(VI) loaded biosorbents for the reutilization process of Cr(VI) ions

5.10 Economic Study of the Adsorbent

According to the results obtained in the present study, 1 m^3 of Cr(VI)-containing wastewater could be treated by using 1.1 kg biosorbent amount derived from Datura *(Datura Stramonium)* fruit. The sorbent derived from Datura *(Datura Stramonium)* used in the present study has no cost associated with it. However, cost estimation for processing and transporting the biosorbents has been carried out by considering 1 kg of biosorbents and the cost involved in each step of preparation process is summarized in Table 5.6. Generally, the cost of the activated carbon utilized as an adsorbent for removing toxic metal from wastewater is approximately $2000 USD/ton in India [Rangabhashiyam and Selvaraju, 2015a, 2015b]. Considering the account of expense, it is clear from Table 5.6 that the cost of derived biosorbent from Datura *(Datura Stramonium)* is very low and reasonable ($124.51, $517.76, and $1079.01 USD/ton for RDSF, SDSF, and PDSF biosorbents respectively) compared to conventionally activated carbon. Hence, it can be inferred that the derived biosorbent from Datura *(Datura Stramonium)* fruit may be employed as an alternatively inexpensive potential biosorbent for removing Cr(VI) from wastewater.

5.11 Comparison with Other Adsorbents

Comparison of biosorption capacities of PDSF, SDSF, and RDSF with earlier reported biosorbents are shown in Table 5.7. It is observed that biosorption capacity of the prepared biosorbents is higher than the other reported biosorbents for removal of Cr(VI). The adsorption capacity is attributed to several important factors such as the extent of surface modification and physical characteristics of biosorbents.

Table 5.6: Cost estimation for the biosorbent derived from Datura *(Datura Stramonium)* fruit

Sr. No.	Material used	Unit cost (Rs.)	RDSF		SDSF		PDSF	
			Amount used	Net price (Rs.)	Amount used	Net price (Rs.)	Amount used	Net price (Rs.)
1	Transportation	4		4	-	-	-	-
2	Sulphuric acid	10/kG	0	0	1 kg	10	-	-
3	Phosphoric acid	50/kG	0	0	-	-	1 Kg	50
4	$NaHCO_3$	0.554/L	0	0	5L	2.77	5L	2.77
5	Cost of drying-1	5/KWh	0.83 KWh (80 °C for 24 h)	4.15	0.83 KWh (105 °C for 24 h)	4.15	0.83 KWh (110 °C for 24 h)	4.15
6	Cost of heating-1	5/KWh	-	-	4 KWh (105°C for 24 h)	20	-	-
7	Cost of heating-2	5/KWh	-	-	-	-	4 KWh (105°C for 24 h)	20
8	Net cost (Rs.)	-	-	8.96	-	36.91	-	76.92
9	Other charges (1% of net cost)	-	-	0.815	-	0.3691	-	0.7692
10	Total cost (Rs./Kg)	-	-	8.96	-	37.27	-	77.68
11	Total cost (US$/ton)	-	-	124.51	-	517.76	-	1079.01

Table 5.7: Comparison of adsorption capacity of biosorbents

Biosorbent	Solution pH	Biosorption capacity (mg g^{-1})	References
Chemically modified Swieteniamahagoni Shells (SSMS , PSMS, RSMS)	2	47.61, 58.82 and 37.03	[Rangabhashiyam et al., 2016]
Coconut coir	2	26.8	[Gonzalez et al., 2008]
Rice husk carbon (RHC) and saw dust carbon (SDC)	2	48.31 and 53.48	[Bansal et al., 2009]
Chemically Syzygiumjambolanum nut	2	39.81	[Muthukumaran et al., 2010]
CAC-S , OS-S	1.5	71.4 and 25.6	[Attia et al., 2010]
Neem sawdust	2	58.82	[Vinodhini and Das, 2010]
Melaleuca diosmifolia leaf	2	62.5	[Kuppusamy et al., 2016]
Tobacco-leaf	1	113.2	[Chen et al., 2009]
Mangrove leaf powder	2.0	60.24	[Sathish et al., 2015]
Boiled sunflower head	2	7.9	[Jain et al., 2009]
Peanut shell (P. Shell), sawdust and Cassia fistula leaves	2	4.32, 3.66 and 4.48	[Ahmad et al., 2017]
Humane hair	2	9.85	[Mondal et al., 2019]
Cranberry (Cornus mas) kernel shell (CKS), rosehip (Rosa canina) seed shell (RSS), and banana (Musa cavendishii) peel (BP)	2	10.42, 15.17, and 681	[Parlayic et al., 2019]
Acid activated banana peel (AABP) and organo-montmorillonite	4	15.1 and 6.67	[Ashraf et al., 2017]
Raw and activated chestnut shells	2	4.44 and 33	[Niazi et al.,2018]
RDSF	**2**	**85.91**	**Present study**
SDSF	**2**	**119.63**	**Present study**
PDSF	**2**	**138.07**	**Present study**

5.12 Conclusion

The present investigation is focused on potential of chemically modified and untreated biosorbent as low cost biosorbent for removal of Cr(VI) from wastewater. The chemical and physical characteristics of biosorbents were observed by various techniques like FTIR, SEM, and EDX. The equilibrium data is well explained by Langmuir isotherm model with high R^2 and low χ^2 value. The maximum monolayer biosorption capacity of Cr(VI) is 85.916, 119.632, and 138.074 mg g^{-1} on RDSF, SDSF and PDSF respectively at optimum pH 2.0. The kinetics analysis revealed that biosorption is better followed by pseudo-second-order model with high R^2 and low χ^2 value. Among all the studied biosorbents, PDSF showed the maximum adsorption capacity (Q = 138.074 mg g^{-1}). The estimated activation energy and mean free energy (by Dubinin–Radushkevich model) suggested that adsorption process is mainly governed by physisorption mechanism. Thermodynamic investigation indicated the feasibility, spontaneous, and endothermic nature of adsorption. The present studies showed that PDSF offers an economical and efficient alternative biosorbent for Cr(VI) biosorption from wastewater.

RESULTS AND DISCUSSION
CHAPTER - 6

Chapter-6
Performance of Acid Activated Water Caltrop (*Trapa Natans*) Shell in Fixed Bed Column for Hexavalent Chromium Removal from Simulated Wastewater

6. Results and Discussion

The removal of Cr(VI) from waste water using activated carbon derived from water caltrop shell using H_3PO_4 by continuous adsorption process is reported in this chapter. The preparation about the activated carbon from water caltrop shell is given in chapter- 3. The fixed bed study is performed in a glass column at optimum bed height and at given conditions. The details about column methodology are reported in chapter- 3, section 3.5.2 column experiments. In the present study, the effect of various parameters such as inlet flow, bed height and initial concentration of solute are investigated by pumping synthetic solution in up flow direction. Furthermore, the performance of column is studied by using breakthrough curve for the given conditions. In addition, the characterization of prepared adsorbent is investigated in the present study.

6.1 Characteristic Analysis of Adsorbent

6.1.1 Surface Area and CHNS Analysis

In order to evaluate the adsorptive capability of an adsorbent, surface area and functional groups of adsorbent's surface play an important role. The BET total pore analysis revealed that BET surface area and t-Plot micropore volume are 782.89 m^2g^{-1} and 0.134 cm^3 g^{-1}, respectively. In addition, the BJH adsorption and desorption average pore diameter are 3.26 nm and 3.15 nm,

respectively, which signifies that the adsorbent is mesoporous in nature. The percentage of *C*, *H*, *N*, and *S* of derived adsorbent are 46.14%, 6.69%, 3.09%, and 0%, respectively.

6.1.2 FESEM and EDX Analysis

The examination of the morphological properties of the adsorbent was performed by FESEM. Fig. 6.1a and 6.1b elucidates the micrograph of adsorbent prior and after uptake of Cr(VI) species. Prior to adsorption, the adsorbent surface has rough and porous surface morphology due to the presence of pores and cavities as shown in Fig. 6.1a. It is attributed to the release of volatile gases from the inner surface of biomass during its thermal decomposition which leads to rougher and porous surface of adsorbent. At the same time, after the Cr(VI) adsorption, these cavities tend to fill and thus the surface turns into smooth surface morphology as shown in Fig. 6.1b, and this result can also be supported by FTIR and EDX analysis. EDX spectral analysis is used to describe the qualitative elemental constitution. As shown in Fig. 6.2b, EDX revealed the presence of Cr(VI) species after the adsorption; however, no such characteristic peak of Cr(VI) was obtained before the adsorptions shown in Fig. 6.2a. Similar analysis and reasoning were reported by Majumder et al., [2017]. FTIR spectral analysis FTIR spectral analysis allows us to understand the interaction behavior of different functional groups on the adsorbent with metal ion. In order to observe the result, the biomass was complexed with KBr powder in the ratio of 1:100 (weight by weight) and spectral analysis were verified in the range of 4000–500 cm^{-1}. FTIR spectra of PWCS (activated adsorbent) prior and after the loading of Cr(VI) species show the complex nature of adsorbent as shown in Fig. 6.3a and 6.3b. The band peaks at 3450.23, 2867.91, 2346.91, 1713.86, 1546.51, 1384.46 and 1065.66 were assigned to O–H stretching, aliphatic C–H stretching, nitrile C≡N stretch, the C=O stretching, amide C–O stretching,

carboxylate anion C=O stretching, and CO of alcohols and carboxylic acids respectively [Singha et al., 2011]. As shown in FTIR spectra (Fig. 6.3b), the adsorption peak intensities of adsorbent after loading the Cr(VI) either decreased or shifted. For example, the adsorption peaks at 3450.23, 2867.91, 2346.91, 1713.86, 1546.51, 1384.46, and 1065.66 were shifted to 3434.33, 2827.02, 2351.47, 1738.85, 1551.81, 1197.42, and 999.78 cm^{-1}, respectively, indicating the involvement of these functional groups in binding of Cr(VI) ion on adsorbent.

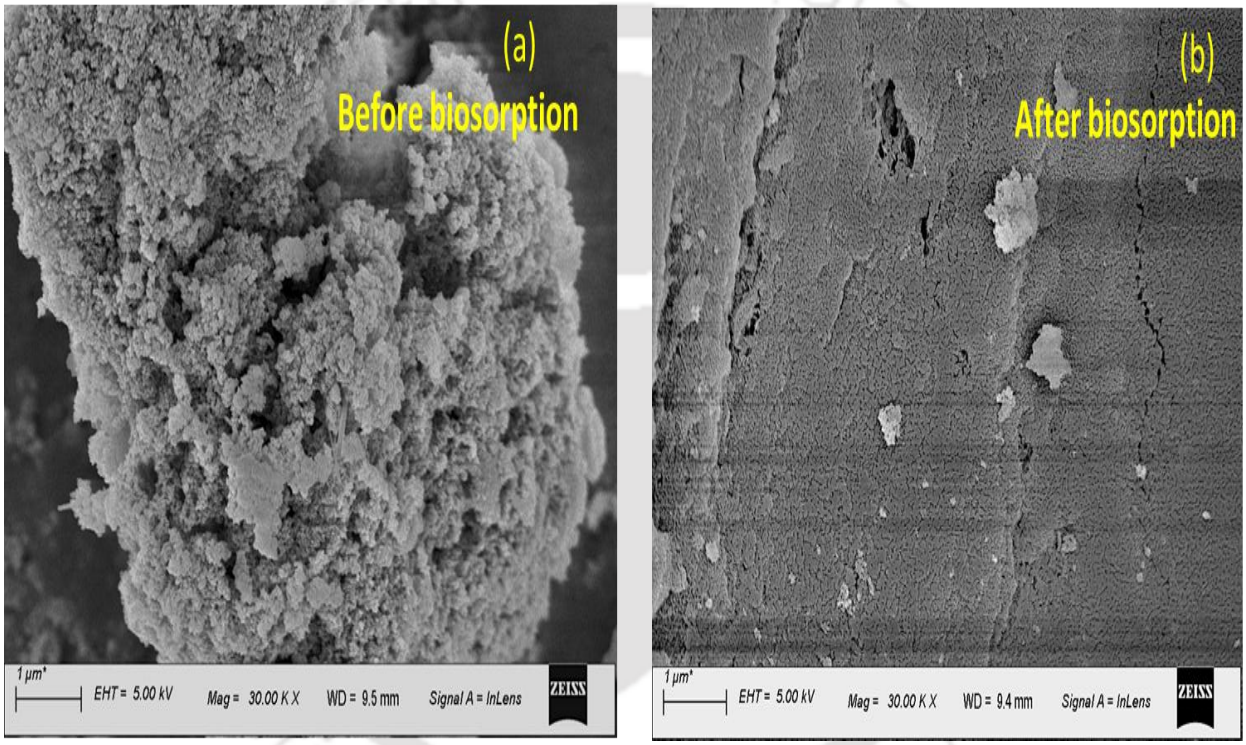

Fig. 6.1: SEM micrographs: (a) before adsorption and (b) after Cr (VI) loaded on PWCS

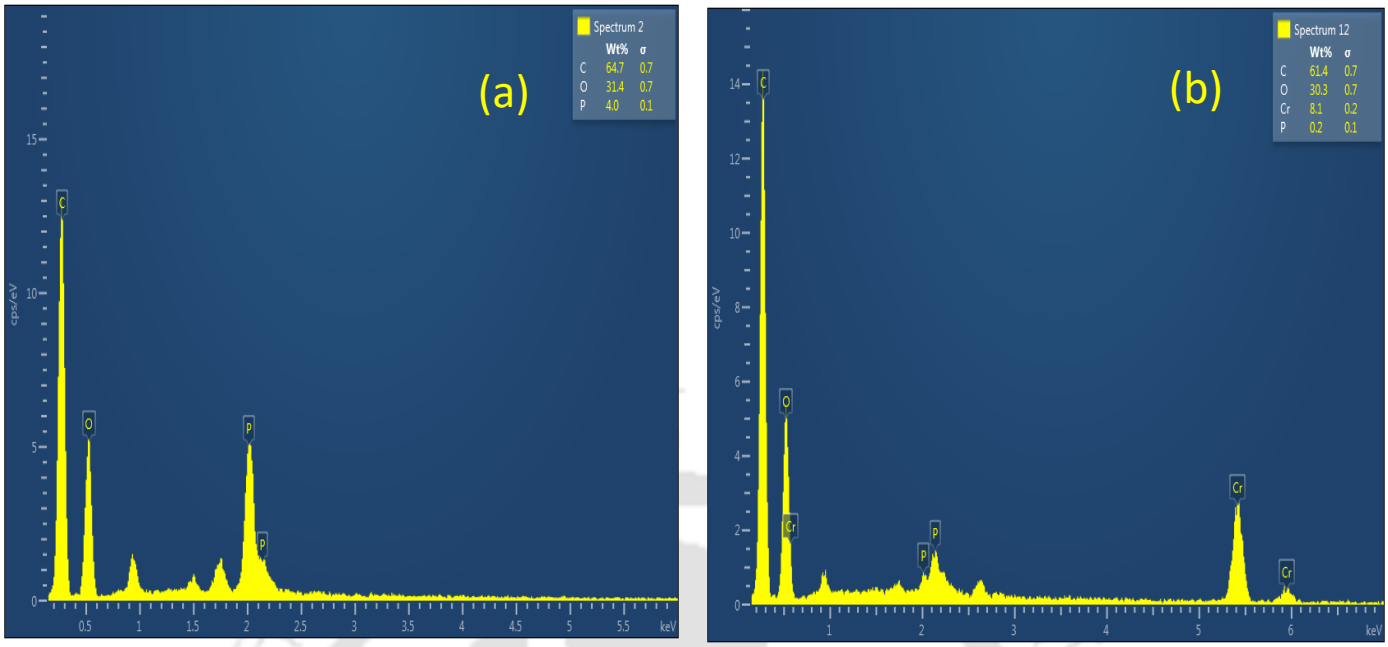

Fig. 6.2: (a) The EDS of PWC shell before adsorption, (b) EDS spectra of PWC shell after adsorption

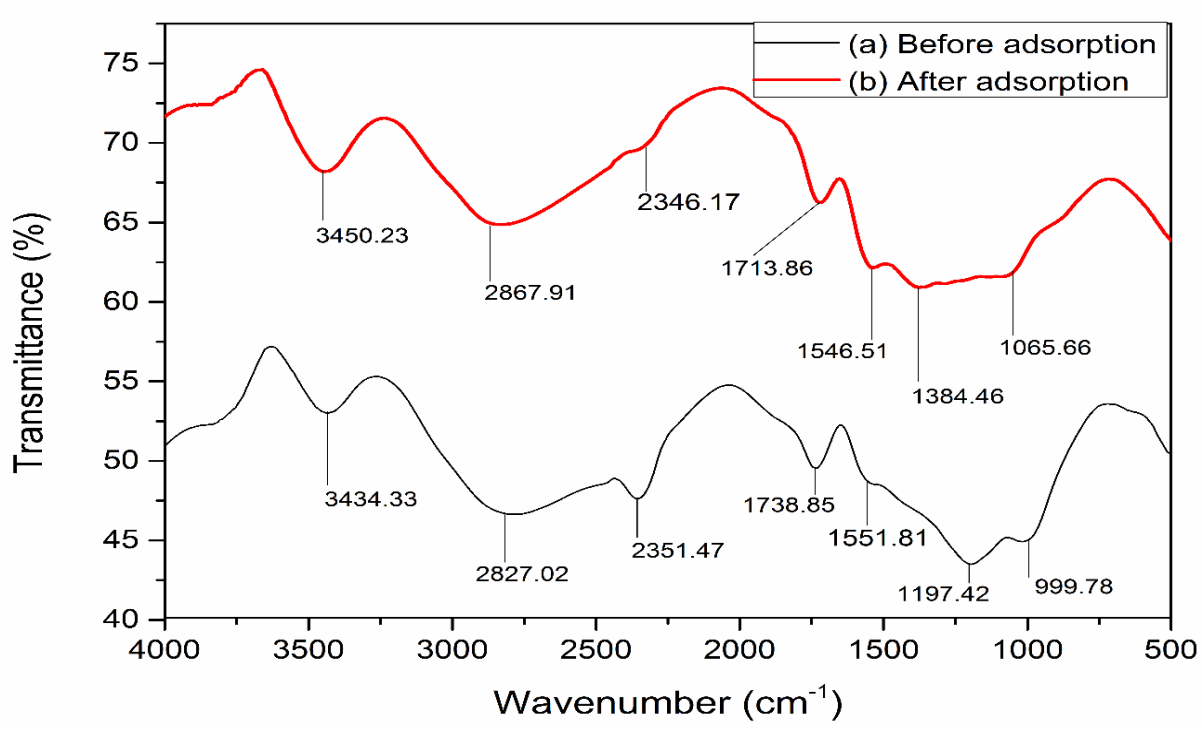

Fig. 6.3: The FTIR spectra of PWC shell before and after adsorption of Cr(VI)

6.2 Biosorption Influence Parameters in Packed Bed Column

In order to perform the experiment in packed bed column, the primary objective was to investigate the effect of several parameters like column bed height, inlet flow rate and initial metal concentration.

6.2.1 Influence of Column Bed Height

Adsorption of Cr(VI) ions in packed bed column was examined by altering the adsorbent's bed height in the column from 1 to 3 cm at initial sorbate concentration of 50 mg L^{-1} and at constant column flow rate of 2 mL min^{-1}. Moreover, 1, 2, and 3 g of PWCS powder were added to yield adsorbent column bed heights of 1, 2, and 3 cm, respectively. As elucidated in Fig. 6.4, elevated breakthrough time and exhaustion time were achieved with elevated adsorbent's column bed height. Furthermore, the adsorption capacity, volume treated, and percent removal on PWCS adsorbent for Cr(VI) removal increased with increased adsorbent's bed height, and the results are shown in Table 6.1. It may be because the increase in contact time of adsorbate with adsorbent due to increase in bed height allows more diffusion of Cr(VI) species into PWCS. However, increased bed height resulted in higher surface area which in turn provided more availability of active site on adsorbent surface for adsorption of Cr(VI) species. Similar analysis and reasoning were reported by Yüksel and Orhan [2019]; Nakkeeran et al., [2018].

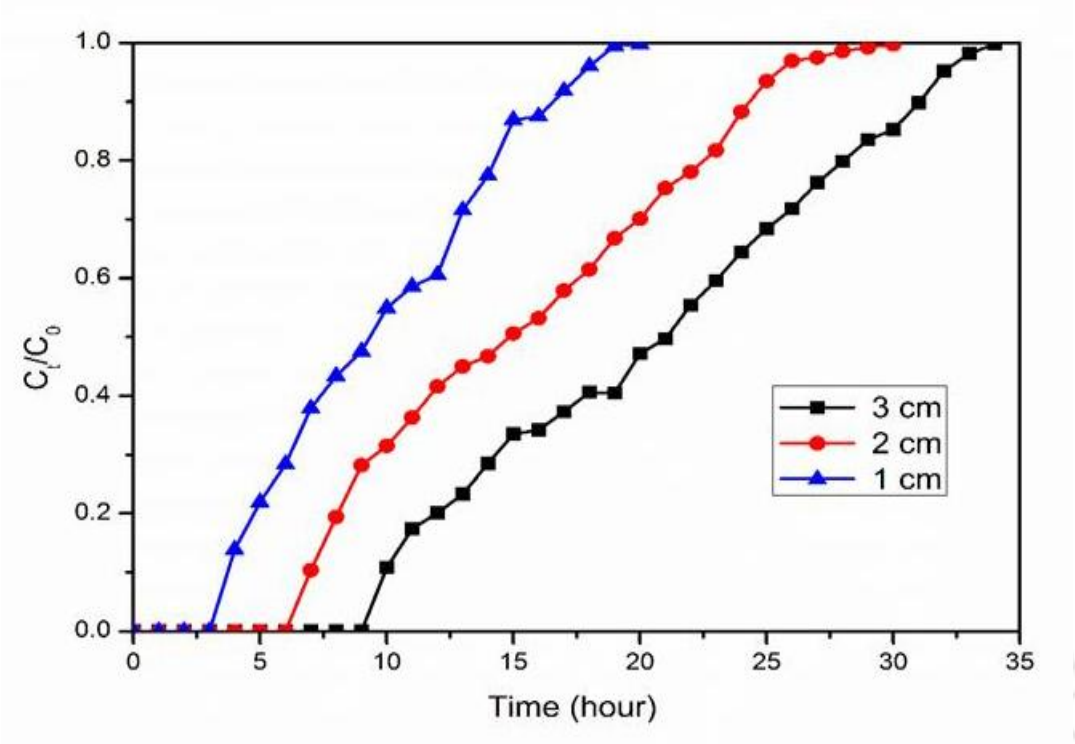

Fig. 6.4: Breakthrough curves of Cr(VI) removal by PWC shell for different bed depth

6.2.2 Influence of Sorbate Flow Rate

Efficient adsorptive performance of the packed bed column was significantly affected by sorbate flow rate. The sorbate's flow rate in the column was altered from 2 to 6 mL min^{-1} with an initial Cr(VI) ion concentration of 50 mg L^{-1} and with 2 cm of adsorbent's column bed height. Column breakthrough curve was achieved by plotting the C_t/C_0 versus *(t)* time as depicted in Fig. 6.5. Here, C_0 and C_t represent the Cr(VI) species concentration in the influent and effluent, respectively. Fig. 6.5 verifies the breakthrough time (t_b) and exhaustion point (t_e) of time have depreciated with elevated flow rates of influent. In addition, as flow rates of the influent elevated from 2.0 to 6.0 mL min^{-1}, this resulted in decreased Cr(VI) species removal efficiency from 51.06% to 48.59% as shown in Table 6.1. This attributes to the decreased sorbate–sorbent contact time and lowered external film mass resistance with increased influent rate. As a result,

Cr(VI) species leaving the adsorbent without being adsorbed in column from the effluent resulted in decreased saturation time. Similar consistency has been reported by other researches also like Banerjee et al., [2017]; Jain et al., [2013] and Rangabhashiyam et al., [2016].

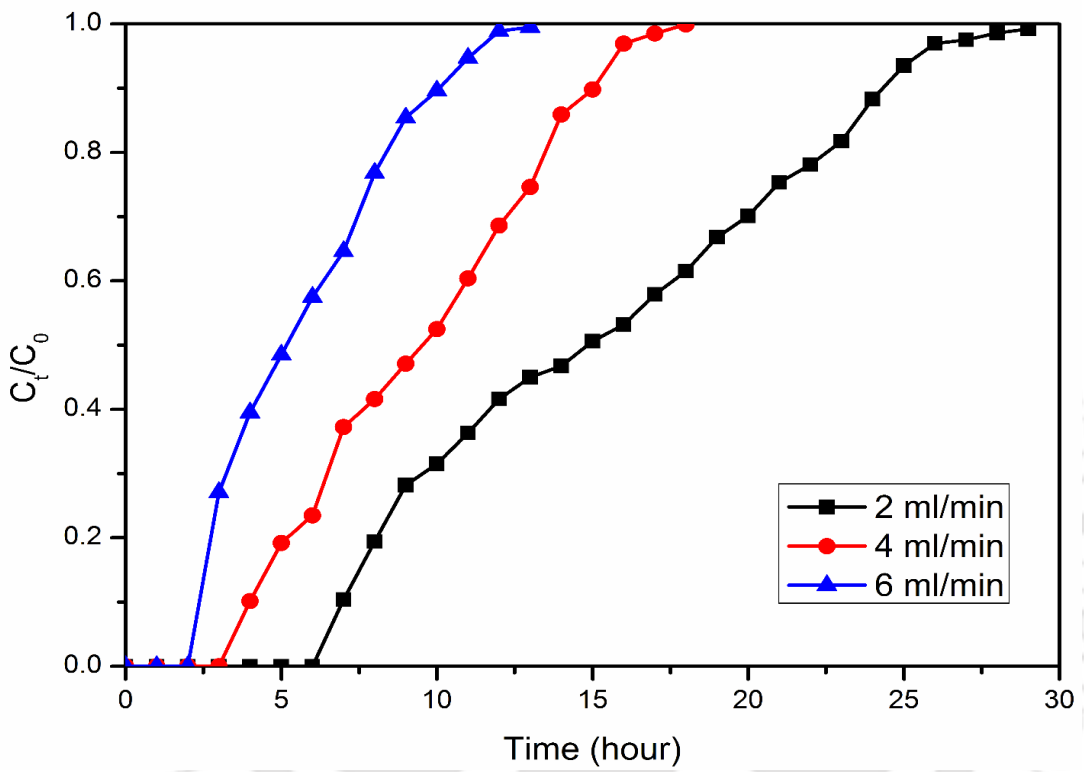

Fig. 6.5: Breakthrough curves of Cr(VI) removal by PWC shell for different flow rate

6.2.3 Influence of Inlet Cr(VI) Species Concentration

To study the influence of initial sorbate concentration, the Cr(VI) species concentration was altered from 50 to 150 mg L^{-1} while other variables were held constant such as sorbate flow rate of 2 mL min^{-1} and sorbent's column bed height of 2 cm. As depicted in Fig. 6.6, the fixed bed exhaustion time (t_e) and breakthrough time (t_b) depreciated from 29 to 19 hour and 7 to 2 hour, respectively, with elevating sorbate concentration from 50 to 150 mg L^{-1}. This could possibly be

due to quicker saturation of sorbate binding sites of PWCS at elevated sorbate concentration, hence breakthrough curve becomes steeper. As reported in Table 6.1, the Cr(VI) species removal efficiency reduced with elevated initial Cr(VI) species concentration. This may be due to the additional amount of solute entering in the column at high concentration while less amount was adsorbed on the adsorbent. The adsorption capacity of the column elevated with increased sorbent influent concentration. This could be due to concentration gradient of the Cr(VI) metal ion in the sorbate solution and on the adsorbent. Thus, higher inlet concentration causes more driving force which is responsible for elevated diffusion coefficients or mass transfer coefficients and hence adsorption capacity increased. Similar investigations have been carried out by Radnia, [2013], Jain et al., [2013], and Banerjee et al., [2017].

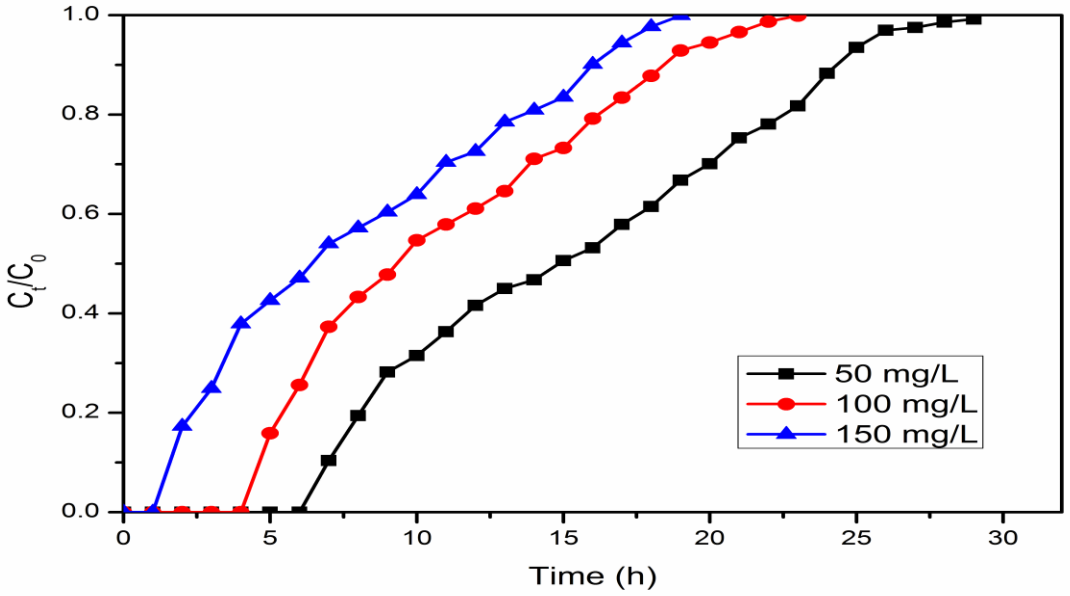

Fig. 6.6: Breakthrough curves of Cr(VI) removal by PWC shell for different initial Cr(VI) concentrations

Table 6.1: Column data analysis at various operating parameters for Cr(VI) adsorption using PWC shell

Z (cm)	Q (L/h)	C_0 (mg/L)	t_{total} (h)	m_{total} (mg)	q_{total} (mg)	$q_{e(exp)}$ (mg/g)	V_{eff} (mL)	Y (%)
1	0.12	50	21	126	64.33	64.33	2.52	51.06
2	0.12	50	29	174	91.27	45.63	3.48	52.46
3	0.12	50	35	216	122.63	40.87	4.32	56.78
2	0.24	50	18	216	113.29	56.64	4.32	52.45
2	0.36	50	13	234	102.00	51.00	4.68	43.59
2	0.12	100	23	276	127.80	63.90	2.76	46.30
2	0.12	150	19	342	140.40	70.20	2.28	41.05

6.3 Modeling of the Packed Bed Column Data

Breakthrough curves and dynamic behavior of column was investigated at given conditions like sorbate column flow rate, initial Cr(VI) species concentration, and adsorbent column bed height. Adsorption data thus obtained from the column study was analyzed by several column models like Adams–Bohart model, Thomas model, Yoon–Nelson model, and BDST model. The laboratory-scale result tested by these models could be used for industrial-grade fixed bed column design.

6.3.1 Thomas Model

This model has been widely employed to define the performance of the packed bed column and it follows the Langmuir assumption adsorption process without axial dispersion. It explains about the adsorption process which adheres to reversible second-order kinetics and the linear form of the equation can be represented as [Baral et al., 2009]. The empirical equation and detail about this model are discussed in chapter- 3, section 3.5.2 column study. The unknown values of K_{TH} and q_0 of Thomas equation was determined by slope and intercept, respectively, of linear plot for ln $((C_0/C_t) - 1)$ versus t using linear regression form (figures not shown) and results are tabulated in Table 6.2. Regression values (R^2) of this model range from 0.801 to 0.945 suggesting the best fit as compared to other models. Table 6.2 also denotes that as adsorbent's bed height of the column increased, q_0 values also elevated with reduction of K_{TH} values. Elevation in Cr(VI) initial concentration resorted to increased q0 values while reducing K_{TH} values. Adsorption driving force refers to difference of sorbate concentration on the adsorbent (PWCS) and in the solution. In addition, an elevated volumetric flow rate resulted in decreased q_0 values with increased K_{TH}. This possibly could be due to less residence time between the Cr(VI) ions and adsorbent in the packed column bed. Similar trends were reported by other researchers like Chen et al., [2012]; Zang et al., [2017] and Baral et al., [2009].

6.3.2 Adams–Bohart Model

Adams–Bohart model uses surface reaction theory to define the fundamental equations. It explains the initial breakthrough curve C_t/C_0 against t values of the fixed bed column. This approach is based on some assumptions like equilibrium does not occur suddenly and the extent of adsorption is proportionally related to the extent of vacant active sites left over the

adsorbent's surface [Goel et al., 2005; Sharma and Singh, 2013]. The ability of the adsorbent in adsorbing the sorbate molecules can be observed by the following equation: The mathematical expression of this model is given in chapter- 3, section 3.5.2 column study. The plot ln (C_t /C_0) versus time was used to determine the unknown parameters, i.e., K_{AB} and N_{AB} using slope and intercept, respectively, and the data for the same are tabulated in Table 6.2. As shown in Table 6.2, the elevated adsorbent's bed height of column as well as sorbate flow rate causes a decrease in value of N_{AB} and K_{AB}. In addition, elevated initial concentration of Cr(VI) species resulted in increased and decreased N_{AB} and K_{AB} values, respectively. Such results can be attributed to the external mass transfer in adsorption of Cr(VI) ions at initial part of the column. The determined linear regression values (R^2) ranged from between 0.880 and 0.920. Low values of R^2 suggest Bohart–Adams model is inappropriate in predicting the behavior of fixed bed column [Mahmoud, 2016].

6.3.3 Yoon–Nelson Model

Yoon–Nelson model assumes that the feasibility of reduced rate of sorption directly depends on the possibility of sorbate adsorption on the sorbent and the possibility of sorbate breakthrough on the sorbent surface [Chen et al., 2012]. Theory and mathematical expression about this model are explained in chapter- 1 and 3, under column study section. The two unknown parameters of Yoon–Nelson model, i.e., K_{YN} and τ can be verified from the linear plot of ln ($C_t/C_0 - C_t$) versus time using its slope and intercept, respectively, and the calculated data are as represented in Table 6.2. Table 6.2 verifies that the time needed to reach 50% breakthrough (τ) is elevated and the rate constant K_{YN} is reduced with the elevation of the adsorbent's bed height column. An increase in sorbate flow rate resulted in increased rate constant K_{YN} and decreased τ values.

These results attribute to quick saturation of packed bed column and less residence time of the Cr(VI) species in the adsorbent bed. Regression values (R^2) from Table 6.2 suggest the applicability of Thomas and Yoon–Nelson models for adsorption of Cr(VI) species in the fixed bed column. Similar analysis and reasoning were reported by other authors [Chen et al., 2012; Ahmad and Hameed, 2010].

Table 6.2: Parameters of various models for Cr(VI) adsorption by PWC shell in packed bed adsorption at various conditions

Experimental conditions			**Thomas model**			**Adams–Bohart model**			**Yoon–Nelson model**		
Z (cm)	**Q (L/h)**	**C_0 (mg/L)**	**q_0 (mg/g)**	**k_{TH} (L/mg-h)**	**R^2**	**N_{AB} (mg/L)**	**k_{AB} (L/mg-h)**	**R^2**	**k_{YN} (1/h)**	**τ (h)**	**R^2**
1	0.12	50	55.44	0.008	0.890	8340.88	0.0021	0.880	0.407	9.241	0.890
2	0.12	50	87.31	0.005	0.930	6141.86	0.0016	0.854	0.262	14.552	0.930
3	0.12	50	117.36	0.005	0.876	5042.04	0.0015	0.920	0.238	19.560	0.876
2	0.24	50	107.92	0.010	0.880	7524.31	0.0028	0.875	0.503	8.993	0.880
2	0.36	50	96.17	0.012	0.945	8178.71	0.0024	0.892	0.589	5.343	0.945
2	0.12	100	121.68	0.003	0.866	9578.00	0.0008	0.829	0.338	10.140	0.866
2	0.12	150	129.02	0.002	0.801	11993.78	0.0006	0.855	0.329	7.168	0.801

6.3.4 Bed Depth Service Time (BDST) Model

This model was studied to extend the laboratory-scale design for pilot-scale application to presume the behavior of fixed bed column. BDST model explains the physical adsorption without considering the external mass resistance and intraparticle mass transfer resistance [Vimala et al. 2011; Vinodhini and Das, 2010]. Mathematical expression is described in chapter-3, section 3.5.2 column study. The plot for service time versus bed height gave a straight line at the sorbate flow rate of 2 mL min^{-1} and it is represented in Fig. 6.7. Regression values (R^2 = 1) were calculated using linear regression, and it suggests the better fitting of BDST model for fixed bed column. Rate constant (K_a) and sorption capacity (N_0) were calculated using the intercept and slope from the straight-line equation of BDST model and data thus calculated are represented in Table 6.3. The observed values of K_a and N_0 were observed to be 0.043071 and 1433.121 respectively. Notably, if K_a values are large, a short column bed height will avoid the breakthrough while decreasing K_a values suggest the requirement of longer bed heights to avoid the breakthrough [Hasan et al., 2010]. BDST model parameters can be implemented for further pilot-scale trials.

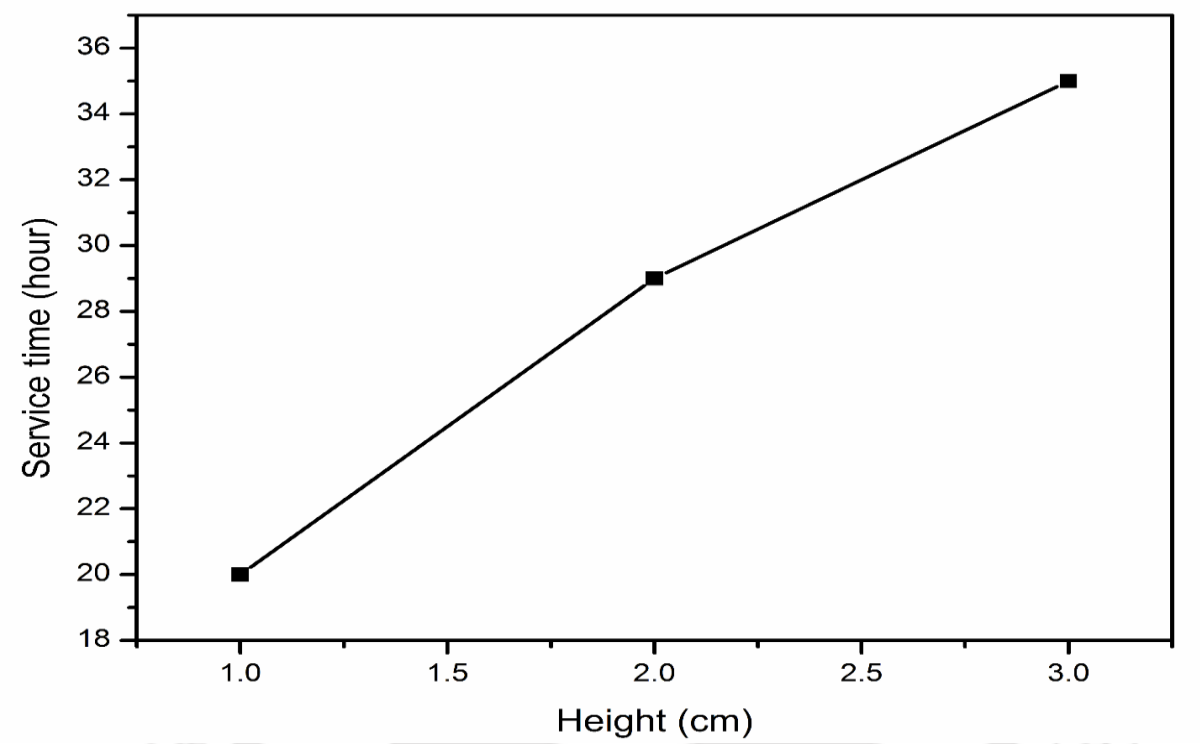

Fig. 6.7: Linear plots of bed depth service time model

Table 6.3: Bed depth service time (BDST) model parameters values

N_0 (mg/L)	K_a (L/mg h)	Slope	Intercept	R^2
3582.803	0.003313	7.5	13	0.9868

6.4 Conclusion

The present investigation verifies the activated carbon derived from phosphoric treated Water caltrop shell (*Trapa Natans*) (PWCS) waste as a adsorbent for efficiently removing Cr(VI) species from simulated solutions using fixed bed column. Influence of sorbate initial concentration, adsorbent's column bed height, and sorbate flow rate on breakthrough curves were studied for fixed bed column. A low initial metal ion concentration, a higher bed height, and a lower flow rate cause higher exhaustion time and breakthrough point. Adsorption efficiency (%) of Cr(VI) species elevated with rising bed height and it reduced with elevated influent Cr(VI) species and sorbent inlet flow rate. The experimental result revealed that percentage removal for Cr(VI) from aqueous solution having pH 2 and temperature 303.15 K was observed to be 52.46% at 2 cm height, 50 mg L^{-1} influent concentration, and 1.2 L h^{-1} flow rate. The maximum adsorption capacity was estimated to be 87.31 mg g^{-1} according to the Thomas model. Several mathematical models such as the Adams–Bohart, Thomas, Yoon–Nelson, and BDST model were used to verify the experimental data of fixed bed column. Performance of breakthrough curve was better explained by Thomas model due to its good correlation coefficient R^2 (0.801 - 0.945) than other models. The BDST model was successfully able to assume the parameters for design of pilot scale plant and observed K_a (L mg^{-1} h^{-1}) value and R^2 was 0.003 and 0.98, respectively. The study revealed that acid-treated Water caltrop (*Trapa Natans)* shell proved a efficient alternative for adsorption of Cr(VI) ion removal from simulated wastewater in a fixed bed column.

CONCLUSION AND FUTURE SCOPE
CHAPTER - 7

Chapter -7

Summary and Future Scope

7.1 Summary

The objective of the present study is to remove the Cr(VI) from waste water using alternative adsorbents which passes with following properties such as low cost, effective and easily available environmental friendly material. In order to search alternative adsorbents, water caltrop (*Trapa Natans*) shell and Datura (*Dataura Stramonium)* fruit were explored and experiments were carried out in batch and continuous modes. In addition, it is also aimed to evaluate the efficiency of derived activated carbon for removal of Cr(VI) from waste water.

The main conclusions drawn from the extensive experimental investigation are given as follow:

a) Water caltrop (*Trapa Natans*) and Datura (*Dataura Stramonium)* fruit containing high carbon and nitrogen percentage such as *C* = 46.14%, *N* = 3.09% and *C* = 44.66 %, *N* = 1.91 % respectively which proved to be a promising adsorbent and precursor for preparation of activated carbon.

b) Chemical activation was carried out by H_3PO_4 and H_2SO_4 to produce activated carbon of several surface characteristics.

c) Characterization of used biosorbents in this study was performed by several technologies such as Surface area analyzer, Scanning electron microscope (SEM), Energy-dispersive X-ray spectroscopy (EDS) and Fourier transform infrared spectroscopy (FT-IR). Characterization showed a rough and complex nature of biosorbents with several functional groups which facilitate Cr(VI) removal from waste water due to chemical or physical interaction in biosorption process.

Significant findings of investigation using aforementioned biosorbents are listed as below:

7.1.1 Cr(VI) Removal from Waste Water in Batch System Using Water Caltrop (*Trapa Natans*) Shell and Datura *(Datura Stramonium)* Fruit.

- The effect of various adsorption parameters such as pH, biosorbent dose, initial Cr(VI) concentration, particle size and temperature experiments were performed on uptake capacity of the developed novel biosorbents in Batch mode. In case of WC (*Trapa Natans*) shell biosorbent, the optimized parameters like pH, temperature, particle size, agitation speed, adsorbent doses, and initial Cr(VI) concentration, were found to be 2, 303 K, 150 mm, 100 rpm, 1 g L^{-1}, and 100 ppm respectively. Further, the optimized parameters like pH, temperature, adsorbent doses, initial Cr(VI) concentration for Datura *(Datura Stramonium)* fruit biosorbent were observed to be 2, 303 K, 1 g L^{-1}, 100 ppm respectively.

- Solution pH is an imperative parameter to control the biosorption of Cr(VI) as it is highly pH depended and the maximum adsorption was observed at pH 2 of solution.

- Various isotherms such as Langmuir, Freundlich and D-R model, and kinetic models like pseudo-first-order, pseudo-second–order and interparticle diffusion model are used to understand the biosorption behavior of different biosorbents when exposed to Cr(VI) solution in batch system.

- Among the tested isotherm and kinetics models, equilibrium data of water caltrop shell are better fitted with Langmuir isotherm (R^2 = 0.989) and pseudo-second-order (R^2 = 0.998) model with high correlation coefficient compared to that of other models.

- The low chi square χ^2 and the high R^2 values associated with nonlinear and linear transformed equation is obtained for Langmuir and pseudo-second-order models among all the tested models in the case of RDSF, PDSF and SDSF biosorbents for Cr(VI) biosorption.

- The maximum monolayer adsorption capacity of water caltrop shell was found to be 98.04 mg g^{-1} at pH 2 of solution.

- The maximum monolayer adsorption capacity was obtained as 85.916, 119.632 and 138.074 mg g^{-1} on RDSF, SDSF, and PDSF respectively at pH 2 of solution.

- The negative values of ΔG^o and positive values of ΔH^0 and ΔS^o obtained for all the tested biosorbents in batch system in this research confirms that biosorption of Cr(VI) was spontaneous , endothermic and randomness in nature.

- Chemically treated carbonized adsorbents showed the high monolayer adsorption capacity.

- To ensure the reuse possibility of adsorbents potential, multiple adsorptions-desorption cycle's process were performed using 0.1 M HCl eluant. The regeneration investigation for the WC (*Trapa Natans*) shell biosorbent showed better recyclable capacity up to five cycle with following adsorption capacity such as 52.77 mg g^{-1} (1^{st} cycle), 41.55 mg g^{-1} (2^{nd} cycle), 29.68 mg g^{-1} (3^{rd} cycle), 23.24 mg g^{-1} (4^{th} cycle), and 20.87 mg g^{-1} (5^{th} cycle). Further, the regeneration study for PDSF, SDSF and RDSF adsorbent revealed better reusability up to three cycle with following percentage removal like 71.12% (1^{st} cycle), 62.45% (2^{nd} cycle), to 42.34% (3^{rd} cycle) for PDSF, from 64.43% (1^{st} cycle), 51.01% (2^{nd} cycle), to 29.87% (3^{rd} cycle) for SDSF, and from 52.54% (1^{st} cycle), 34.70% (2^{nd} cycle), to 12.09% (3^{rd} cycle) for RDSF biosorbents.

- To know the economic viability of the adsorbent, cost analysis was performed to develop the adsorbents. The cost analysis associated with preparation of all the studied adsorbent likes WC (*Trapa Natans*) shell, RDSF, SDSF and PDSF was observed to be $ 93.39, $124.51, $517.76, and $1079.01 USD/ton respectively which are reasonable compared to commercially activated carbon.

7.1.2 Fixed Bed Study for Cr(VI) Removal by H_3PO_4 Treated Water Caltrop (*Trapa Natans*) Shell

- This research revealed that breakthrough time increases with increase in bed height and decreases with increase in inlet flow rate and initial metal concentration.

- The results further showed that the percentage removal of Cr(VI) increases with increase in bed height while decreases with increase in influent flow rate and initial Cr(VI) concentration.

- Thomas and Yoon–Nelson models are fitted better with experimental data obtained studies from column and it is appropriate for scaling up of fixed bed. According to Thomas model, the maximum adsorption capacity was found to be 87.31 mg g^{-1}

The research carried out in this present study precisely concluded that developed adsorbents in this work are economical, biodegradable, efficient and promising tool which act as potential adsorbent for the treatment of hexavalent chromium containing wastewater.

7.2 Future Scope

Biosorption process is a promising tool for sequestration of Cr(VI) from waste water. Therefore, to understand the large scale applicability and complex mechanism of biosorption process, further investigation is required.

Based on observed results of the present investigation, the following suggestions are given for future work:

1. To evaluate and optimize the packed bed column parameters with real effluent for commercial application.
2. To carry out biosorption studies with objective of removing multiple heavy metal pollutants from waste water.
3. To analyze the kinetics, isotherm and thermodynamics parameters for multiple heavy metal pollutants system.
4. To study the desorption properties of synthesize adsorbent at several temperature.
5. The developed adsorbent can also be tested for removal of dyes from effluent stream.

REFERENCES

References

1. Albadarin, A. B., Mangwandia, C., Al-Muhtaseb, A. H., Walkera, G. M., Allena, S.J., Ahmad, M. N. M.(2012). Kinetic and thermodynamics of chromium ions adsorption onto low-cost dolomite adsorbent. *Chemical Engineering Journal, 179, 193– 202.*

2. Anandkumar, J., Mandal B.(2009). Removal of Cr(VI) from aqueous solution using Bael fruit (Aegle marmelos correa) shell as an adsorbent. *Journal of Hazardous Materials, 168, 633–640.*

3. Ali , A., Saeed , K., Mabood, F. (2016). Removal of chromium (VI) from aqueous medium using chemically modified banana peels as efficient low-cost adsorbent. *Alexandria Engineering Journal, 55, 2933–2942.*

4. Abdelnaeim, M. Y., Sherif , I.Y. E., Attia , A. A., Fathy , N.A., Shahat, M.F. E. (2016). Impact of chemical activation on the adsorption performance of common reed towards Cu(II) and Cd(II). *International Journal of Mineral Processing, 157, 80–88.*

5. Abdolali, A., Ngo, H.H., Gao, W., Zhou, L. J., Du, B., Wei, Q.,Wang, C.X., Nguyen, D.P. (2015). Characterization of a multi-metal binding biosorbent: Chemical modification and desorption studies. *Bioresource Technology, 193, 477-487.*

6. Ahalya, N., Kanamadi R. D., and Ramachandra T. V. (2008). Biosorption of chromium (VI) by tamarindus indica pod shells. *Journal of Environmental Science Research International, 1 (2),77-81.*

7. Aliabadi, M., Khazaei, I., and Fakhraee, H. (2012). Hexavalent chromium removal from aqueous solutions by using low-cost biological wastes: equilibrium and kinetic studies. *Int. J. Environ. Sci. Technol, 9, 319–326.*

8. Abbas, S. H., Ismail, I. M., Mostafa, T. M., Sulaymon, A. H. (2014). Biosorption of Heavy Metals: A Review. *Journal of Chemical Science and Technology, 3 (4), 74-102.*

9. Altun, T., Pehlivan, E. (2012). Removal of Cr(VI) from aqueous solutions by modified walnut shells. *Food Chemistry, 132(2), 693-700.*

10. Ahmad, A., Ghazi, Z.A., Saeed, M., Ilyas, M., Ahmad, R., Khattak, A.M., Iqbal, A. (2017). A comparative study of the removal of Cr(VI) from synthetic solution using natural biosorbents. *New J. Chem., 41, 10799–10807.*

11. Akram, M., Bhatti,H. N., Iqbal , M., Noreen, S., Sadaf, S.(2017). Biocomposite efficiency for Cr(VI) adsorption: Kinetic, equilibrium and thermodynamics studies. *Journal of Environmental Chemical Engineering, 5(1), 400-411.*

12. Ashraf, A., Bibi,I., Niazi, N. K., Ok, Y. S., Murtaza, G., Shahid, M., Kunhikrishnan, A., Li D., and Mahmood T. (2017) . Chromium(VI) sorption efficiency of acid-activated banana peel over organo-montmorillonite in aqueous solutions. *International Journal of Phytoremediation, 19(7), 605-613.*

13. Amuda, O.S., Adelowo, F.E., Ologunde M.O. (2008). Kinetics and equilibrium studies of adsorption of chromium(VI) ion from industrial wastewater using Chrysophyllum albidum (Sapotaceae) seed shells. *Colloids and surfaces. B, Biointerfaces, 68(2), 184-192.*

14. Afroze, S., Sen, T.K., H. M. Ang, H.M. (2016). Adsorption performance of continuous fixed bed column for the removal of methylene blue (MB) dye using Eucalyptus sheathiana bark biomass. *Res Chem Intermed, 42, 2343–2364.*

15. Agarwal, G.S., Bhuptawat, H.K., Chaudhari, S.(2006). Biosorption of aqueous Cr(VI) by Tamarindus indica seeds. *Bioresource Technology, 97, 949–956.*

16. Arul, N. M., Alemu, A.K.,Goswami, L., Pakshirajan, K., Pugazhenthi, G. (2016). Waste Litchi Peels for Cr(VI) removal from synthetic wastewater in batch and continuous systems: sorbent characterization, regeneration and reuse study. *Journal of Environmental Engineering, 142, C4016001–11.*

17. Apiratikul, R., and Pavasant, P. (2008). Batch and column studies of biosorption of heavy metals by Caulerpa lentillifera. *Bioresource Technology, 99, 2766–2777.*

18. Argun, M. E., and Dursun, S. (2008). A new approach to modification of natural adsorbent for heavy metal adsorption. *Bioresource Technology, 99, 2516–2527.*

19. Attia, A. A., Khedr, S. A., and Elkholy, S. A. (2010). Adsorption of chromium ion (VI) by acid activated carbon. *Brazilian Journal of Chemical Engineering, 27, 183–193.*

20. Ahmad, A.A., Hameed, B.H. (2010). Fixed-bed adsorption of reactive azo dye onto granular activated carbon prepared from waste. *J Hazard Mater, 175,298–303.*

21. Barakat, M.A. (2011). New trends in removing heavy metals from industrial wastewater. *Arabian Journal of Chemistry, 4, 361–377.*

22. Babula, P., Adam, V., Opatrilova, R., Zehnalek, J., Havel, L., and Kizek, R. (2008). Uncommon heavy metals, metalloids and their plant toxicity: a review. *Environmental Chemistry Letters, 6 (4), 189–213.*

23. Balan, C., Volf, I., Bilba , D. (2013). Chromium (VI) Removal From Aqueous Solutions By Purolite Base Anion-Exchange Resins With Gel Structure. *Chemical Industry & Chemical Engineering Quarterly, 19 (4), 615−628.*

24. Banerjee, M., Basu, R. K., Das, S. K. (2018). Cr(VI) adsorption by a green adsorbent walnut shell: Adsorptionstudies, regeneration studies, scale-up design and economic feasibility. *Process Safety and Environmental Protection, 116, 693–702.*

25. Bishnoi, N. R., Bajaj, M., Sharma, N., Gupta, A . (2004). Adsorption of Cr(VI) on activated rice husk carbon and activated alumina. *Bioresource Technology, 91, 305–307.*

26. Bhatnagar, A., Minochaa, A.K. (2017). Biosorption optimization of nickel removal from water using Punica granatum peel waste. *Colloids and Surfaces B: Biointerfaces, 76, 544–548.*

27. Bohart, G.C., Adams, E.Q. (1920). Some aspect of the behavior of charcoal with respect to chlorine. *J. Am. Chem. Soc. 42,523–529.*

28. Baral, S.S., Das, N., Ramulu, T.S., Sahoo, S.K., Das, S.N., Chaudhury, G.R. (2009). Removal of Cr(VI) by thermally activated weed Salvinia cucullata in a fixed-bed column. *Journal of Hazardous Materials 161 (2009) 1427–1435.*

29. Bind, A., Goswami, L., and Prakash, V. (2018). Comparative analysis of floating and submerged macrophytes for heavy metal (copper, chromium, arsenic and lead) removal: sorbent preparation, characterization, regeneration and cost estimation. *Geology, Ecology, and Landscapes, 2(2), 61-72.*

30. Brunauer, S., Emmett,P. H., and Teller, E.(1938). Adsorption of gases in multimolecular layers. *Journal of the American Chemical Society 60(2), 309–319.*

31. Bhaumik, M., Setshedi ,K., Maity, A., Maurice S., Onyango, M.S. (2013). Chromium(VI) removal from water using fixed bed column of polypyrrole / Fe_3O_4 nanocomposite. *Separation and Purification Technology, 110, 11–19.*

32. Bansal, M., Singh, D., Garg, V.K. (2009). A comparative study for the removal of hexavalent chromium from aqueous solution by agriculture wastes' carbons. *Journal of Hazardous Materials, 171, 83–92.*

33. Burakov, A.E., Galunin, E.V., Burakova, I.V., Kucherova, A. E., Agarwal,S., Tkachev, A.G., Gupta V.K. (2018) . Adsorption of heavy metals on conventional and nano structured materials for wastewater treatment purposes: A review. *Ecotoxicology and Environmental Safety ,148, 702-712.*

34. Barkakati, P., Begum, A., Das, M.L., Rao, P.G. (2010). Adsorptive separation of Ginsenoside from aqueous solution by polymeric resins: equilibrium, kinetic and thermodynamic studies. *Chemical Engineering Journal, 161, 34–45.*

35. Bansal, M., Singh, D., Garg, V.K., Rose, P. (2008). Mechanisms of Cr(VI) removal from synthetic wastewater by low cost biosorbents. *Journal of Environmental Research and Development, 3, 228–243.*

36. Blazquez, G., Hernáinz, F., Calero, M., Martín-Lara, M. A., and Tenorio, G. (2009). The effect of pH on the biosorption of Cr (III) and Cr (VI) with olive stone. *Chemical Engineering Journal, 148, 473–479.*

37. Banerjee, M., Bar, N., Basu, R.K., Das, S.K. (2017). Comparative study of adsorptive removal of Cr(VI) ion from aqueous solution in fixed bed column by peanut shell and almond shell using empirical models and ANN. *Environ Sci Pollut Res Int., 24,10604–10620.*

38. Chen, J., Yang, P., Song, D., Yang, S., Zhou, L., Han, L., Lai, B. (2014). Biosorption of Cr(VI) by carbonized Eupatorium adenophorum and Buckwheat straw: thermodynamics and mechanism. *Frontiers of Environmental Science & Engineering, 8, 960–966.*

39. Chwastowski, J., Staroń, P., Kołoczek, H., Banach, M., (2017). Adsorption of hexavalent chromium from aqueous solutions using Canadian peat and coconut fiber. *Journal of Molecular Liquids, 248, 981-989.*

40. Chen, S., Yue, Q., Gao, B., Li, Q., Xu, X., Fu, K., (2012). Adsorption of hexavalent chromium from aqueous solution by modified corn stalk: a fixed-bed column study. *Bioresource Technology, 113, 114-120.*

41. Chen, Y., Tang, G., Yu, Q.J., Zhang, T., Chen, Yan, Gu, T.,(2009). Biosorption properties of hexavalent chromium on to biomass of tobacco-leaf residues. *Environmental Technology, 30, 1003–1010.*

42. Cimino, G., Passerini , A., Toscano G., (2000) . Removal of Toxic Cations and Cr(VI) from Aqueous Solution by Hazelnut Shell. *Water Research, 34(11), 2955-2962.*

43. Chowdhury, S., Mishra, R., Saha, P., Kushwaha, P. (2011). Adsorption thermodynamics, kinetics and isosteric heat of adsorption of malachite green onto chemically modified rice husk. *Desalination, 265, 159–168.*

44. Chen, Z., Ma, W., & Han, M. (2008). Biosorption of nickel and copper onto treated alga (Undaria pinnatifida): application of isotherm and kinetic models. *Journal of Hazard Materials, 155, 327–333.*

45. Chen,Y., Tang,G.,Yu,Q. J., Zhang, T., Chen,Y., and Gu, T. (2009). Biosorption properties of hexavalent chromium on to biomass of tobacco-leaf residues. *Environmental Technology, 30, 1003–1010.*

46. Chen, S., Yue, Q., Gao, B., Li, Q., Xu, X., Fu, K. (2012). Adsorption of hexavalent chromiumfrom aqueous solution bymodified corn stalk: a fixed-bed column study. *Bioresour. Technol., 113:114–120.*

47. Demirbas, A. (2008). Heavy metal adsorption onto agro-based waste materials: A review. *Journal of Hazardous Materials, 157(2–3), 220-229.*

48. Das, A.P., Singh, S. (2011). Occupational health assessment of chromite toxicity among Indian miners. *Indian Journal of Occupational and Environmental Medicine, 15(1), 6-13.*

49. Dhal, B., Thatoi, H. N., Das, N.N., Pandey B.D. (2013). Chemical and microbial remediation of hexavalent chromium from contaminated soil and mining/metallurgical solid waste: A review. *Journal of Hazardous Materials, 250– 251, 272– 29.*

50. Das, A. P., and Mishra, S. (2008). Hexavalent Chromium (VI) : Environment Pollutant And Health Hazard. *Journal of Environmental Research and Development, 2(3), 386-39.*

51. Dong, X., Ma, L. Q., Yuncong Li, Y. (2011). Characteristics and mechanisms of hexavalent chromium removal by biochar from sugar beet tailing. *Journal of Hazardous Materials, 190, 909–915.*

52. Dias, J. M., Alvim-Ferraz, M. C. C. M., Almeida, M. F., Utrilla, J. R. (2007). Manuel Sánchez-Polo. Waste materials for activated carbon preparation and its use in aqueous-phase treatment: A review. *Journal of Environmental Management , 85(4), 833-846.*

53. Doke, K. M., Khan, E.M. (2017). Equilibrium, kinetic and diffusion mechanism of Cr(VI) adsorption onto activated carbon derived from wood apple shell. *Arabian Journal of Chemistry,10(1),S252-S260 .*

54. Dai, Y., Sun, Q., Wang, W., Lu, L., Liu, M., Li, J., Yang, S., Sun, Y., Zhang, K., Xu, J., Zheng, W., Hu, Z., Yang, Y., Gao, Y., Chen, Y., Zhang, X., Gao, F., Zhang, Y. (2018). Utilizations of agricultural waste as adsorbent for the removal of contaminants: A review. *Chemosphere, 211, 235-253.*

55. Dubey, S. P., Gopal, K. (2007). Adsorption of chromium(VI) on low cost adsorbents derived from agricultural waste material: A comparative study. *Journal of Hazardous Materials, 145(3), 465-470.*

56. Dehghani, M.H., Sanaei, D., Ali, I., Bhatnaga, A. (2016). Removal of chromium(VI) from aqueous solution using treated waste newspaper as a low-cost adsorbent: Kinetic modeling and isotherm studies. *Journal of Molecular Liquids, 215, 671-679.*

57. Dabrowski, A., Hubicki, Z., Podkoscielny, P., Robens, E. (2004). Selective removal of the heavy metal ions from waters and industrial wastewaters by ion-exchange method. *Chemosphere, 56, 91–106.*

58. Dąbrowski, A. (2001). Adsorption from theory to practice. *Advances in Colloid and Interface Science, 93,135–224.*

59. Dada, A. O., Olalekan, A. P., Olatunya, A.M., and Dada, O. (2012). Langmuir, Freundlich, Temkin and Dubinin–Radushkevich isotherms studies of equilibrium sorption of zn^{2+} unto phosphoric acid modified rice husk. *IOSR Journal of Applied Chemistry, 3(1), 38 -45.*

60. Enniya, I., Rghioui, L., Jourani A. (2018). Adsorption of hexavalent chromium in aqueous solution on activated carbon prepared from apple peels. *Sustainable Chemistry and Pharmacy, 7, 9-16 .*

61. Elangovan, R., Philip, L., Chandraraj, K. (2008). Biosorption of chromium species by aquatic weeds: kinetics and mechanism studies. *Journal of Hazardous Materials, 152, 100–112.*

62. Fu , F., Wang, Q. (2011). Removal of heavy metal ions from wastewaters: A review. *Journal of Environmental Management, 92, 407-418.*

63. Feng, B., Shen, W., Shi, L., and Qu, S. (2018). Adsorption of hexavalent chromium by polyacrylonitrile-based porous carbon from aqueous solution. *R. Soc. open sci., 5, 171662. http://dx.doi.org/10.1098/rsos.171662*

64. Fomina, M., Gadd, G.M . (2014). Biosorption: current perspectives on concept, definition and application. *Bioresource Technology, 160, 3–14.*

65. Fawzy, M., Nasr, M., Gaber, A.A., and Fadly, S. (2016). Biosorption of Cr(VI) from aqueous solution using agricultural wastes, with artificial intelligence approach. *Separation Science and Technology, 51(3), 416-426.*

66. Ferreira, G. L.R., Vendruscolo, F., Filho, N. R. A. (2019). Biosorption of hexavalent chromium by Pleurotus ostreatus. *Heliyon, 5(3), e01450. doi:10.1016/j.heliyon.2019.e01450*

67. Foo, K.Y., Hameed, B.H. (2010). Insights into the modeling of adsorption isotherm systems. *Chemical Engineering Journal, 156, 2–10.*

68. Freundlich, H., Helle, W. (1939). On adsorption in solution. *Journal of the American Chemical Society, 61, 2228–2230.*

69. Febrianto, J., Kosasih, A. N., Sunarso, J., Ju, Y.H., Indraswati , N., Ismadjia, S. (2009). Equilibrium and kinetic studies in adsorption of heavy metals using biosorbent: A summary of recent studies. *Journal of Hazardous Materials, 162, 616–645.*

70. Fan, T., Liu, Y., Feng, B., Zeng, G., Yang, C., Zhou,M., Zhou, H., Tan, Z., Wang , X. (2008).Biosorption of cadmium(II), zinc(II) and lead(II) by Penicillium simplicissimum: Isotherms, kinetics and thermodynamics. *Journal of Hazardous Materials, 160 , 655–661.*

71. Feng, N., Guo, X., Liang, S., Zhu, Y., Liu, J. (2011). Biosorption of heavy metals from aqueous solutions by chemically modified orange peel. *Journal of Hazardous Materials, 185(1), 49-54.*

72. Farooq, U., Kozinski , J.A., Khan, M. A., Athar, M. (2010). Biosorption of heavy metal ions using wheat based biosorbents – A review of the recent literature. *Bioresource Technology , 101, 5043–5053.*

73. Ghosh, S., and Mitra , D. (2018). Elimination of Chromium(VI) from Waste Water Using Various Biosorbents . *Water Science and Technology Library, 84, 237-284.*

74. Gonzalez, M. H., Georgia C.L. Araujob, Claudia B. Pelizaroa, Eveline A. Menezes, Lemos, S. G., Sousa, G. B. D., Nogueira, A. R. A. (2008). Coconut coir as biosorbent for Cr(VI) removal from laboratory wastewater. *Journal of Hazardous Materials, 159, 252–256.*

75. Gadd , G.M. (2009). Biosorption: critical review of scientific rationale, environmental importance and significance for pollution treatment. *J Chem Technol Biotechnol, 84,13–28.*

76. Ghosal, P. S., Gupta, A.K .(2017). Determination of thermodynamic parameters from Langmuir isotherm constant-revisited. *Journal of Molecular Liquids, 225, 137–146.*

77. Gupta, V.K., Nayak, A., Agarwal, S. (2015). Bioadsorbents for remediation of heavy metals: Current status and their future prospects. *Environ. Eng. Res., 20(1), 1-18.*

78. Garg, U. K., Kaur, M.P., Garg, V.K., Suda, D. (2007) . Removal of hexavalent chromium from aqueous solution by agricultural waste biomass. *Journal of Hazardous Materials, 140 (1–2), 60-68.*

79. Gao, H., Liu, Y., Zeng, G., Xu, W., Li, T., Xia, W. (2008). Characterization of Cr(VI) removal from aqueous solutions by a surplus agricultural waste--rice straw. *Journal of Hazardous Materials, 150 (2),446-452 .*

80. Gupta, S., Babu, B.V. (2009). Utilization of waste product (tamarind seeds) for the removal of Cr (VI) from aqueous solutions: equilibrium, kinetics, and regeneration studies. *Journal of Environmental Management, 90 (10), 3013-3022.*

81. Gupta, V. K., Rastogi, A., Nayak, A. (2010). Adsorption studies on the removal of hexavalent chromium from aqueous solution using a low cost fertilizer industry waste material. *Journal of Colloid and Interface Science, 342, 135–141.*

82. Goel, J., Kadirvelu, K., Rajagopal, C., Kumar, V.G. (2005). Removal of lead(II) by adsorption using treated granular activated carbon: batch and column studies. *J Hazard Mater 125:211–220.*

83. Huang, Z., Wang, X., Yang, D. (2015). Adsorption of Cr(VI) in wastewater using magnetic multi-wall carbon nanotubes. *Water Science and Engineering, 8, 226–232.*

84. Hyder, A.H.M.G., Begum , S. A., Egiebor, N.O. (2015). Adsorption isotherm and kinetic studies of hexavalent chromium removal from aqueous solution onto bone char. *Journal of Environmental Chemical Engineering, 3, 1329–1336.*

85. Hegazi, H. A. (2013). Removal of heavy metals from wastewater using agricultural and industrial wastes as adsorbents. *HBRC Journal, 9, 276–282.*

86. Hutson, N.D., and Ralph, T. Y. R . (1997). Theoretical Basis for the Dubinin-Radushkevitch (D-R) Adsorption Isotherm Equation. *Adsorption, 3, 189-195.*

87. Hanif, M. A., Nadeem, R., Bhatti, H. N., Ahmad, N. R., Ansari, M. T. (2007). Ni(II) biosorption by Cassia fistula (Golden Shower) biomass. *Journal of Hazardous Materials, B139, 345–355.*

88. Hashem, M.A. (2007). Adsorption of lead ions from aqueous solution by okra wastes. *Int. J. Phys. Sci., 2,178–184.*

89. Hachair, A. S., Hofmann, A. (2018). Hexavalent chromium quantification in solution: Comparing direct UVvisible spectrometry with 1,5-diphenylcarbazide colorimetry. *C. R. Chimie , 21, 890-896.*

90. Hernaández, M.E. P., Argteaga, A. K. A., Vidal, C. A. G., Pardaveá, M. P. (2005).Mercury ions removal from aqueous solution using an activated composite membrane. *Environ. Sci. Technol., 39, 7667–7670.*

91. Ho, Y., McKay, G. (1999). Pseudo-second order model for sorption processes. *Process Biochemistry, 34,451–465.*

92. Hutchins, R. A. (1973a). Optimum sizing of activated carbon systems. *Industrial Water Engineering, 10(3), 40–43.*

93. Hasan, S.H., Singh, K.K., Prakash, O., Talat, M., Ho, Y. S. (2008). Removal of Cr(VI) from aqueous solutions using agricultural waste 'maize bran'. *Journal of Hazardous Materials, 152, 356–365.*

94. Hasan, S.H., Ranjan, D., Talat, M. (2010). Agro-industrial waste "wheat bran" for the biosorptive remediation of selenium through continuous upflow fixed-bed column. *J Hazard Mater, 18, 1134–1142.*

95. Iftikhar, A.R., Bhatti, H.N., Hanif, M.A., Nadeem, R. (2009). Kinetic and thermodynamic aspects of Cu(II) and Cr(III) removal from aqueous solutions using rose waste biomass. *Journal of Hazardous Materials, 161, 941–947.*

96. Ilyas, M., Ahmad, A., Saeed, M. (2013). Removal of Cr(VI) from aqueous solutions using peanut shell as adsorbent. *Journal of the Chemical Society of Pakistan, 35, 760 768.*

97. Jain, M., Garg, V.K., Kadirvelu, K. (2009). Equilibrium and Kinetic Studies for Sequestration of Cr(VI) From Simulated Wastewater Using Sunflower. *Waste Biomass. J Hazard Mater, 171(1-3), 328-34.*

98. Jain, M., Garga, V.K. , Kadirvelu, K. (2009). Chromium(VI) removal from aqueous system using Helianthus annuus (sunflower) stem waste. *Journal of Hazardous Materials 162 , 365–372.*

99. Jobby, R., Jha, P., Yadav, A.K., Desai, N. (2018). Biosorption and biotransformation of hexavalent chromium. *Chemosphere, 207, 255–266.*

100. Jain, M., Garg, V.K., Kadirvelu, K. (2013). Cadmium(II) sorption and desorption in a fixed bed column using sunflower waste carbon calcium– alginate beads. *Bioresour Technol 129, 242–248.*

101. Jianying, Q., Gaosheng, Z., Haining, L. (2015). Efficient removal of arsenic from water using a granular adsorbent: Fe–Mn binary oxide impregnated chitosan bead. *Bioresource Technology 193, 243–249.*

102. Khan, N., Hussain, S. T., Saboor, A., Jamila, N., and Kim, K. S. (2013). Physicochemical investigation of the drinking water sources from Mardan, Khyber Pakhtunkhwa, Pakistan. *International Journal of Physical Sciences, 8(33), 1661-1671.*

103. Keshavarzi, B., Hassanaghaei, M., Moore, F., RastegariMehr, M., Soltanian, S., Lahijanzadeh, A.R., Sorooshian, A. (2018). Heavy metal contamination and health risk assessment in three commercial fish species in the Persian Gulf. *Marine Pollution Bulletin, 129, 245–252.*

104. Ksakas, A., Loqman ,A., Bali, B. E., Taleb , M., Kherbeche, A. (2015). The adsorption of Cr (VI) from aqueous solution by natural materials. *J. Mater. Environ. Sci. 6 (7), 2003-2012.*

105. Kan , C.C., Ibe , A. H., Rivera, K.K.P., Arazo, R.O., Luna,M. D. G. (2017). Hexavalent chromium removal from aqueous solution by adsorbents synthesized from groundwater treatment residuals. *Sustainable Environment Research, 27, 163-171.*

106. Kumar, A., Jena, H. M. (2017). Adsorption of Cr(VI) from aqueous solution by prepared high surface area activated carbon from Fox nutshell by chemical activation with H_3PO_4. *Journal of Environmental Chemical Engineering, 5, 2032–2041.*

107. Kaur, R., Singh, J., Khare, R., and Ali, A. (2012). Biosorption the possible alternative to existing conventional technologies for sequestering heavy metal ions from aqueous streams: A Review. *Universal Journal of Environmental Research and Technology, 2(4), 325-335.*

108. Kulkarni, P. S., Kalyani, V., and Mahajani, V.V. (2007). Removal of Hexavalent Chromium by Membrane-Based Hybrid Processes. *Ind. Eng. Chem. Res., 46, 8176-8182.*

109. Ku, Y., and Jung, I. L. (2001). Photocatalytic reduction of C(VI) in aqueous solutions by UV irradiation with the presence of titanium dioxide . *Wat. Res., 35(1), 135±142.*

110. Kononova ,O. N., Bryuzgina , G. L., Apchitaeva, O.V., Kononov, Y.S. (2015). Ion exchange recovery of chromium (VI) and manganese (II) from aqueous solutions. *Arabian Journal of Chemistry, 12(8), 2713-2720 .*

111. Kobya , M., Demirbas , E., Senturk , E., Ince, M. (2005) . Adsorption of heavy metal ions from aqueous solutions by activated carbon prepared from apricot stone. *Bioresource Technology, 96, 1518–1521.*

112. Kumar, A., and Jena, H. M. (2017). Adsorption of Cr(VI) from aqueous phase by high surface area activated carbon prepared by chemical activation with $ZnCl_2$. *Process Safety and Environmental Protection, 109, 63–71.*

113. Kavitha, D., Namasivayam, C. (2007). Experimental and kinetic studies on methylene blue adsorption by coir pith carbon. *Bioresource Technology, 98, 14–21.*

114. Kuppusamy, S., Thavamani, P., Megharaj, M., Venkateswarlu, K., Lee, Y. B., Naidu, R., (2016). Potential of Melaleuca diosmifolia leaf as a low-costadsorbent for hexavalent chromium removal fromcontaminated water bodies. *Process Safety and Environmental Protection, 100, 173–182.*

115. Kobya, M., (2004). Removal of Cr(VI) from aqueous solutions by adsorption onto hazelnut shell activated carbon: kinetic and equilibrium studies . *Bioresource Technology, 91(3), 317-321.*

116. Khan, T., Isa, H.M., Mustafa, M. R. U., Chia, H. Y., Baloo, L., Manan, T.S.B.A., and Saeed, M. O., (2016). Cr(VI) adsorption from aqueous solution by an agricultural waste based carbon. *RSC Adv., 6, 56365- 56374.*

117. Khan, T. A., Mukhlif, A. A., Khan, E. A., Sharma, D.K. (2016). Isotherm and kinetics modeling of Pb(II) and cd(II) adsorptive uptake from aqueous solution by chemically modified green algal biomass. *Model Earth Syst. Environ, 2, 117.*

118. Khoubestani, R. S., Mirghaffari, N., and Farhadian, O. (2015). Removal of three and hexavalent chromium from aqueous solutions using a microalgae biomass-derived biosorbent. *Environmental Progress & Sustainable Energy, 34, 949–956.*

119. Liu, W., Yang, L., Xu, S., Chen, Y., Liu, B., Li, Z., and Jiang, C. (2018). Efficient removal of hexavalent chromium from water by an adsorption–reduction mechanism with sandwiched nanocomposites. *RSC Adv., 8, 15087-15093.*

120. Lagergren, S. (1898). Zur theorie der sogenannten adsorption Geloster stoffe. *Kungliga Svenska Vetenskapsakademiens. Handlingar, 24 (4), 1–39.*

121. Liu, L.Y., Qin, J.C., Li, K., Mehmood, M. A., Liu, C.G. (2017). Impact of moisture content on instant catapult steam explosion pretreatment of sweet potato vine. *Bioresources and Bioprocessing, 4 (49), doi:10.1186/s40643-017-0179-z.*

122. Langmuir, I. (1918). The adsorption of gases on plane surfaces of glass, mica and platinum. *Journal of the American Chemical Society, 40, 1361–1403.*

123. Levan, L.k., Muthukumaran, V., Gobinath, M. B. (2009). Batch adsorption and kinetics of chromium (VI) removal from aqueous solutions by Ocimum americanum L. seed pods. *Journal of Hazardous Materials, 161, 709–713.*

124. Lagergren, S. (1898). About the theory of so-called adsorption of soluble substances, Zur theorie der sogenannten adsorption gelster stoffe. *Kungliga Svenska Vetenskapsakademiens, Handlingar Band, 24(1898), 1–39.*

125. Miretzky, P., Cirelli , A. F. (2010). Cr(VI) and Cr(III) removal from aqueous solution by raw and modified lignocellulosic materials: A review. *Journal of Hazardous Materials, 180, 1–19.*

126. Mishra, A., Dubey , A., Shinghal, S. (2015). Biosorption of chromium(VI) from aqueous solutions using waste plant biomass. *Int. J. Environ. Sci. Technol., 12, 1415 – 1426.*

127. Mohan, D., Singh, K. P. (2002). Single- and multi-component adsorption of cadmium and zinc using activated carbon derived from bagasse Fan agricultural waste. *Water Research, 36, 2304–2318.*

128. Mohan, S., Sreelakshmi, G. (2008). Fixed bed column study for heavy metal removal using phosphate treated rice husk. *Journal of Hazardous Materials, 153, 75–82.*

129. Mohanty, K., Jha, M., Meikap, B.C., Biswas, M.N. (2005). Removal ofchromium (VI) from dilute aqueous solutions by activated carbon developed fromTerminalia arjuna nuts activated with zinc chloride. *Chemical Engineering Science, 60, 3049 – 3059.*

130. Mubarak, N. M. , Sahu, J. N., Abdullah, E. C., & Jayakumar, N. S. (2014). Removal of heavy metals from wastewater using carbon nanotubes. *Separation & Purification Reviews, 43(4), 311-338.*

131. Mohan, D., Singh, K. P., and Singh, V. K. (2005). Removal of hexavalent chromium from aqueous solution using low-cost activated carbons derived from agricultural waste. *Ind. Eng. Chem. Res, 44, 1027-1042.*

132. Madrid, A. S., Barrera, L. M., García, E. A., Urbina, E. C.,(2011) . Nickel(II) Biosorption by Rhodotorula Glutinis. *J Ind Microbiol Biotechnol,* 38(1), 51-64.

133. Munoz, A.J., Espínola,F., Moya,M., and Ruiz E. (2015). Biosorption of Pb(II) Ions by Klebsiella sp. 3S1 Isolated from a Wastewater Treatment Plant: Kinetics and Mechanisms Studies. *Bio Med Research International, Article ID 719060, 12.*

134. Mahmood , Z., Zahra, S., Iqbal, M., Raza, M. A., Saqib Nasir, S., (2017). Comparative study of natural and modified biomass of Sargassum sp. for removal of Cd^{2+} and Zn^{2+} from wastewater. *Appl Water Sci, 7, 3469–3481.*

135. Malkoc, E., Nuhoglu, Y., Dundar, M. (2006). Adsorption of chromium(VI) on pomace--an olive oil industry waste: batch and column studies. *Journal of Hazardous Materials, 138(1), 142-151.*

136. Marin, A.B.P., Aguilar, M.I., Meseguer, V.F., Ortuño, J.F., Sáez, J., Lloréns , M. (2009). Biosorption of chromium (III) by orange (Citrus cinensis) waste: Batch and continuous studies. *Chemical Engineering Journal, 155(1–2), 199-206.*

137. Muthukumaran, K., Beulah, S., (2010). Removal of Chromium (VI) from wastewater using chemically activated Syzygiumjambolanum nut carbon by batch studies. *Procedia Environmental Sciences, Urban Environmental Pollution, 4, 266–280.*

138. Matlock, M.M., Howerton, B.S., Atwood, D.A. (2002). Chemical precipitation of lead from lead battery recycling plant wastewater. *Ind. Eng. Chem. Res., 41, 1579–1582.*

139. Moon, C.J., Lee, J.H. (2005). Use of curdlan and activated carbon composed adsorbents for heavy metal removal. *Process Biochem., 40, 1279–1283.*

140. Mansour, M.S., Ossman, M.E., Farag, H.A. (2011). Removal of Cd (II) ion from waste water by adsorption onto polyaniline coated on sawdust. *Desalination, 272, 301–305.*

141. Mahmoud, M. A. (2015). Thermodynamics and kinetics studies of Mn (II) removal from aqueous solution onto powder corn cobs (PCC). *Chromatography Separation Techniques, 6(7), 1000301-1000304.*

142. Mondal, N. K., and Basu, S. (2019). Potentiality of waste human hair towards removal of chromium(VI) from solution: kinetic and equilibrium studies. *Applied Water Science, 9(49).*

143. Mahmoud, M.A. (2016). Kinetics studies of uranium sorption by powdered corn cob in batch and fixed bed system. *J Adv Res., 7, 79–87.*

144. Majumder, R., Sheikh, L., Naskar, A., Vineeta, Mukherjee M, Tripathy, S. (2017) Depletion of Cr(VI) from aqueous solution by heat dried biomass of a newly isolated fungus Arthrinium malaysianum: a mechanistic approach. *Scientific Reports, 7, 11254-11268* .

145. Nunez, P. V. L., García, E. A., Urbina, M. C. C., Barrera, L.M., Urbina, E. C. (2014). Removal of Hexavalent And Total Chromium From Aqueous Solutions By Plum (P. Domestica L.) Tree Bark. *Environmental Engineering and Management Journal, 13(8), 1927-1938.*

146. Nor, N.M., Chung, L.L., Teong, L.K., Mohamed, A. R. (2013). Synthesis of activated carbon from lignocellulosic biomass and its applications in air pollution control a review. *Journal of Environmental Chemical Engineering, 1, 658–666.*

147. Ngah,W.S.W., Hanafiah, M.A.K.M. (2008). Removal of heavy metal ions from wastewater by chemically modified plant wastes as adsorbents: A review. *Bioresource Technology, 99, 3935–3948.*

148. Nakkeeran, E., and Selvaraju, N. (2017). Biosorption of chromium(VI) in aqueous solutions by chemically modified Strychninetree fruit shell. *International Journal of Phytoremediation, 19(12), 1065-1076.*

149. Nguyen, T. A. H., Ngo, H. H., Guo, W. S., Zhang, J., Liang, S., Yue, Q. Y., Li, Q., Nguyen, T. V., (2013). Applicability of agricultural waste and by-products for adsorptive removal of heavy metals from wastewater. *Bioresource Technology, 148, 574-585.*

150. Nemr, A. E. (2007). Pomegranate husk as an adsorbent in the removal of toxic chromium from wastewater. *Chemistry and Ecology, 23, 409–425.*

151. Niazi, L., Lashanizadegan, A., Sharififard, H. (2018). Chestnut oak shells activated carbon: Preparation, characterization and application for Cr (VI) removal from dilute aqueous solutions. *Journal of Cleaner Production, 185,554-561.*

152. Nakkeeran, E., Patra, C., Shahnaz, T., Rangabhashiyam, S., N. Selvaraju, N. (2018). Continuous biosorption assessment for the removal of hexavalent chromium from aqueous solutions using Strychnos nux vomica fruit shell. *Bioresource Technology Reports , 3,256–260.*

153. Nasseh, N., Taghavi, L., Barikbin, B., & Harifi-Mood, A. R. (2017). The removal of Cr(VI) from aqueous solution by almond green hull waste material: kinetic and equilibrium studies. *Journal of Water Reuse and Desalination, 7, 449–460.*

154. Owalude , S. O., Tella, A. C. (2016). Removal of hexavalent chromium from aqueous solutions by adsorption on modified groundnut hull. *Beni suef university journal of basic and applied sciences, 5, 377–388.*

155. Othman,Z. A. A., Ali, R., Naushad, M. (2012). Hexavalent chromium removal from aqueous medium by activated carbon prepared from peanut shell: adsorption kinetics, equilibrium and thermodynamic studies. *Chem. Eng. J., 184, 238–247.*

156. Owa, F.W. (2014). Water pollution: sources, effects, control and management. *International Letters of Natural Sciences, 3, 1-6.*

157. Pawari, M.J., Gawande, S. (2015). Ground water pollution and its consequence. *International journal of engineering research and general science, 3(4), 773-76.*

158. Pal, A., Datta, S., and Paul A. K. (2013). Hexavalent Chromium Reduction by Immobilized Cells of Bacillus sphaericus AND 303. *Brazilian Archives Of Biology And Technology, 56(3), 505-512.*

159. Pena, S. V., Diaz, C.B., Hernández, I. L., Bilyeu, B., and Delgadillo, S.A. M. (2012). An Effective Electrochemical Cr(VI) Removal Contained in Electroplating Industry Wastewater and the Chemical Characterization of the Sludge Produced. *Ind. Eng. Chem. Res., 51(17), 5905–5910.*

160. Ponou, J., Kim, J. , Wang, L.P., Dodhiba, G., Fujita, T. (2011). Sorption of Cr(VI) anions in aqueous solution using carbonized or dried pineapple leaves. *Chem. Eng. J., 172, 906–913.*

161. Papirio, S., Frunzo, L., Mattei, M. R. , Ferraro, A., Race, M., Acunto, B. D., Pirozzi, F., and Esposito, G. (2017). Heavy Metal Removal from Wastewaters by Biosorption: Mechanisms and Modeling. *Springer International Publishing AG, Sustainable Heavy Metal Remediation, EnvironmentalChemistry for a Sustainable World, 8, DOI 10.1007/978-3-319-58622-9_2*

162. Pradhan, D., Sukla, L. B., Mishra, B.B., Devi, N. (2019).. Biosorption for removal of hexavalent chromium using microalgae Scenedesmus sp. *Journal of Cleaner Production, 209, 617-629.*

163. Park, D., Yun,Y. S., and Park, J. M. (2010). The past, present, and future trends of biosorption. *Biotechnology and Bioprocess Engineering, 15, 86–102.*

164. Pakade, V. E., Ntuli, T. D., Ofomaja, A. E. (2017). Biosorption of hexavalent chromium from aqueous solutions by Macadamia nutshell powder. *Appl Water Sci., 7, 3015–3030.*

165. Panday, K.K., Prasad, G., Singh,V.N. (1985). Copper(II) removal from aqueous solutions by fly ash. *Water Research, 19(7), 869-873.*

166. Pandey, P. K., Sharma, S. K., and Sambi, S. S. (2010). Kinetics and equilibrium study of chromium adsorption on zeolite NaX. *International Journal of Environmental Science & Technology, 7, 395–404.*

167. Parlayici, Ş., and Pehlivan, E. (2019). Comparative study of Cr(VI) removal by bio-waste adsorbents: equilibrium, kinetics, and thermodynamic. *Journal of Analytical Science and Technology, 10(15).* , https://doi.org/10.1186/s40543-019-0175-3

168. Pourfadakari, S., Jorfi, S., Ahmadi, M., and Takdastan, A. (2017). Experimental data on adsorption of Cr(VI) from aqueous solution using nanosized cellulose fibers obtained from rice husk. *Data in Brief, 15, 887–895.*

169. Rakhunde , R., Deshpande, L., and Juneja, H.D. (2012). Chemical Speciation of Chromium in Water: A Review. *Critical Reviews in Environmental Science and Technology, 42,776–810.*

170. Rangabhashiyam, S., Nandagopal, M.S. G., Nakkeeran, E., and Selvaraju, N. (2016). Adsorption of hexavalent chromium from synthetic and electroplating effluent on chemically modified Swietenia mahagoni shell in a packed bed column. *Environ Monit Assess ,188, 411*. DOI 10.1007/s10661-016-5415-z

171. Rai, M.K., Shahi, G., Meena, V., Meena R., Chakraborty, S., Singh, R.S., Rai, B.N.(2016). Removal of hexavalent chromium Cr (VI) using activated carbon prepared from mango kernel activated with H_3PO_4. *Resource-Efficient Technologies, 2, S63–S70.*

172. Rafatullaha, M., Sulaiman, O., Hashim, R., Ahmad, A. (2009). Adsorption of copper (II), chromium (III), nickel (II) and lead (II) ions from aqueous solutions by meranti sawdust. *Journal of Hazardous Materials, 170, 969–977.*

173. Rao, R. A. K., Rehman F. (2010). Adsorption studies on fruits of Gular (Ficus glomerata): Removal of Cr(VI) from synthetic wastewater. *Journal of Hazardous Materials, 181(1–3), 405-412.*

174. Rangabhashiyam , S., Selvaraju N., (2015b) . Efficacy of unmodified and chemically modified Swieteniamahagoni shells for the removal of hexavalent chromium from simulated wastewater. *Journal of Molecular Liquids, 209, 487–497.*

175. Rangabhashiyam, S., and Selvaraju, N. (2015a). Evaluation of the biosorption potential of a novel Caryota urens inflorescence waste biomass for the removal of hexavalent chromium from aqueous solutions. *Journal of the Taiwan Institute of Chemical Engineers, 47, 59–70.*

176. Radnia, H. (2013). Adsorption of Fe(II) from aqueous phase by chitosan: application of physical models and artificial neural network for prediction of breakthrough. *International Journal of Engineering, 26(8), 845-858.*

177. Sud, D., Mahajan, G., Kaur, M.P. (2008). Agricultural waste material as potential adsorbent for sequestering heavy metal ions from aqueous solutions – A review. *Bioresource Technology, 99, 6017–6027.*

178. Srivastava , N.K., Majumder C.B. (2008). Novel biofiltration methods for the treatment of heavy metals from industrial wastewater. *Journal of hazardous Materials, 151(1), 1-8.*

179. Shahid, M., Shamshad, S., Rafiq, M., Khalid, S., Bibi , I., Niazi, N. K., Dumat , C., Rashid, M. I. (2017).Chromium Speciation, Bioavailability, Uptake, Toxicity and Detoxification in Soil-Plant System: A Review. *Chemosphere, 178, 513-533.*

180. Saha, R., Nandi, R., and Saha, B. (2011). Sources and toxicity of hexavalent chromium. *Journal of Coordination Chemistry, 64 (10), 1782–1806.*

181. Shrivastava, R., Upreti, R.K., Seth, P.K., Chaturvedi U. C. (2002). Effects of chromium on the immune system. *FEMS Immunology and Medical Microbiology, 34, 1-7.*

182. Shrestha, B., Kour, J., Ghimire, K. N. (2016). Adsorptive Removal of Heavy Metals from Aqueous Solution with Environmental Friendly Material Exhausted Tea Leaves. *Advances in Chemical Engineering and Science, 6, 525-540.*

183. Shukla, S. S., Yu, L. J., Dorris, K. L., & Shukla, A. (2005). Removal of nickel from aqueous solutions by sawdust. *Journal of Hazardous Materials, 121, 243–246.*

184. Srivastavaa, S., Agrawala, S.B., Mondalb, M.K. (2015). Biosorption isotherms and kinetics on removal of Cr(VI) using nativeand chemically modified Lagerstroemia speciosa bark. *Ecological Engineering, 85, 56–66.*

185. Sooksawat, N., Meetam, M., Kruatrachue, M., Pokethitiyook , P., and Duangrat Inthorn, D. (2016). Equilibrium and kinetic studies on biosorption potential of charophyte biomass to remove heavy metals from synthetic metal solution and municipal wastewater. *Bioremediation Journal, 20(3), 240-251.*

186. Shinde V.B., and Singarvelu M. (2014). Thermo Gravimetric Analysis of Biomass Stalks For Briquetting. *Journal of Environmental Research And Development, 9, 151-160.*

187. Singh, K.K., Rastogi, R., Hasan, S.H. (2005). Removal of Cr(VI) from wastewater using rice bran, *Journal of Colloid and Interface Science ,290 (1),61-68.*

188. Sathish, T., Vinithkumar, N. V., Dharani, G., & Kirubagaran, R. (2015). Efficacy of mangrove leaf powder for bioremediation of chromium (VI) from aqueous solutions: kinetic and thermodynamic evaluation. *Applied Water Science, 5, 153–160.*

189. Sharma, D. C., and Forster, C. F. (1994). A preliminary examination into the adsorption of hexavalent chromium using low-cost adsorbents. *Bioresource Technology, 47, 257–264.*

190. Srivastava, V.C., Mall, I.D., Mishra, I.M. (2006). Characterization of mesoporous rice husk ash (RHA) and adsorption kinetics of metal ions from aqueous solution onto RHA. *Journal of Hazardous Materials, 134, 257–267.*

191. Saranya, N., Nakkeeran, E., Shrihari, S., Selvaraju, N. (2017). Equilibrium and kinetic studies of hexavalent chromium removal using a novel biosorbent: Ruellia Patula Jacq. *Arabian Journal for Science and Engineering, 42, 1545–1557.*

192. Saha, P., Chowdhury, S., Gupta, S., Kumar, I. (2010). Insight into adsorption equilibrium, kinetics and thermodynamics of Malachite Green onto clayey soil of Indian origin. *Chemical Engineering Journal, 165, 874–882.*

193. Sarin, V.,Pant, K.(2006). Removal of chromium from industrial waste by using eucalyptus bark. *Bioresource Technology, 97, 15–20.*

194. Singha, B., and Das, S. K. (2011). Biosorption of Cr(VI) ions from aqueous solutions: kinetics, equilibrium, thermodynamics and desorption studies. *Colloids and Surfaces B: Biointerfaces, 84, 221–232.*

195. Singha, B., Naiya, T. K., Bhattacharya, A. K., and Das, S. K. (2011). Cr(VI) ions removal from aqueous solutions using natural adsorbents – FTIR studies. *Journal of Environmental Protection, 2, 729–735.*

196. Sharma, R., Singh, B. (2013). Removal of Ni (II) ions from aqueous solutions using modified rice straw in a fixed bed column. *Bioresour Technol., 146, 519–524.*

197. Taweel, Y. A.E., Nassef , E. M., Elkheriany, I., Sayed, D. (2015). Removal of Cr(VI) ions from waste water by electrocoagulation using iron electrode. *Egyptian Journal of Petroleum, 24, 183–192.*

198. Tatah, V.S., Ibrahim,K.L.C., Ezeonu ,C.S., Otitoju, O. (2017).Biosorption kinetics of heavy metals from fertilizer industrial waste water using groundnut husk powder as an adsorbent. *Journal of Applied Biotechnology & Bioengineering, 2(6), 221–228.*

199. Thomas, H.C.(1994). Heterogeneous ion exchange in a flowing system. *J. Am. Chem. Soc., 66,1664–1666.*

200. Torresdey, J.L. G., Tiemann, K.J., Armendariz, V., Oberto, L. B., Chianelli, R.R., Rios, J., Parsons, J. G., Gamez, G. (2000). Characterization of Cr(VI) binding and reduction to Cr(III) by the agricultural by products of Avenamonida (Oat) biomass . *J Hazard Mater., B, 80, 175-188.*

201. Tsamo, C., Djonga, P.N. D., Dikdim, J.M. D., Kamga, R.(2018). Kinetic and equilibrium studies of Cr(VI), Cu(II) and Pb(II) removal from aqueous solution using red mud, a low-cost adsorbent. *Arabian Journal for Science and Engineering, 43, 2353–2368.*

202. Tewari, N., Vasudevan, P., Guha, B.K. (2005). Study on biosorption of Cr(VI) by Mucorhiemalis. *Biochemical Engineering Journal, 23, 185–192.*

203. Tan, W.T., Ooi, S.T., Lee, C.K. (1993). Removal of chromium(VI) from solution by coconut husk and palm pressed fibres. *Environmental Technology, 14,277–282.*

204. Timbo, C.C., Schulz, M. k., Amuanyena, M., Kwaambwa, H.M. (2017). Adsorptive removal from aqueous solution of Cr(VI) by green moringa tea leaves biomass. *Journal of Encapsulation and Adsorption Sciences, 07, 108–119.*

205. Vendruscolo, F., Ferreira, G. L. D. R., Filho, N. R. A. (2017). Biosorption of hexavalent chromium by microorganisms. *International Biodeterioration and Biodegradation, 119,87- 95.*

206. Volesky, B. (2001). Detoxification of metal-bearing effluents: biosorption for the next century. *Hydrometallurgy, 59(2–3), 203-216.*

207. Venugopal, V., Mohanty, K. (2011) . Biosorptive uptake of Cr(VI) from aqueous solutions by Parthenium hysterophorus weed: Equilibrium, kinetics and thermodynamic studies. *Chemical Engineering Journal, 174(1), 151-158.*

208. Vinodhini, V., Das, N., (2010). Packed bed column studies on Cr (VI) removal from tannery wastewater by neem sawdust. *Desalination, 264(1–2), 9-14* .

209. Vinodhini, V., Das, N. (2010). Relevant approach to assess the performance of sawdust as adsorbent of Cr(VI) ions from aqueous solutions. *International Journal of Environmental Science & Technology, 7, 85–92.*

210. Vimala, R., Charumathi, D., Das, N. (2011). Packed bed column studies on cd(II) removal from industrial wastewater by macro fungus Pleurotus platypus. Desalination, 275 (1-3), 291–296.

211. Weber, W.J., Morris, J.C. (1963). Kinetics of adsorption on carbon from solution. *Journal of the Sanitary Engineering Division, American Society of Civil Engineering, 89 (1), 31–60.*

212. Wojciechowska, M. (1999). Structure and catalytic activity of double oxide system: Cu–Cr–O supported on MgF_2. *Journal of Molecular Catalysis A: Chemical, 141, 155–170.*

213. Xie , B., Shan ,C., Xu , Z., Li , X., Zhang ,X., Chen , J., Pan, B. (2017). One-step removal of Cr(VI) at alkaline pH by UV/sulfite process: Reduction to Cr(III) and in situ Cr(III) precipitation. *Chemical Engineering Journal 308, 791–797.*

214. Xu, F., Zhu, T.T., Rao, Q.Q., Shui , S. W., Li, W. W., He, H. B., Yao, R. S. (2017). Fabrication of Mesoporous Lignin-Based Biosorbent From Rice Straw and Its Application for Heavy-Metal-Ion Removal. Journal of Environmental Science, *53, 132-140.*

215. Yoon, Y.H., Nelson, J.H. (1984).Application of gas adsorption kinetics 1 a theoretical model for respirator cartridge service time. *Am. Ind. Hyg. Assoc. J., 45,509–516.*

216. Yüksel, Ş., Orhan, R. (2019). The removal of Cr(VI) from aqueous solution by activated carbon prepared from apricot, peach stone and almond shell mixture in a fixed-bed column. *Arabian Journal for Science and Engineering ,44,5345-5357.*

217. Zayed, A.M., Terry, N. (2003). Chromium in the environment: factors affecting biological remediation, *Plant and Soil., 249 (1), 139–156.*

218. Zewail, T. M., Yousef, N.S. (2015). Kinetic study of heavy metal ions removal by ion exchange in batch conical air spouted bed. *Alexandria Engineering Journal, 54, 83–90.*

219. Zhua, C. S., Wang, L. P., Chena, W.B. (2009). Removal of Cu(II) from aqueous solution by agricultural by-product: Peanut hull. *Journal of Hazardous Materials, 168, 739–746.*

220. Zafar, M. N., Aslam, I., Nadeem , R., Munir, S., Rana, U.A., Khan, S. U.D. (2015). Characterization of chemically modified biosorbents from rice bran for biosorption of Ni(II). *Journal of the Taiwan Institute of Chemical Engineers, 46, 82–88.*

221. Zhang, R., Wang, B.,Ma, H. (2010) . Studies on Chromium (VI) adsorption on sulfonated lignite. *Desalination, 255, 61–66.*

222. Zang, T., Cheng, Z., Lu, L., Jin, Y., Xu, X., Ding, W., Qu, J. (2017). Removal of Cr(VI) by modified and immobilized Auricularia auricula spent substrate in a fixed-bed column. *Ecological Engineering*, 99, 358–365.

Research Output from The Thesis

Research Publications

1. Kumar, S., Selvaraju, N., & Prasanna, V. R., 2018. Removal of Cr(VI) from synthetic solutions using water caltrop shell as a low-cost biosorbent. *Separation Science and Technology*, 2783-2799. https://doi.org/10.1080/01496395.2018.1560333

2. Kumar, S., Shahnaz, T., Selvaraju, N., & Prasanna, V. R., 2020. Kinetic and thermodynamic studies on biosorption of Cr(VI) on raw and chemically modified Datura (Datura Stramonium) fruit . *Environ Monit Assess.*, 192-248. https://doi.org/10.1007/s10661-020-8181-x

3. Kumar, S., Patra, C., Selvaraju , N., Prasanna, V. R., 2020. Study the performance of fixed bed column for the hexavalent chromium removal using activated carbon derived from Water caltrop cell using phosphoric acid . *Environmental Science and Pollution Research*, **27**, 28042–28052. https://doi.org/10.1007/s11356-020-09155-8

Conferences Presentations (National and International)

1. Kumar, S., Selvaraju, N., & Prasanna, V. R., (2019). Activated carbon derived from water caltrop shell as a potentially low cost biosorbent for sequestration of Cr(VI) from waste water. *Fourth International Conference on Sustainable Energy & Environmental Challenges, at CSIR NEERI Nagpur 27-29 November.*

2. Kumar, S., Selvaraju, N., & Prasanna, V. R., (2020). Biosorption of Cr(VI) from aqueous solutions by Cassia fistula fruit. *3rd International Conference on* Waste Management, Recycle *, at IIT Guwahati Assam. 13-14 February.*

3. Kumar, S., Selvaraju, N., & Prasanna, V. R., (2020). Biosorption of Cr(VI) from aqueous solution using activated carbon prepared by Cassia fistula fruit using chemical activation with $ZnCl_2$. *National Conference on Issue & Challenges in water Treatment & Allied research for Sustainable Environment, at IIT Guwahati Assam. 23-25 January.*